

OPTIMAL POLICY IN THE PRESENCE OF SOCIAL IMAGE CONCERNS

Edward Jee^{*†} Anne Karing[‡] Karim Naguib[§]

September 2024

Abstract

Economic theory suggests that social image concerns can strengthen or dampen the effects of economic incentives. We explore these interactions through a large-scale field experiment in which we vary the cost and visibility of deworming decisions in Kenya. We randomly assign communities to either close or far from deworming treatment locations and introduce signals for adults to broadcast their deworming status to community members. First, we find that take-up of deworming decreases with travel distance to treatment locations, while allowing adults to signal their status increases take-up and does so significantly more at farther distances. Second, we build a structural model through which we show that changes in the cost of deworming shift equilibrium beliefs about the prosociality of those who deworm compared to those who do not, meaningfully altering the social image returns from deworming. Third, we show that ignoring endogenous shifts in social image returns leads to a suboptimal allocation of treatment points, placing them 8 to 13 percent closer to communities than the welfare maximizing optimum. Our findings suggest that knowledge of these interactions could lead to meaningful expansions of access to health services.

Keywords: incentives, social image, social multiplier, optimal policy
JEL codes: D01, D82, H21, I12, O10

*We thank Stefano DellaVigna, Edward Miguel and Ned Augenblick, and numerous seminar participants at Berkeley, Bocconi, Chicago, New York, Pompeu Fabra, Stanford and the NBER Summer Institute Development Economics for helpful discussions and feedback. Arthur Baker provided outstanding research assistance in Kenya. The field experiment would not have been possible without the invaluable support and collaboration of the Ministry of Health Kenya, Evidence Action, and REMIT. Funding for this project was provided by the Children’s Investment Fund Foundation. The experiment and data collection were approved by the UC Berkeley IRB and the Kenya Medical Research Institute. The experiment was registered at AEA RCT registry (RCT ID: AEARCTR-0001643). All errors are our own.

[†]University of Chicago. Email: edjee@uchicago.edu.

[‡]University of Chicago. Email: akaring@uchicago.edu.

[§]AstraZeneca. Email: karimn2.0@gmail.com.

1 Introduction

Markets often fail to achieve socially optimal outcomes. To address this, governments shape economic incentives – the benefits and costs of actions – realigning individual choices with the social optimum. Yet, these choices are also governed by social image concerns, carrying reputational benefits and costs. Economic theory predicts that social motivations can interact with economic incentives, strengthening or weakening their effects (Bénabou and Tirole 2011).

Understanding how social image and economic incentives interact is crucial for optimal policy design. For example, driving an electric vehicle signals environmental consciousness. A government subsidy for electric vehicles can increase adoption among consumers with a lower valuation for clean energy, thereby weakening the signaling value of driving an electric vehicle and reducing the subsidy’s efficacy. Similarly, taxing firms for emitting pollutants increases both the economic and reputational costs of doing so – firms that continue polluting will be perceived as cheats and suffer a “double whammy”.

Despite the intuitive nature of these interactions, empirical evidence of their importance remains scarce. This paper aims to causally identify and quantify the interactions between economic incentives and social image concerns in a real-world setting and assess their significance for the optimal allocation of public resources.

We collaborate with the Government of Kenya to implement a field experiment within a new community deworming program targeting 200,000 adults. The context is well-suited for studying the interactions between image concerns and economic incentives. Deworming is a well-known and accepted health treatment that sends a positive signal when taken. Sixty-eight percent of adults report that they would look down on a person who decided not to take part in community deworming, and 93% said they would praise a person for taking part. Yet, similar to many preventative health behaviors, take-up is low despite treatment being available for a nominal fee at clinics and pharmacies. Deworming has positive externalities, lowering the risk of transmission to others.

A government has three key levers to achieve the target level of deworming take-up: introducing material incentives, setting up treatment centers closer to communities, and leveraging social image concerns by increasing the visibility of actions.

To quantify the interactions between economic incentives and social image concerns, our research design uses the concept of the social multiplier (Bénabou and Tirole 2011). This concept illustrates how changes in the costs and benefits of prosocial actions influence the social image returns from these actions by shifting beliefs about the prosociality of those who take the action versus those who do not. To detect these interactions, we thus need to vary both the cost and social image associated with deworming take-up at a community level.

The large geographic scale of the deworming program allows us to create exogenous

variation in both. First, we vary the cost of deworming and its equilibrium take-up level by randomly assigning communities to treatment points that are either close or far away. On average, communities assigned to the farther locations need to travel one additional kilometer to reach treatment points compared to those assigned to closer locations.

Second, we credibly vary the visibility of deworming and thus the ability to signal. We introduce two forms of signals for adults who take up treatment: a colorful bracelet and ink on the thumb. The former is potentially more visible, while the latter is almost costless to provide and is an established signal commonly used for voting. To control for the consumption value of the bracelet, we introduce a material incentive in the form of a wall calendar.¹ The calendar also allows us to capture potential differences in the effects of incentives on take-up across far and close communities, independent of changes in the returns from signaling.

Increasing the visibility and salience of deworming decisions could lead individuals to update about the importance of deworming treatment, learn about community take-up, or serve as a reminder to deworm. To control for these effects, we send text messages reminding about the availability of treatment and providing information about the proportion of community members who already dewormed to a random subsample of individuals across both incentive and control communities. We then test for differential treatment effects between those who received the message and those who did not.

Our design, by randomizing at the community level, creates common knowledge about travel cost and signals within each community, such that beliefs about those who participate in community deworming and those who do not can shift accordingly.

We show that deworming decisions in a campaign setting are highly visible: in control group communities, for 70% of peers, individuals believe that they know their deworming status. Visibility decreases by 12 percentage points ($p=0.04$) when comparing close and far control communities. Qualitative data suggest that in the absence of signals, adults primarily learn about others' actions through direct encounters at treatment locations or by observing them going for treatment. Thus, as distance increases, it becomes harder for adults to observe others going to treatment, and because they are less likely to go themselves, they are also less likely to observe others at treatment points.

The introduction of bracelet and ink as signals changes this pattern: knowledge of peers' deworming status in far communities increases by 22 ($p<0.001$) and 15 ($p=0.006$) percentage points, respectively. This effectively reduces the decline in visibility caused by distance. However, signals increase the visibility of deworming decisions only by 3 ($p=0.56$) to 6 ($p=0.24$) percentage points in close communities, suggesting that individuals paid less attention to them. As distance and associated costs increase, signals become more informative about an individual's motivation to care for their own and the

¹We implement a willingness-to-pay experiment and show that the calendar serves as an appropriate placebo treatment for the bracelet.

community’s health. This leads individuals to pay more attention to signals in distant communities than in closer ones.

The reduced form analysis generates three main findings. First, in the absence of signals, far communities have a deworming take-up rate that is 17 percentage points ($p < 0.001$) lower than close communities. This is corroborated by individuals’ beliefs: they correctly predict that greater travel distance reduces take-up by 13 percentage points ($p = 0.002$). Second, individuals value the opportunity to signal with a bracelet, increasing deworming take-up from 34% to 42% ($p = 0.008$), compared to the control group. Individuals assign a negative utility to the ink, resulting in no significant increases in take-up for this signaling treatment. The impacts of bracelet signals are not significantly smaller in the presence of text messages, ruling out that reminder effects or learning can explain our results. We also find a significant increase in take-up by 5.5 percentage points when comparing the bracelet to the calendar incentive ($p = 0.019$), providing further evidence for the value of social image. Third, bracelet and ink show the same pattern of effects when comparing close and far communities: the effect of any signal on deworming take-up is nearly 2 times larger ($p = 0.054$) for communities far from treatment points compared to those closer. This suggests that high travel costs increase the return from signaling. Our willingness-to-pay experiment validates that bracelets are valued similarly to calendars across close and far communities, ruling out that these effects are driven by increases in private value due to scarcity of bracelets in far communities.

Next, we integrate our theoretical framework and experimental data into a structural model that explicitly models the private benefits, costs, and social image utility from deworming. This enables us to: (a) quantify the change in deworming take-up that stems from a change in social image returns as cost change, and (b) determine the optimal allocation of treatment locations under various policymaker scenarios.

In [Bénabou and Tirole \(2011\)](#)’s framework, an increase in the cost of an action, by changing who takes the action, increases the signaling value and therefore blunts the impact of rising costs on take-up. However, the extent to which signaling blunts the effect of cost depends on the visibility of the action, and thus the ability to signal. In the absence of visibility of actions, the social multiplier is 1, meaning that every increase in cost results in a proportional decrease in take-up. In the presence of visibility, the social multiplier is greater than or smaller than 1 depending on the response of visibility to cost. In the context of our experiment, when social signals are provided, we find a social multiplier between 0.9 and 0.8. As deworming decisions remain equally visible across close and far communities, an increase in social image returns dampens the negative effect of increased travel cost. In contrast, in the absence of social signals, the social multiplier falls between 1.1 and 1.3 and amplifies the negative effect of an increase in travel cost on take-up. The decline in visibility of the action outweighs the increase in perceived prosociality of taking the action.

In the final part of the paper, we use the parameter estimates from the structural model and combine them with geographic data on community locations and feasible treatment points to determine optimal policy actions in two specific scenarios. First, we determine the social planner’s optimal distribution of deworming treatment locations, when aiming to reach a target level of take-up. In this instance, she minimizes the number of treatment centers within the program’s designated area. Ignoring the effects of changes in acceptance on beliefs about the prosociality of those who take up deworming treatment, compared to those who do not, leads to non-trivial differences in the optimal allocation of treatment centers. A social planner would build too many treatment centers (7 percent) in the presence of social signals, and build too few centers in the absence of social signals.

Secondly, we calculate the optimal Pigovian and Ramsey subsidies: in our setting, the ideal distance to a deworming treatment location, in the presence of social image utility. We find that the optimal placement of points of treatment is approximately one kilometer further away when offering social signals compared to the control scenario. We show that a social planner who is cognizant of the social multiplier would place points of treatment 8 to 13% further apart compared to a planner who treats the effect of social image utility as constant with respect to distance. Importantly, we find that when visibility of deworming decisions is high, a policymaker who increases the private benefit of deworming would have to move points of treatment closer to maximize welfare.

Our paper makes three contributions. First, we jointly experiment with social signaling and economic incentives to understand their interactions and impact on policy efficacy in shaping socially optimal behaviors. Previous experiments focus on the static case, using signals to increase take-up or affect outcomes (Bursztyn and Jensen 2017; Bursztyn et al. 2018; Chandrasekhar et al. 2018; Dellavigna et al. 2017; Karing 2024; Breza and Chandrasekhar 2019) without considering changes in equilibrium beliefs about the prosociality of individuals taking the action predicted by Bénabou and Tirole (2006). This paper shows policymakers unaware of these interactions would overprovide public goods in one area, and potentially preventing the expansion of the program to a wider population. Our findings highlight that the effects of signals vary as a function of equilibrium beliefs and therefore not only shift the demand curve for a good but also change the slope or elasticity of demand as a function of equilibrium take-up.

Secondly, we contribute to a growing literature that seeks to understand the mechanisms underlying social image concerns and their role in motivating public good provision (Karlan and McConnell 2014; Kessler 2017; Perez-Truglia and Cruces 2017). We show that bracelets can be effective in increasing deworming take-up, and that individuals derive utility from the ability to signal their value for health. Furthermore, this signaling utility is higher at greater distances, as individuals are able to credibly signal their increasingly prosocial type as equilibrium beliefs change.

Third, this paper contributes to a large literature focused on using structural models to estimate relevant policy counterfactuals (Butera et al. 2022; Hurwicz 1966; Heckman and Vytlacil 2001). By microfounding individuals decision to deworm applying theory we allow for endogenous shifts in the prosociality of individuals taking up deworming compared to those who do not, and therefore allow equilibrium beliefs to change in response to policies. Our structural model allows us to decompose the effects of policies that counterfactually vary signals into a direct effect on visibility and an indirect effect on the equilibrium beliefs about the prosociality of individuals taking the action, and corresponding social image return.

Our results offer important insights for policymakers: economic incentives, such as a small cash payment or reduced travel cost, can lower the social image returns from taking an action by shifting equilibrium beliefs about the prosociality of individuals who take the action, leading to a potentially smaller than expected increase in take-up.

However, policymakers can leverage existing social image concerns by making actions more visible for individuals to broadcast their type, to effectively increase the take-up of and access to a public health good. Specifically, not only does increased visibility increase take-up levels, it reduces the effect of travel cost by increasing social returns, allowing policymakers to reduce investments without compromising take-up.

The remainder of the paper is organized as follows. Section 2 discusses the empirical setting. Section 3 provides the theoretical framework and predictions. Section 4 describes the implementation and design of the experiment. Section 5 presents the reduced form model results whilst Section 6 shows how we take the model to the data and provide structural estimates. Section 7 calculates the policymaker’s allocation of deworming points of treatment using estimates from the structural model whilst Section 8 concludes.

2 The Setting

Intestinal worms are a development burden to children and adults in many developing countries. According to the World Health Organization (2023) approximately 24% of the world’s population are infected with soil-transmitted helminths.² Severe infections lead to abdominal pain, iron-deficiency, anemia, malnutrition, and stunting. While significant progress has been made in deworming children through school programs, treating adults requires encouraging them to seek treatment.

Community deworming and the context of Western Kenya provide an empirically relevant and suitable setting to study prosocial behavior and the potential of social signaling. First, deworming is a public good. Most of its benefits come through reduced disease transmission to others, while private health benefits are low for many individuals.

²World Health Organization, Fact Sheet Soil-transmitted helminth infections, January 2023 <http://www.who.int/mediacentre/factsheets/fs366/en/>.

Second, deworming is an established health behavior in Kenya. In 2009 the Government of Kenya launched a National School-Based Deworming program (NSBDP) through which between 2012 and 2017 over 5 million children got dewormed in high endemic areas including our study area. Partly as a result, 78% of adults in our baseline survey sample know about deworming treatment and 61% are aware that treatment should be taken regularly, every three to twelve months. When asked who is at risk of worm infections, 94% of adults answer children and 67% answer that adults are at risk too. Only 4% say that deworming treatment is for sick people only.

Third, there is strong social judgment around deworming. Ninety-five percent of adults at baseline say they would praise someone who would come for free deworming treatment, while 69% said they would look down on a person who did not come. Figure A2 shows that image concerns for deworming are comparable to those for open defecation and childhood immunization. Individuals consider deworming as the “right thing to do” to protect one’s health, while those who do not deworm are considered careless and ignorant. While there could be concerns about adults’ interpreting others’ decision to deworm as a sign of them having worms or “being dirty” (i.e. revealing a negative health characteristic), baseline data suggests that this is not the case. Deworming treatment is regarded as something people should take frequently irrespective of their symptoms. Similar to other contexts, these social image concerns exist even in the absence of externality concerns. Our baseline data shows that adults have a limited understanding of externalities. A mere 27% of adults know that worms can spread between people.³

Lastly, adults underinvest in deworming despite treatment being readily available at a low cost (\$US 0.50-2 at pharmacies). While 68% of adults at baseline report to have taken treatment before, only 38% say they dewormed in the past 12 months. Adults in endemic areas are advised to deworm every 6 to 12 months but there is currently no formal program that provides free treatment to adults.

In collaboration with the Kenyan Government, we implement a new community deworming program that offers free deworming treatment to over 200,000 adults in Western Kenya. The program is implemented across three counties, Busia, Siaya and Kakamega, where soil-transmitted helminths are endemic. Over the course of 12 consecutive days, from 8am until 5pm, adults ages 18 and above were able to receive deworming treatment for free at a central location. Treatment was administered by local Community Health Volunteers (CHVs).⁴

³When asked if a person sick with worms can spread worms to others, only 31 percent answered yes, 56% said no and 13% were uncertain. When asked “If you have worms, does that affect your neighbors or relatives health?” 27% and “If your neighbors or relatives have worms, does that affect your health?” 25% answered yes. Only 18% answered yes to all three questions, having full understanding of externalities. 41% answered yes to one of the three questions, suggesting a partial understanding of externalities.

⁴We implement the program and experiment in two waves: wave one of deworming was implemented from early to mid-October in Busia and Siaya County, and wave two was implemented from late October until early November in Kakamega County.

3 Model

We adapt the theoretical framework by [Bénabou and Tirole \(2011\)](#) and extend it to endogenize the visibility of actions. The model discussion serves two purposes: (1) we lay out the main objects that we consider when introducing experimental variation and building a structural framework; (2) we define the social multiplier and state its main predictions on behavioral responses.

3.1 The Decision to Deworm in the Presence of Social Image Concerns

An individual’s decision to take-up deworming treatment $y_i \in \{0, 1\}$ depends on the net private benefit of deworming, the prosocial desire to look after one’s health and that of others, and the social image utility from being seen as highly prosocial. We model an individual’s utility as:

$$U_i = (b - c + v_i + u_i)y_i + \mu(c)E_{-i}(v_i|y_i)$$

where the first term, $b - c$, represents the net private benefit, composed of the health benefit b and the cost of taking up treatment c . Individuals differ in their type v_i , that is, their prosociality, which is known to them but unobservable to others. $\mu(c)E_{-i}[v_i|y_i]$ denotes the social image utility an individual receives based on others’ inferences about his or her type. The parameter $\mu(c) \equiv x(c)\lambda$ captures both the visibility of actions—that is, the extent to which others know whether an individual was dewormed ($x > 0$)—and the value individuals place on their social image in the context of deworming ($\lambda \geq 0$). u_i is an idiosyncratic cost or taste shock with variance σ_u , distributed independently of v , and unobservable to others.⁵ We combine the two margins of unobserved heterogeneity in one variable $w_i = u_i + v_i$. Following the logic of [Bénabou and Tirole \(2006, 2011\)](#) there exists a unique set of actions under visibility such that each individual chooses an action y_i , given the equilibrium actions of all other individuals. This equilibrium is characterized by the cutoff type $w^*(c)$ —who is indifferent between taking deworming treatment and not—and the social image returns, which solve the fixed-point equation:⁶

$$w^*(c) - c + b + \mu(c)[E(v|w > w^*(c)) - E(v|w \leq w^*(c))] = 0$$

The focus of our study is the final term, the social image returns from deworming, $\Delta(w^*(c)) = E(v|w > w^*(c)) - E(v|w \leq w^*(c))$. This term represents the difference in how

⁵One microfoundation for u_i is that the community doesn’t directly observe individuals’ private cost but knows the expected, cluster level cost, c , and the variation in costs, σ_u , around expected cost.

⁶ $w^*(\cdot)$ is a function of all the model primitives, $b, c, \mu(c)$. For simplicity, we focus on cost c as it is the main variable we consider when generating predictions.

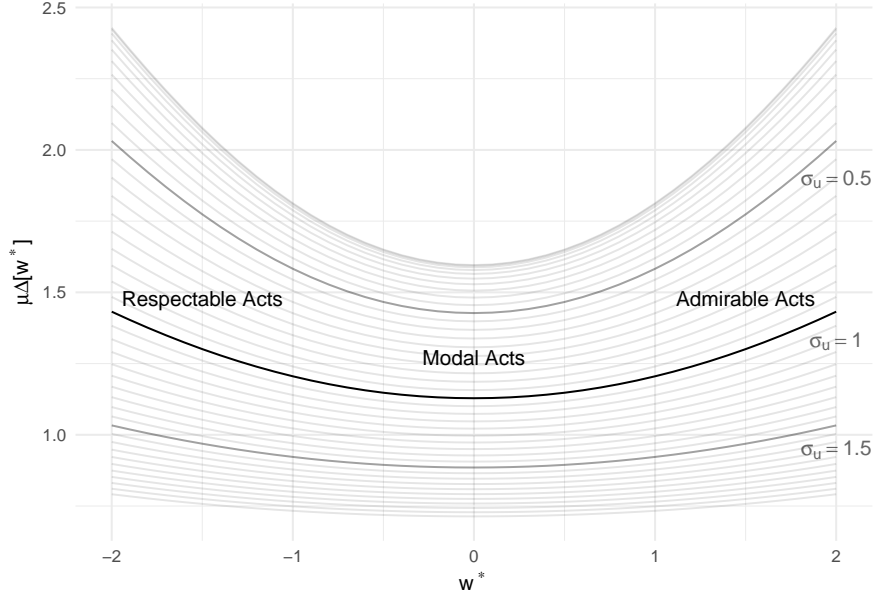


Figure 1: Equilibrium Social Image Returns

Notes: This figure shows how the expected social image return, $\mu(c)\Delta[w^*]$, varies as the cutoff type, w^* , changes. As σ_u increases, the social image returns fall as it becomes harder to infer someone's type based on actions. To generate this figure we fix $\mu(c) = 1$ and calculate $\mu(c)\Delta[w^*]$ across a grid of w^* and σ_u values. In Appendix Figure A1 we show a similar plot of social image returns as a function of take-up, since the proportion of individuals taking the action varies across each line as σ_u changes.

others perceive an individual's type based on whether they deworm, $y = 1, w > w^*(c)$, or not, $y = 0, w \leq w^*(c)$.

We augment the original model described by [Bénabou and Tirole \(2006\)](#) by allowing for visibility, μ , to vary as a function of the cost, c , incurred to perform the action, and therefore equilibrium deworming take-up. When an action is harder to perform and the signal is therefore more costly to obtain, the latter might be more valued, and individuals may be more likely to promote the signal. Others might also pay greater attention to signals when they are more informative about someone's type. On the other hand, as fewer people participate in deworming, the observability of the action may decline, and therefore the visibility of the action may decline too.

We assume u_i and v_i are normally distributed⁷ which gives w_i a normal distribution with standard deviation σ_w so the proportion of those who take up deworming is:⁸

$$\bar{y}(c) = 1 - F_w(w^*(c)), \quad (1)$$

where $F_w(w) = \Phi\left(\frac{w}{\sigma_w}\right)$ is the CDF of w . The social image return $\Delta(w^*(c))$ is based

⁷We use the normal distribution since it delivers an analytical characterisation of the net social image return, defined later in the paper. Any non-uniform type distribution will create an interaction between incentives and visibility.

⁸In Appendix I we derive the density of w when v is bounded, as described in [Bénabou and Tirole \(2011\)](#).

on others' inference about one's prosocial motivation in the presence of two forms of uncertainty: (i) the individual's true type and (ii) the heterogeneity in private benefit caused by the idiosyncratic shock.

Figure 1 displays how social image returns change as the cutoff type w^* (the equilibrium take-up level of deworming) changes. Social image returns are U-shaped with respect to the level of take-up.⁹ For “modal” acts (w^* close to zero) inferences about individuals' types are close to average, thus uninformative, and social image returns $\mu(c)\Delta(w^*)$ are low. For “respectable” acts ($w^* \ll 0$), everyone but the lowest types are taking the action, generating strong type inferences and increasing social image returns as w^* is falling. For “admirable” or “heroic” acts ($w^* \gg 0$), only the most virtuous or prosocial people take the action, allowing for strong type inferences and increasing social image returns as w^* is increasing.

Allowing for individual level shocks u_i makes it harder for others to draw inferences about v_i from observed actions. Intuitively, when the variance σ_u is small, as shown at the top of Figure 1, communities can easily infer one's type based off actions as the contribution of idiosyncratic shocks is small in expectation. However, as the variance σ_u increases, communities are unable to determine whether individuals primarily deworm out of intrinsic motivation or due to a large u_i . The social image returns to deworming $\mu(c)\Delta(w^*)$ decrease at each level of w^* and the U-shaped returns curve flattens (see Figure 1).¹⁰

3.2 Predictions

The model gives rise to the following predictions.

Prediction 1. Direct Visibility Effect

An increase in visibility, μ , will increase deworming take-up:

$$\frac{\partial \bar{y}}{\partial \mu} = f_w(w^*(c)) \underbrace{\frac{\Delta(w^*(c))}{1 + \mu\Delta'(w^*(c))}}_{\partial w^*/\partial \mu} > 0$$

where $f_w(w)$ is the PDF of w .

An increase in visibility of the act of deworming a_i increases the utility from social image returns, raising individuals' incentives to deworm either to avoid stigma or to be praised.¹¹

⁹Bénabou and Tirole (2011) prove that this holds provided the distribution of types is unimodal.

¹⁰Flattening and not simply falling of social image returns: Holding v fixed and increasing σ_u has greater effects in the tail of the w^* distribution, since a higher proportion of individuals take the action due to noise rather than because of being highly prosocial.

¹¹Following Bénabou and Tirole (2011), we assume that $1 + \mu\Delta'(w^*) > 0$ which ensures the indirect

Prediction 2. Direct Cost Effect *An increase in the cost of deworming, c , will lower aggregate take-up:*

$$\frac{\partial \bar{y}}{\partial c} = -f_w(w^*(c)) \underbrace{\frac{1 - \mu' \Delta(w^*(c))}{1 + \mu \Delta'(w^*(c))}}_{\partial w^* / \partial c} < 0$$

provided $1 - \mu' \Delta(w^(c)) > 0$.*

Since cost enter negatively into an individual's utility function, a rise in cost will decrease deworming take-up for all μ sufficiently small.

Prediction 3. Amplification & Mitigation

If the semi-elasticity of social image returns with respect to cost, $\frac{\partial \Delta}{\partial c} \frac{1}{\Delta}$, is greater than the semi-elasticity of visibility with respect to cost, $\frac{\partial \mu}{\partial c} \frac{1}{\mu}$, then the effect of an increase in costs on deworming take-up is dampened:

$$-\frac{\partial \mu}{\partial c} \frac{1}{\mu} < \frac{\partial \Delta}{\partial c} \frac{1}{\Delta} \implies \frac{\partial \bar{y}}{\partial c} = -f_w(w^*(c)) \frac{1 - \mu' \Delta(w^*(c))}{1 + \mu \Delta'(w^*(c))} > -f_w(w^*(c)) \quad (2)$$

If the reverse is true, then an increase in costs is amplified:

$$-\frac{\partial \mu}{\partial c} \frac{1}{\mu} > \frac{\partial \Delta}{\partial c} \frac{1}{\Delta} \implies \frac{\partial \bar{y}}{\partial c} = -f_w(w^*(c)) \frac{1 - \mu' \Delta(w^*(c))}{1 + \mu \Delta'(w^*(c))} < -f_w(w^*(c)) \quad (3)$$

The second term in Equations (2) and (3) represents the *social multiplier*—the change in social image returns as the equilibrium cutoff type changes with cost changes, $\partial w^* / \partial c$. This change either strengthens or dampens the marginal effect of private benefits and costs. If $\Delta'(w^*(c))$ is zero, such as when the type distribution is uniformly distributed, or individuals are not concerned about their social image or there is no visibility ($\mu = 0$), then we have a unit multiplier; i.e., there is no additional effect on the demand for deworming from a change in the private costs or benefits. If $\Delta'(w^*(c))$ is negative, the multiplier is greater than 1, increasing the sensitivity to changes in costs or benefits. Conversely, if $\Delta'(w^*(c))$ is positive, the multiplier is less than 1, decreasing sensitivity. The multiplier shifts from being greater than 1 to less than 1 as $w^*(c)$ increases, as shown in Figure 1. Thus, as w^* increases and deworming becomes more of an “admirable” act rather than a “modal” act, the marginal effect of private benefits diminishes.

Allowing for μ to change with c alters the social multiplier, as defined in [Bénabou and Tirole \(2011\)](#). For ranges of cutoff types w^* where social image returns $\Delta(w^*(c))$ increase as costs increase, but visibility μ decreases, the net social image returns can decrease or

effect of greater visibility on the cutoff type, w^* , does not outweigh the direct effect, which will hold for μ sufficiently small. In Appendix Figure A4 we verify that an extension of this condition, shown later, holds for all distances and parameter values considered in this paper using estimates from our structural model.

increase, depending on which effect is more dominant. This leads to a prediction where the amplifying or mitigating effect of the social multiplier depends on the semi-elasticities of visibility and social image returns.

This interaction between economic and social image benefits and costs presents a challenge for policymakers when choosing optimal incentives. Increasing private incentives when an act is “modal” will have different effects on deworming take-up than if a policymaker increases an incentive for an “honorable” act.

We will test Predictions 1 to 3 using our reduced form model (Section 5), examining whether visibility increases take-up, distance reduces take-up, and the treatment effect of increased visibility is more pronounced at lower take-up equilibria than at higher ones. Subsequently, we will use a structural model (Section 6) to (re)assess Predictions 1 to 2 and directly estimate the social multiplier, Prediction 3, thereby quantifying the amplification and mitigation effects that private incentives induce in the presence of social image concerns.

4 Experimental Design

Identifying the social multiplier requires exogenous variation in equilibrium take-up of deworming as well as in social image concerns. The former induces changes in the equilibrium cutoff type, since a given individual’s actions are a function of their community’s actions.

4.1 Distance Treatments

To create exogenous variation in equilibrium deworming take-up, we introduce a distance condition, $d \in \{\text{close, far}\}$. We randomly assign communities’ closest point of treatment to be either a “Close” (0-1.25km) or “Far” (1.25-2.5km) deworming location.¹² The distance to the assigned treatment location is, for all but two clusters, shorter than the distance to any other deworming treatment location. The site selection and randomization procedure for points of treatment and clusters is described in detail in Appendix A. Randomizing distance to the nearest deworming location at the community level changes the cost individuals must incur to get dewormed and our campaign creates common knowledge of such costs within a community. When an individual in a community observes an individual taking (or deciding not to take) the decision to get dewormed they can correctly infer an individual’s type, v_i . The distance condition shifts the equilibrium take-up of deworming since in Far communities, only those with higher types will still choose to get dewormed. Since a community centroid’s distance to the treatment location

¹²Due to small changes in the actual location of treatment points and the dispersion of households within targeted areas, actual distance to points of treatment were distributed as shown in Figure A3 and occasionally some Close communities had to walk slightly more than 1.25km and vice versa.

is common knowledge amongst households and distance, as a travel cost, directly enters individuals’ utility function, our preferred distance measure is the centroid’s distance to the treatment location – we present robustness checks using the randomized distance condition and controlling for a household’s distance to the treatment location in Appendix B. Our community-level randomization of communities to a Close or Far point of treatment successfully created a mean difference in walking distance of 1.02 kilometers, as shown in Figure A3. We verify, using a permutation test, that there is no statistically significant relationship between the distance between a community’s centroid and treatment locations across a range of observed covariates in Figure C1.

4.2 Incentive Treatments

To create variation in social image concerns, we introduce two incentives aimed at increasing the visibility of deworming, a bracelet and indelible ink marked on the thumb of those dewormed, shown in Figure A5. We cross-randomize the distance conditions with these incentives at the community level: 39 treatment locations individuals received a bracelet when coming for deworming and at 36 they received ink. The color green was chosen as it is not associated with any political parties and was liked most by individuals during piloting. We test two different signals since it was unclear upfront which one could be more cost-effective.¹³

Each of these incentives also introduces a private benefit (or cost, if ink is disliked), which we need to disentangle from the incentive’s signaling value. To do so, we also introduced a low-visibility incentive with a comparable private benefit: a simple paper wall calendar shown in Figure A6 in 35 communities.¹⁴ Due to its durability and visibility inside the home, the calendar would also act as a self-signal to individuals, reminding them of their participation in deworming.

Finally, 34 treatment locations were randomized into a control arm where no incentives were provided, giving four total incentive arms $z = \{\text{control, ink, calendar, bracelet}\}$ across 144 communities. Randomization at the community level, alongside our information campaign, ensures common knowledge within a community about what a given signal means about an individual’s deworming choice.

¹³Ink and bracelets vary as signals across important dimensions:

- i) Ink is known for its use during elections. Bracelets are not commonly worn among adults in Kenya.
- ii) Ink has zero or negative consumption utility if individuals perceive it as messy or distrust it due to its link to voting. Bracelets could provide positive consumption value but cannot cause disutility since it is a voluntary signal.
- iii) Bracelets have a high visibility as they are worn around the wrist. Ink’s visibility is lower as it is applied to the thumb and only lasts for about 3 days to 2 weeks (on the skin/on the nail).
- iv) The cost of ink is close to zero while a bracelet costs \$0.20. Our research partner, a non-profit, had a strong interest in testing ink.

¹⁴Wall calendars are popular in Kenya as people use them to decorate the walls of their homes and often have many calendars for the same year put up. The cost of the calendar is 50 Kenyan Shillings (50 US Cents).

Our study randomization incorporates county-level stratification and is summarized in Figure [A7](#).

4.3 Information Treatment

One week before the launch of the community deworming program CHVs together with research staff visited each of the selected 144 communities to inform households about the upcoming program. The objective of the community visits was to create common knowledge about a key set of information, namely: (i) inform households about the upcoming deworming program, including when and where treatment would be available, and send a strong message that (ii) regular deworming, even in the absence of symptoms, is not only important for children but also for adults and (iii) deworming is a public good. In addition, CHVs informed community members that ink, calendars and bracelets would be given when coming for deworming, and distributed flyers that displayed the incentives (see Appendix Figure [A8](#)).

4.4 Experiment Data

Our analysis uses several data sources, including administrative data on deworming take-up and survey data that was collected before and after the intervention:

1. *Household census*: We conducted a census of all adults (18 years age or older) residing in the 144 selected communities: surveyors visited each household, captured their geographic coordinates, and collected basic information of each household member that would allow us to follow-up with individuals and stratify over relevant characteristics (e.g., phone ownership). In total we listed 38,019 adults. Using the census lists we randomly sampled individuals to be surveyed at base- and/or endline.
2. *Baseline survey data*: From each of the 144 communities we randomly sampled 15 households and from each household one adult was randomly picked to respond to the baseline survey. We surveyed 4,823 adults about their knowledge about private and social benefits, prior experience and beliefs about deworming take-up and social norms. We reported outcomes under in Section [2](#).
3. *Endline survey data*: We surveyed 5,664 adults to verify the correct implementation of all treatments, the visibility of signals, first and second order beliefs and to conduct a separate choice experiment to elicit preferences for calendar and bracelets.
4. *Monitored deworming sample*: A sample of 9,805 adults whose deworming status was monitored at the point of treatment by enumerators. This sample includes our main outcome variable since it provides a verifiable measure of deworming sta-

tus. While CHVs distributed the deworming drugs and incentives, field researchers recorded personal information on electronic devices.

We detail the timeline of the experiment implementation and main data collection activities in Figure A9.

4.5 Sample Definition and Randomization Checks

The control group mean and standard error for each covariate, along with pairwise comparisons between control and treatment groups and their corresponding p -values, are presented in Table B1. In the final column of Panel A, all the F -tests for joint significance show p -values above 0.1 across all comparisons apart from ‘Distance to PoT’, which we would expect since by design communities in the Close condition have to walk less than Far communities. Since our identification strategy leverages differences both within each distance condition across incentive arms and within incentive arm across distance we report within incentive across distance pairwise differences in Appendix Table B2.

There is evidence of some imbalance within the far treatment for ‘Distance to PoT’, as communities in the ink arm are, on average, 344 meters further away (p -value = 0.02) than control communities. To alleviate concerns arising from imbalanced travel distance we show that the randomization inference p -values for all covariates regressed on continuous distance are greater than 0.1 in Figure C1 and in our main specification we control for distance continuously in the reduced form Probit model to capture any effect of greater average walking distance on deworming decisions. Estimates from our structural model also condition on distance directly in order to measure the private cost incurred by individuals choosing to deworm.

Overall, baseline characteristics do not statistically differ across treatment and control, Table B1 Panels A-D contains 15 imbalances at the 10% level and three at the 5% level against an expected 18 and nine imbalances respectively across 184 comparisons. Whilst the pairwise distance differences in Appendix Table B2 has only eight imbalances at the 10% level from 88 comparisons. Covariates collected at endline to establish implementation success are shown in Table B1 Panel D. Overall, levels of recall about the program are high with 86% and 79% of respondents reporting remembering a CHV visiting in the Close and Far control conditions, whilst 80% and 96% recall an announcement about deworming program being conducted in their community.

5 Reduced Form Estimates

5.1 Treatment Effects

In this section, we estimate the effect of the distance and incentive treatments on visibility and deworming take-up. Our visibility specification uses OLS to regress first-order beliefs on material and signaling incentives interacted with a community centroid’s distance to the point of treatment, where first-order beliefs are measured as the proportion of community members an individual reports having knowledge of their deworming status. Our main deworming specification is a Probit model, which captures the probability of getting dewormed, Y_{ivs} , for individual i in community v and strata s :

$$Pr(Y_{ivs} = 1 | d_{vs}) = \Phi \left(\alpha_s + \sum_{z \in Z} \beta_z \text{treat}_{z,vs} + \sum_{z \in Z} \gamma_z \text{treat}_{z,vs} \times \text{Distance to PoT}_{vs} \right) \quad (4)$$

that is, a saturated model where we interact our material and signaling incentives with the community centroid’s distance to the point of treatment; where α_s represent stratification dummies.

5.1.1 Increasing the Cost of Deworming

We first show that introducing variation in distance leads to meaningful changes in first-order beliefs about others’ deworming decisions.¹⁵ We find high levels of visibility in the Control group shown by Column 1 of Table 1, with 69.6% of respondents reporting knowing the deworming status of others. Knowledge of others’ deworming decisions is significantly higher in the Close communities at 75.3% compared to 62.8% in the Far communities ($p=0.04$). Both the high baseline level of visibility and greater visibility at Close communities is consistent with the effect of the mass information campaign. The limited number of days deworming treatment is available and the single point of treatment per community makes the observation of individuals’ participation in deworming easier. With naturally lower take-up in Far communities, observing someone taking treatment is less likely in these areas.

We turn to the primary outcome of the experiment which is the fraction of individuals taking deworming treatment. Columns 1 to 4 of Table 2 show the average treatment effects using the reduced form Probit model. Even during a large, community-wide deworming campaign take-up of treatment is not the modal act: only 33% of individuals on average receive deworming treatment in the Control group which suggests there is scope for interventions to have a large, positive impact. Travel to central locations is seen as costly: 40.7% of adults in Close communities come for deworming treatment, while only 23.5% attend from Far communities, a 17.3 percentage points ($p<0.001$) difference.

¹⁵Appendix Table B3 shows similar results using second-order beliefs as a robustness check.

Table 1: The Effects of Incentives on the Visibility of Deworming Decisions

Dependent variable: First-order beliefs	Reduced Form			
	Combined (1)	Close (2)	Far (3)	Far - Close (4)
Control	0.691 [0.03]	0.747 [0.042]	0.622 [0.044]	-0.125 [0.06]
$H0$: Any Signal \neq No Signal, p -value	<0.001	0.431	<0.001	0.001
$H0$: Bracelet \neq Calendar, p -value	0.001	0.583	<0.001	0.002
Ink	0.084 [0.04]	0.032 [0.053]	0.147 [0.052]	0.115 [0.068]
Calendar	0.039 [0.039]	0.03 [0.052]	0.049 [0.055]	0.019 [0.074]
Bracelet	0.135 [0.037]	0.051 [0.047]	0.237 [0.053]	0.185 [0.068]

Notes: Point estimates show the probability an individual responded that they knew about a community member’s deworming status when asked the question: “Do you think this person came for deworming?” conditional on the respondent recognizing the person within the community randomly drawn by the enumerator. Respondents were asked 10 times. ‘Control’ denotes the control mean, whilst other rows denote treatment effects relative to the control mean. “Combined”, “Close”, “Far”, and “Far - Close” average treatment effect estimates are calculated by aggregating over the predicted deworming take-up in each cell using the Probit model with continuous distance. $H0$: Any signal $>$ No signal pools the ink and bracelet arms and the control and calendar arms and computes the p -value for the one sided t-test that treatment effects are greater in the signal arms than non-signal arms. $H0$: Bracelet $>$ Calendar shows the p -value for a one sided t-test that the Bracelet treatment effect is greater than the Calendar treatment effect. Sample consists of 999 respondents and estimates are generated using a probit model with strata dummies and saturated dummies for incentive treatment and incentive treatment interacted with distance to the nearest point of treatment. Results are clustered at the community level using the cluster bootstrap. Parentheses denote standard errors. Far - Close shows the difference between the close and far treatment effect. Figure A15 breaks down the reasons individuals gave when prompted why they answered “Yes”, “No”, “Don’t Know” using a GPT model to classify free-text reponses. Table B3 shows quantitatively similar results using second-order beliefs.

Importantly, the experimental variation in distance shifted the equilibrium take-up level across Close and Far communities which is essential to generate variation in the cutoff type, used in our structural model.

5.1.2 Increasing the Visibility of Deworming Take-up

We next show that introducing social signals increases the visibility of deworming decisions, and closes the knowledge gap between Far and Close communities. The Bracelet and Ink conditions increase knowledge of others’ deworming status by 13 percentage points ($p < 0.001$) and 8.4 percentage points ($p = 0.04$), respectively. However, the Far treatment effects are much larger than the Close treatment effects: the Bracelet increases visibility by 21.7 percentage points ($p < 0.001$) in Far communities compared to a mere 5.8 percentage points ($p = 0.24$) in Close communities. Similarly, the Ink had effects of 14.6 ($p = 0.006$) and 3.2 ($p = 0.56$) percentage points in Far and Close communities, re-

Table 2: The Effects of Incentives on Deworming Take-up

Dependent variable: Take-up	Reduced Form			
	Combined (1)	Close (2)	Far (3)	Far - Close (4)
Control	0.33 [0.023]	0.407 [0.024]	0.235 [0.033]	-0.173 [0.032]
<i>H0</i> : Any Signal \neq No Signal, <i>p</i> -value	0.407	0.642	0.075	0.049
<i>H0</i> : Bracelet \neq Calendar, <i>p</i> -value	0.03	0.269	0.02	0.341
Ink	-0.019 [0.031]	-0.053 [0.033]	0.023 [0.042]	0.076 [0.041]
Bracelet	0.084 [0.028]	0.06 [0.033]	0.115 [0.042]	0.055 [0.049]
Calendar	0.034 [0.028]	0.026 [0.031]	0.043 [0.036]	0.017 [0.037]

Notes: This table shows average marginal effects from a Probit model with saturated interactions between incentive treatment arms and distance to the point of treatment and strata fixed effects. “Combined”, “Close”, “Far”, and “Far - Close” average treatment effect estimates are calculated by aggregating over the predicted deworming take-up in each cell using the Probit model with continuous distance. Estimates show treatment effects compared to the control group, apart from Control which displays the level of deworming take-up in the control group. Square brackets show standard errors clustered at the community level calculated using the cluster bootstrap. Far - Close shows difference between the close and far treatment effects. *H0*: Any signal $>$ No signal pools the ink and bracelet arms and the control and calendar arms and computes the *p*-value for the one sided t-test that treatment effects are greater in the signal arms than non-signal arms. *H0*: Bracelet $>$ Calendar shows the *p*-value for a one sided t-test that the Bracelet treatment effect is greater than the Calendar treatment effect. We present a Bayesian probit model in Table B10 using a parametric form of clustering to aid comparability with the structural model. Appendix Tables B9 and B8 show results including the squared distance to a cluster’s centroid and replacing continuous distance with a binary treatment indicator for the Close and Far group respectively.

spectively. The large disparity in effects on visibility across Close and Far motivates our decision to allow μ to vary directly with distance. The greater treatment effect for Bracelets compared to the Ink is corroborated by our endline checks, shown in Table B11.

As expected, the Calendar had little effect on visibility: the point estimate for all communities combined is 2.4 percentage points ($p=0.53$), and the Bracelet-Calendar difference in treatment effects on first-order beliefs is significant ($p<0.05$) for all but the Close treatment arm ($p=0.22$). Given the Calendar has little effect on visibility and a similar private utility as the Bracelet condition, it is an appropriate control for the signaling effect of bracelets in the reduced form analysis.

Having established that signaling incentives increase visibility about community members’ deworming decisions, we now show that increasing the visibility of deworming by providing an opportunity to signal is an effective way of increasing take-up. Bracelets increase take-up by 8.4 percentage points ($p=0.003$) compared to the Control Group. The Calendar incentive had a positive but non-significant impact on take-up of 3.4 percentage points ($p=0.218$). Since it has a similar private valuation compared to bracelets, but a

lower signaling component, the difference in treatment effects across Bracelet - Calendar ($p=0.03$) acts as a naive estimate of the effect of signaling in the reduced form model. In the Close treatment group this difference is positive, at 3.3 percentage points, but not statistically significant ($p=0.279$). While the treatment effects of the Calendar incentive are almost identical for close and far communities (difference of 0.017, $p = 0.656$), the Bracelet effect on take-up for far communities is 5.5 percentage points larger than for close communities ($p=0.258$). As a result, the Bracelet-Calendar difference in the Far condition increases to 7.11 percentage points ($p=0.022$). The Ink incentive has no discernible impact on overall deworming take-up, but reveals a similar pattern in treatment effects across Close and Far communities, with an increase by 7.6 percentage points ($p=0.069$). The p -value from a two-sided test that compares the treatment effects of Any Signal to No Signal— a ‘Difference-in-Differences’ approach that pools the two signaling incentives (Any Signal) and compares the Calendar incentive with the Control Group (No Signal) across Far and Close communities— is 0.049, as shown in the second row of column 4. This suggests that there are interactions between distance costs and the social image returns from signaling.

5.2 Alternative Mechanisms and Robustness

5.2.1 Reminder and Social Learning Effects

Adults had the opportunity to come for deworming treatment across twelve consecutive days, creating an opportunity not only for bracelet and ink incentives to be used as signals, but also to work as reminders or provide information about take-up in their community leading to social learning. To identify the relevance of these alternative mechanisms, we implemented a text message treatment for a random subsample of 1,228 adults from the census lists.¹⁶ We randomly sampled 20 adults in each of the 144 communities, of which 10 were assigned to treatment and received text messages that reminded them about the availability of deworming (SMS reminder), and provided information about the proportion of adults in their community who had already come for deworming (SMS social info).¹⁷ Individuals received the first text message the day before deworming started and then one message every other day of the deworming campaign until the final day.

When comparing the treatment effects of incentives for individuals who received the SMS treatment to those who did not, the overall treatment effects and significance remain similar. Figure [A10](#) shows the difference in incentive treatment effects across the SMS

¹⁶Only individuals who owned a phone were included in the eligible sample for treatment. 75% of adults in our sample had a phone.

¹⁷We only sampled ten adults per community, in order to mitigate the risk of spillover effects on non-treated individuals and avoid that the treatment shifted beliefs about aggregate take-up of deworming in the community. Only individuals in the control condition were eligible to receive SMS reminders, whilst all incentive conditions were eligible for the SMS social info treatment arm.

treatment and SMS control condition. The red horizontal bars display the additional effect of social info SMS messages and show they are very similar to the main sample treatment effects. The blue bars show the treatment effects when individuals received only the reminder message. If the Bracelet and Ink also worked as reminders or led to social learning, we would expect their effect to be significantly lower in the presence of our SMS messages. Whilst the social info arm tends to have slightly larger treatment effects, these differences all include 0 within their 95% confidence intervals.

5.2.2 Bracelets as Consumption Goods

An alternative explanation is that bracelets are more valued than calendars as a consumption item, potentially due to their fashion appeal. This perceived value might be higher in Far communities, where bracelets are rarer (scarcity value).

To estimate any difference in monetary valuation between the two items, we elicited individuals' willingness to pay (WTP) for calendars and bracelets in Control group communities during the endline survey. First, participants were asked to choose between a calendar or a bracelet. Second, participants were offered a random amount of cash, between US\$0 and 1, if they agreed to switch from the item they selected to the other item. We find that individuals value the calendar over the bracelet uniformly across distance conditions, as shown in Table [B12](#).

One caveat of the WTP survey being done in Control group communities is that it was implemented with only a small number of individuals per community (10-12 people) and therefore could not capture any social utility. To address this concern, we offered the same choice between a bracelet and calendar as a gift at endline to survey participants in bracelet and calendar communities. In these communities, individuals would have common knowledge about the share of individuals with a bracelet or calendar, and their gift choice would reflect the social utility of having the item. If bracelets are more valued as rare status items, our signaling effects could be confounded with a demand for scarce goods. Scarcity would suggest that in the Bracelet treatment arm, due to higher deworming take-up in close compared to far communities, individuals who did not deworm would have a higher WTP for bracelets in far communities. The same logic could apply to the calendar incentive. We find that individuals have homogeneous preferences for the bracelet and calendar across distance conditions, $p=0.39$ and $p=0.32$, respectively. This suggests that the difference in treatment effects between far and close communities cannot be attributed to differences in the consumption value of bracelets or to scarcity influencing higher WTPs across distance conditions.

5.2.3 Distance Measurement

Another concern may be how distance, and therefore deworming cost, is measured by the econometrician versus how communities perceive the distance cost of deworming. For instance, whilst our preferred specification uses the distance between a community’s centroid and the treatment location, if individuals have perfect knowledge of everyone’s location in a community, using the community centroid’s distance to the treatment location will overestimate the cost some face whilst underestimating the cost of households who happen to be located closer to the treatment location within the community. Therefore, in Appendix Tables B4 and B6 we present visibility and deworming take-up results robust to controlling for the distance measured from each household’s location to the treatment location.

Finally, we test the sensitivity of the reduced form results to the cost of distance’s functional form and allow distance to have a non-linear effect on deworming take-up in Appendix Tables B7, B8, and B9 which show results using saturated dummies for the assigned distance group, Close and Far, and results using distance and its square, instead of just the distance between a community’s centroid and the treatment location used in our main specification. We find that results are qualitatively similar, the Bracelet and Ink treatment effects are always greater than Calendar in the Far treatment group and the Any Signal to No Signal, Far -Close comparison is always significant at the 5% level.

5.3 Summary

The reduced form results demonstrate that the distance condition effectively generated exogenous variation in equilibrium deworming take-up, while the social signaling treatments increase the visibility of deworming decisions. Additionally, the positive double difference estimate, which compares the effect of the Bracelet treatment to that of the Calendar on deworming take-up across Close and Far conditions, provides suggestive evidence that the value of signaling increases as the equilibrium level of deworming take-up decreases in a community. This outcome aligns with the predictions of our model. Importantly, this positive double difference cannot be fully explained by alternative behavioral mechanisms. Factors such as salience, scarcity, or social learning alone cannot account for the observed increases in deworming take-up at both far and close distances, nor can they explain the commensurate increase in treatment effects when moving from close to far, observed only in conditions with a signaling incentive.

6 Structural Estimates

In this section, we use the model described in Section 3 to directly estimate the social multiplier and perform counterfactuals in Section 7. First, we verify that the average

treatment effects implied by the model replicate the reduced form results presented earlier. Second, we leverage our structural model to decompose treatment effects into an effect attributable to signals versus the effect of treatment driven by the private valuation of the incentives. Next, we estimate the social multiplier the social planner faces across each treatment arm, benchmarked against a scenario with no visibility and therefore a 1:1 pass-through of distance costs.

6.1 Set-up

The goal is to estimate the net social image return, $\Delta(w^*(z, d))$, which is determined in equilibrium by the equation:

$$w^*(z, d) = -(z \cdot \beta_z - d \cdot \delta) - \mu(z, d)\Delta(w^*(z, d)) \quad (5)$$

where $\Delta(x) = E[v|w > x] - E[v|w \leq x]$ is the net social image return from taking up deworming when the cutoff type is x , costs enter as $d \cdot \delta$, and $z \cdot \beta_z$ represents the incentive private benefit for treatment z . Since we assume the type, v , and idiosyncratic error, u , are normally distributed, with (normalized) variance 1 and σ_u respectively, and w is the sum of these terms we can rewrite the net social image return, $\Delta(w)$, analytically:¹⁸

$$\Delta(w) = \frac{1}{\Phi\left(\frac{w}{\sqrt{\sigma_w^2+1}}\right) \left[1 - \Phi\left(\frac{w}{\sqrt{\sigma_w^2+1}}\right)\right]} \times \frac{1}{\sigma_w} \frac{\exp\left(-\frac{1}{2} \frac{w^2}{\sigma_w^2+1}\right)}{\sqrt{2\pi}} \times \sqrt{\frac{\sigma_w^2}{\sigma_w^2+1}}.$$

Therefore, for each posterior draw we evaluate the likelihood using the probability an individual chooses to deworm, $\Phi_w(-w^*(z_i, d_i))$:

$$L(y; \Theta) = \prod_{i=1}^N \Phi_w(-w^*(z_i, d_i))^{y_i} [1 - \Phi_w(-w^*(z_i, d_i))]^{1-y_i}$$

where the parameters $\delta, \beta_z, \sigma_w$ solve the fixed point described in Equation 5.

We incorporate information from our WTP survey to improve precision when estimating β_z by restricting the private benefit parameter for bracelets in Equation 5 to be $\beta_{\text{bracelet}} = \beta_{\text{calendar}} + \gamma \mu^{\text{wtp}}$.¹⁹ We jointly estimate μ^{wtp} using the modified Probit

¹⁸The derivation using bounded v as in the original Bénabou and Tirole model can be found in the Appendix. It admits a similar closed form expression with additional Owen's T terms.

¹⁹The parameter γ translates the difference in monetary valuation to utility. Since the marginal utility of money isn't identified by the WTP experiment, γ is only estimated off variation in individuals' deworming take-up decisions in the Bracelet and Calendar arm. Therefore, we incorporate extremely conservative priors that suggest this utility value is small. Our conservativeness makes it harder for the model to estimate a larger signaling effect since making γ small increases the private benefit attributed to the Bracelet and therefore reduces the estimated signaling benefit.

likelihood:

$$P(g, \text{switch} \mid m, \mu^{\text{wtp}}, \sigma^{\text{wtp}}) = \begin{cases} P(v^{\text{wtp}} < -m) & \text{switch} = 0 \wedge g = 0 \\ P(v^{\text{wtp}} > m) & \text{switch} = 0 \wedge g = 1 \\ g \cdot (P(v^{\text{wtp}} < g \cdot m) - P(v^{\text{wtp}} < 0)) & \text{switch} = 1. \end{cases} \quad (6)$$

where g_i indicates an individual initially chose the calendar gift, $g_i = \mathbf{1}\{i \text{ chooses calendar} = 1\}$ and $m \in \{0, 10, \dots, 100\}$ denotes the random amount of cash, in Kenyan shillings, offered to switch items, $s \in \{0, 1\}$.²⁰

Next, we complement our take-up and willingness-to-pay surveys with data on beliefs about the observability of signals. In each arm, we conducted a survey to assess how reported knowledge of others' deworming status changes with incentives and distance. For each respondent, we randomly selected ten of their community members and ask them if they recognized them and if so, whether they knew their deworming status. We model the number of reported known statuses as a logistic binomial conditional on the number of recognized community members to estimate the probability an individual reports knowing a member's deworming status, $p^{\text{bel}}(z, d) = \text{logit}^{-1}(\eta^{\text{bel}}(z, d))$ and $\eta^{\text{bel}}(z, d) = z'(\beta^{\text{bel}} + \delta^{\text{bel}} \cdot d)$:

$$P(N_{\text{know status}} = x \mid d, z) = \binom{N_{\text{recognised}}}{N_{\text{know status}}} \cdot p^{\text{bel}, N_{\text{know}}} \cdot (1 - p^{\text{bel}})^{N_{\text{recognise}} - N_{\text{know}}}. \quad (7)$$

To incorporate information from all the sub-experiments we define $\mu(z, d) = \lambda_0 \cdot p^{\text{bel}}(z, d)$ and jointly estimate the fixed point, Equation 5, the WTP model described by Equation 6, and the beliefs likelihood given by Equation 7. Therefore, the parameters β^{bel} , δ^{bel} , β_{calendar} , β_{bracelet} must simultaneously rationalize the observed deworming take-up decisions, the first-order beliefs data, and the WTP survey data. Since we estimate the joint likelihood defined above in a Bayesian framework we place $N(0, 0.25)$ priors over $\beta_z, \delta, \beta^{\text{bel}}, \delta^{\text{bel}}$. These are weakly informative priors that centre effect estimates on zero but guide the sampler towards more plausible effect sizes, speeding up convergence.

6.1.1 Estimation

We estimate the Bayesian model in Stan ([Stan Development Team 2023](#)) using Hamiltonian Monte-Carlo. Each posterior draw calculates the fixed point solution using Stan's internal algebraic solver and samples from the posterior using Markov Chain Monte-Carlo. Throughout we use regularizing, weakly informative priors that centre effects on zero.²¹ A Bayesian model has some attractive advantages when estimating the likelihood above.

²⁰Results for our WTP model parameters can be found in Table B13.

²¹A more detailed discussion of our prior choices can be found in Appendix E.

Firstly, propagating uncertainty across various sub-models and hyperparameters is easier since Bayesian inference requires specifying a full likelihood and jointly estimating all parameters. Next, the Bayesian model allows us to directly estimate the policymaker’s posterior allocation of points of treatment when we turn to optimal policy in Section 7. Instead of solving the allocation problem for a given point estimate we solve for the allocation problem across each posterior draw and calculate the policymaker’s posterior over optimal allocations – fully reflecting the estimation uncertainty the policymaker faces due to sampling variation.

Finally, we use the Bayesian model to directly interrogate the assumptions underlying our structural model. To ensure our assumptions, both concerning the likelihood and our priors, are not unduly influencing reported posterior estimates, we present additional results throughout the paper using the prior predictive distribution - the implied treatment effects if we took our prior as given, before conditioning on the data. This is particularly attractive in contexts with black-box structural models since our priors over model primitives, such as β_z, σ_w , have hard-to-predict implications for deeper structural objects, such as the net social image return, $\Delta(w^*)$, or the shape of the social multiplier. By drawing from the prior over the primitives and calculating the corresponding social multiplier, before conditioning on the data, we can inspect what our choice of likelihood and prior assumptions are imposing on the social multiplier. Comparing the prior predictive and posterior distribution shows the effect of conditioning on the data in the experiment. In our case, the prior predictive distribution is always centred on a null effect and often incredibly wide.

6.2 Identification

We use two sources of exogenous variation to identify the parameters of the model. The distance condition randomly varies the cost communities must pay to get dewormed, measured in terms of walking distance, which induces variation in the equilibrium level of deworming take-up in a community and therefore exogenous variation in the cut-off type, w^* . Our visibility treatment arms create exogenous variation in visibility, μ , by randomly varying the visibility of the prosocial action. Jointly inducing variation in both visibility, μ , and the cut-off type, w^* , allows us to estimate $\mu\Delta(w^*)$ alongside a Gaussian functional form assumption over the type distribution.

The additional structure imposed by [Bénabou and Tirole \(2011\)](#) lets us estimate directly the interaction between social image returns and incentives. For instance, the simple reduced form double-difference comparison between Bracelet-Calendar in Close versus Far conflates changes in the cut-off type w^* with changes in visibility and private benefits. This will be important when we estimate counterfactuals since policies manipulating visibility and private incentives will generate endogenous changes in the cutoff type

alongside their direct effects. Our estimates are structural in the sense of [Hurwicz \(1966\)](#). For instance, a reduced form model can estimate a signaling value, $\hat{s}(d)$, as a function of distance using the calendar as a control for bracelet. However, $\hat{s}(d)$ would have no external validity – it would only accurately estimate effects in contexts with identical levels of equilibrium deworming take-up and private benefits.

6.3 Structural Results

6.3.1 Average Treatment Effects

Appendix Tables [Table B14](#) and [B15](#) show the average treatment effects from the structural model are congruent with our reduced form results, presented previously in [Tables 1](#) and [2](#). We find that distance has a negative effect of 9.2 percentage points on knowledge about others’ deworming status in the control group (reduced form estimate: 12.4 percentage points). Bracelets increase visibility by 14.8 percentage points in the Far communities (reduced form estimate: 15.9 percentage points). In terms of effects on take-up, the structural model estimates display a similar pattern to those shown previously, where distance leads to a large fall in deworming take-up in the Control arm (-15.0 versus -17 percentage points in the reduced form analysis) and treatment effects in the signaling arms are larger in Far than Close. Again, the Bracelet - Calendar, Far - Close double-difference is positive and 95% credibility intervals do not include 0 (3.1 percentage points, CI: [1.4, 5.4]). The Bracelet treatment effect on take-up pooled across distance conditions is 7.3 percentage points (reduced form estimate: 8.4 percentage points).

In [Table B16](#), we decompose treatment effects into a private benefit, β_z , and signaling effect, $\mu_z\Delta(w^*)$. As expected, Bracelet and Ink have the largest signaling treatment effects, increasing deworming take-up by 2.9 (CI: [1.2, 4.9]) and 1.8 (CI: [0.4, 3.6]) percentage points respectively, pooling across the distance condition. Again, we observe a greater effect in Far than Close for both signals, and signaling benefits are larger than private benefits in the Far arm for both signals. Finally, we estimate a large negative private utility for the Ink treatment which suggests individuals resented inking their thumb – perhaps partly due to the connotations associated with using ink to keep track of voting in elections in Kenya.^{22,23}

²²The negative private effect is corroborated by our endline follow-up checks, [Table B11](#), which shows that whilst 81% of surveyed individuals still had their bracelet, only 14.4% of individuals still had ink on their thumb when surveyed.

²³The negative reaction to ink was not expected during the experiment design, however it is particularly useful as a large negative private effect, combined with the distance cost, shifts the cutoff type even higher - i.e. individuals must truly have a very high type, v , if they choose to deworm in Far communities with the ink signal.

6.3.2 Social Multiplier Effects

One of our primary estimands is how the negative effect on take-up caused by an increase in the cost of deworming could be mitigated or amplified because of the social multiplier. The marginal effect of distance is:

$$\frac{\partial E[Y(z, d)]}{\partial d} = -f_w(w^*(z, d)) \cdot \frac{\frac{\partial b(z, d)}{\partial d} - \frac{\partial \mu(z, d)}{\partial d} \Delta(w^*(z, d))}{1 + \mu(z, d) \Delta'(w^*(z, d))}.$$

In Figure 2 we estimate the renormalised social multiplier produced by each incentive arm:²⁴

$$\tilde{S}M(z, d) = \frac{1}{\delta} \cdot \frac{-\delta + \frac{\partial \mu(z, d)}{\partial d} \Delta[w^*]}{1 + \mu(z, d) \Delta'[w^*]} \quad (8)$$

The dashed black line corresponds to the effect on deworming take-up in the absence of visibility, $\mu(z, d) = 0, \mu'(z, d) = 0$, in this case the multiplier is just 1 and so there is no additional pass-through to the elasticity of deworming take-up with respect to changes in cost. The grey dashed line shows the median estimate from the prior predictive distribution, the implied estimate from our Bayesian structural model if we draw from our prior without conditioning on the data. This is centred on 1, comparing the posterior with prior predictive distribution shows the effect of conditioning on data in our model – social multiplier estimates are primarily driven by the data, not any specific functional form or prior choice tied to our model.

²⁴We divide the social multiplier through by the distance cost parameter, δ , so that estimates can be interpreted relative to 1.

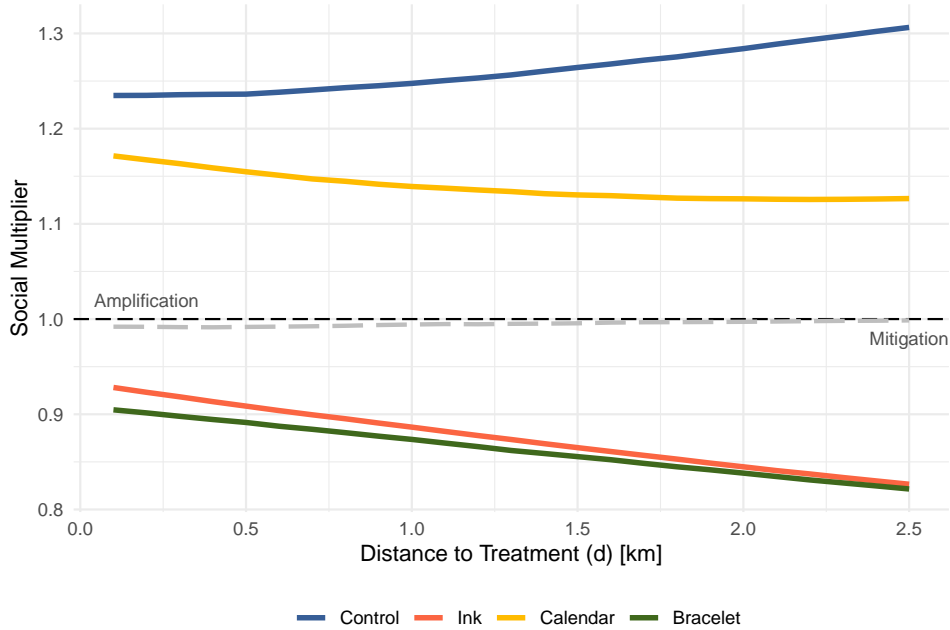


Figure 2: Social Multiplier

Notes: This plot shows the social multiplier estimated using the structural model. The plot shows how sensitive take-up is to changes in cost - as distance increases individuals in the bracelet and ink condition become less and less sensitive to the increased cost due to greater associated social image returns. On the other hand, individuals become more and more sensitive to the increased cost in the control and calendar conditions. At 2.5km individuals in the bracelet condition reduce their take-up 82% as much as individuals without any visibility. The dashed black line corresponds to the expected effect if there is no visibility - $\mu = 0$. The larger, dashed grey line shows the prior predictive median i.e. the prior by default assumes there is no social multiplier or visibility. Line: median.

The area below the dashed black line produces mitigation effects, $\tilde{S}M(z, d) < 1$, and therefore for a given increase in costs, say 10%, there is a relatively smaller pass-through to $\partial y / \partial d$. At 0.75km the ink social multiplier is 0.9 – for a 10% increase in costs, deworming takeup only falls by 9% compared to the no visibility case.²⁵ The bracelet social multiplier is similar to that of ink – at 0km it is equal to 0.925 whilst at 2.5km it falls to 0.82. This directly matches predictions from [Bénabou and Tirole \(2011\)](#) theoretical model – as distance costs increase the social image returns grow ever larger as those taking the action are perceived to be increasingly prosocial.

The Control and Calendar arm, on the other hand, display amplification, $\tilde{S}M(z, d) > 1$. Under the original model this should be impossible in our setting, since distance always enters individuals’ utility function negatively and deworming isn’t a “Respectable Act” so social image returns must increase as distance rises. However, our model endogenizes changes in visibility across distance and it is precisely this reduction in visibility which

²⁵Since the Probit likelihood doesn’t have a constant marginal effect, $\bar{y}' = f_w(w^*)\delta \cdot \tilde{S}M(z, d)$, so a multiplier of 0.9 can’t be directly interpreted as only a 9% fall in deworming takeup when costs increase by 10%.

offsets any gains from social image returns.²⁶ This means at 0km from the point of treatment an increase in costs by one unit is considered 1.2 times more costly by individuals - whilst they gain social image returns from taking the action, the reduction in visibility outweighs this increase and overall signaling utility falls.²⁷

6.3.3 Robustness

Whilst our main specification uses the community centroid’s distance to the treatment location as a common, observable cost it is plausible that communities and individuals form expectations using different information sets. Therefore, in Online Appendix F we explore robustness to different information sets and differences in beliefs formed by over-dispersed clusters through three different models: The first uses the community centroid’s distance to solve for the cut-off type and net social image returns but a household’s distance to the treatment location enters into an individual’s utility function when deciding to take the action or not. This leads to a similar expression for the probability of deworming, $\Phi_w(-w^*(z, \bar{d}) + \delta(\bar{d} - d))$, as our main specification, $\Phi_w(-w^*)$, except an additional term nets off the difference in costs between household, d , and centroid distance, \bar{d} .²⁸

Next, we estimate a full information model where every household knows the distance between a household and the treatment location, and therefore private cost, of every other household. Algebraically, this model is identical to the main specification but the fixed point is solved for all 9,805 individuals in the sample. Finally, we re-estimate the main specification whilst removing any communities that are over-dispersed - defined as communities with a mean squared distance of greater than 0.5km from the cluster centroid - which could generate a wedge between the social image returns households’ earn using the community centroid versus the private cost they face at the household level.

Online Appendix Tables F1, F2, and F3 show results from these adjusted models. Varying the information set leads to very similar results for Bracelet, Calendar, and the Control mean whilst the Ink results are mixed. The model with cluster level social image returns but individual distance costs show a negative Ink treatment effect, even at Far, but again finds a more positive effect at Far than Close. The full information model’s Ink effect is also negative but now flat across Far and Close. Finally, the model removing over-dispersed communities displays similar treatment effects across all conditions as our

²⁶Appendix Figure A11 decomposes the social multiplier into an effect caused by changes in visibility and an effect caused by changes in social image returns. As expected, the social image return component is uniformly positive.

²⁷Comparing across treatment arms is difficult in Figure 2 since for a given distance, moving from one curve to another curve induces a change in private benefit, visibility, *and* a change in the cutoff type, w^* , since this is an endogenous function of private and signaling benefits in equilibrium. Therefore, in Figure F5 we fix w^* at the control level for each distance point and show the derivative of deworming takeup with respect to distance directly $\frac{\partial y(z,d)}{\partial d}$.

²⁸For more details of this derivation, see Section F.1.

main specification. Online Appendix G discusses sensitivity to distributional assumptions over w and provides some simulations using alternative densities.

7 Optimal Incentives with Social Image Concerns

In this section we use results from our structural model to estimate the optimal spatial allocation of treatment locations, or Point of Treatments (PoTs henceforth) for policymakers across various counterfactuals. Next, we focus on the optimal distance a social planner must choose when placing PoTs to maximize welfare in the presence of norms using a Pigovian subsidy, or Ramsey subsidy in the presence of deadweight costs.

7.1 Policymaker’s Allocation of Deworming Sites

We formulate a problem where the policymaker’s goal is to minimize the number of funded PoTs subject to achieving an overall deworming level in an area. We focus on minimizing the number of funded PoTs to avoid specifying the PoT production function a policymaker or planner faces, since we have little evidence on the PoT cost across regions.²⁹

Suppose there are n communities, indexed by i , and m PoTs which we index by j . The policymaker’s goal is to minimize the number of PoTs required, γ , while achieving the expected deworming level, \bar{T}^C , defined as $E_{\Theta} \left[\sum_{i=1}^n T(z = \text{control}, d_{ij}; \theta) \cdot x_{ij}^{\text{experiment}} \right]$. This represents the deworming take-up level that would have been attained if every community in the experiment, assigned to their randomized PoT allocation, $x_{ij}^{\text{experiment}}$, had instead been in the control condition, $z = \text{control}$. We formulate this problem as an integer program:

²⁹That is, we have little sense of how many PoTs a policymaker can afford to produce in a given region and instead reason that for a given target, most policymakers would wish to be parsimonious with their resources and use spare points of treatment elsewhere or budget resources to solve other issues.

$$\begin{aligned}
\gamma(\theta) &= \min_{y_j, x_{ij}} \sum_{j=1}^m y_j & (9) \\
s.t. \quad \sum_{i=1}^n T(z, d_{ij}; \theta) \cdot x_{ij} &\geq \underbrace{E_{\Theta} \left[\sum_{i=1}^n T(\text{control}, d_{ij}; \theta) \cdot x_{ij}^{\text{experiment}} \right]}_{\bar{\gamma}^c} \\
\sum_{j=1}^m x_{ij} &= 1, \forall i \\
x_{ij} &\leq y_j, \forall i, j \\
x_{ij} d_{ij} &\leq D
\end{aligned}$$

where x_{ij} is an indicator corresponding to community i using PoT j , d_{ij} is the distance between community i and PoT j , and y_j is an indicator equal to 1 if PoT j is funded (i.e., available for use by communities) by the policymaker. The remaining constraints ensure every community is assigned to a funded PoT and no assigned community-PoT pair can be more than D meters apart.

$T(d_{ij}; \theta)$ is the policy maker's posterior estimate of demand for deworming when community i is assigned to PoT j . Since the posterior describes a distribution over $T(d_{ij}; \cdot)$ we solve the policymaker's problem for 200 draws from the model estimated in Section 6 and aggregate over these solutions to produce the policymaker's posterior belief about the number of PoTs required, $\bar{\gamma} = E_{\Theta}[\gamma(\theta)]$, shown in Table 3. Figure A12 shows the number of assigned PoTs across counterfactuals evaluated at the posterior median, $\gamma(\theta_{\text{median}})$. Aggregating across posterior draws, instead of using a plugin estimator such as θ_{median} ensures the policymaker's estimates of γ fully reflect estimation uncertainty.

Our preferred specification uses a maximum distance constraint, $D = 3.5\text{km}$. We chose 3.5km as a compromise between limiting extrapolation and constraints imposed by our experimental design - by construction there are almost no treatment locations within 2.5km of multiple communities in our data. Table C2 shows our results are robust extrapolating out to 10km, primarily because the policymaker rarely wishes to set communities and PoTs more than 2km apart as the model places virtually no posterior density on positive take-up past 5km. Additionally, we provide results in Appendix Table C3 that decompose the effect of our modified social multiplier, which accounts for changes in visibility across distance, with the original social multiplier described by Bénabou and Tirole (2006), fixing visibility, μ , and social image returns, $\Delta(w^*)$, one at a time across different distances.

7.1.1 Counterfactual Simulations

Our structural model decomposes $T(d_{ij}; \theta)$, the demand for deworming from pairing community i with PoT j , into a private utility component and social image return from signaling deworming status. Therefore, we fix private utility at the control level and explore the effect of counterfactually varying visibility, μ_z , on the number of required PoTs.

$$T(z, d_{ij}; \theta) = \underbrace{B(z, d_{ij})}_{\text{private benefit}} + \underbrace{\mu(z, d_{ij})\Delta [w^*(z, d_{i,j})]}_{\text{social image return}}$$

To produce a common benchmark we first show the allocation of PoTs and corresponding level of deworming using the randomized allocation used in the experiment, evaluated at the posterior median, in the first panel of Figure A12 and the policymaker’s joint posterior in Table 3 Panel A. In the figure, blue triangles denote unused PoTs and red triangles funded PoTs, the black dots show where our communities are and a black line links communities to their assigned PoT. Under the experimental allocation, if we had assigned every community to the control arm, average deworming takeup would have been 32.92% and communities would have to walk 1.2km on average.

The second panel of Figure A12 shows the effect of solving Equation 9. Essentially, the policymaker assigns every community to their closest possible Point of Treatment instead of randomly assigning community-PoT pairs within the Far and Close conditions. Where possible, the policymaker does not fund a PoT and instead pools communities around a common, central treatment point. This increases the average walking distance to 1.27km at the posterior median and reduces the number of required PoTs to 107.

Varying Visibility

$$T(z, d_{ij}; \theta) = \underbrace{B(\text{control}, d_{ij})}_{\text{private benefit}} + \underbrace{\mu(\text{bracelet}, d_{ij})\Delta [w^*(z_c, z_b, d_{i,j})]}_{\text{social image return}}$$

The third panel of Figure A12 shows the effect of counterfactually varying visibility from the Control incentive, μ_{control} , to the Bracelet incentive, μ_{bracelet} , whilst holding private benefit fixed at the Control level. The policymaker accounts for the updating of agents beliefs over net social image returns, $\Delta[w^*]$, as a change in visibility leads to an endogenous shift in the cutoff type, w^* . Now the policymaker can leverage the mitigating effects of the social multiplier by spacing Points of Treatment even further out – only 90 PoTs are required to serve the population and average walking distance rises to 1.66km.

Table 3: Posterior Estimates of Number of Points of Treatment Required

Private benefit	Visibility	Assigned PoTs	Mean take-up	Mean distance (km)
Panel A: Random allocation				
Control	Control	144	0.33 (0.31, 0.346)	1.2
Panel B: Policymaker allocation				
Control	Control	107 (100, 114)	0.33 (0.329, 0.331)	1.26 (1.11, 1.411)
Control	Signal value fixed at bracelet 0.5km	96 (86, 105)	0.33 (0.329, 0.331)	1.52 (1.297, 1.758)
Control	Bracelet	90 (79, 102)	0.33 (0.329, 0.33)	1.68 (1.364, 1.957)
Control	No Visibility	144 (144, 144)	0.174 (0.101, 0.259)	0.58 (0.58, 0.58)

Notes: Point estimates show posterior medians, parentheses show 95% posterior credibility intervals. Credibility intervals are omitted for the experimental allocation panel for ‘Assigned PoTs’ and ‘Mean distance (km)’ since these are fixed across posterior draws. Posterior medians and credibility intervals are estimated by solving an integer linear program across 200 random posterior samples drawn from the relevant structural model. Estimates shown use a maximum distance constraint of 3.5km. That is, the decision maker cannot assign any point of treatment-community pair if communities must walk more than 3.5km.

Unaware of the Social Multiplier

$$T(z, d_{ij}; \theta) = \underbrace{B(\text{control}, d_{ij})}_{\text{private benefit}} + \underbrace{\mu(\text{bracelet}, d_{ij} = 0.5\text{km})\Delta [w^*(z_c, z_b, d_{i,j} = 0.5\text{km})]}_{\text{social image return}}$$

Next, we fix private benefit at the control level and calculate the value of signals, $\mu\Delta[w^*]$, fixed at 0.5km to simulate a policymaker that is aware of the value of social signaling but is unaware of the interaction between incentives and norms. That is, they perceive the static increase in demand for deworming created by introducing visibility but are unaware that the social multiplier changes the shape of the demand curve, shown by the bracelet (red) and control (yellow) demand curves in Appendix Figure A13. In our setting the bracelet demand curve becomes flatter at further distances due to mitigation, the social image returns from actions perceived as “heroic” grow larger as costs increase, and the control demand curve becomes steeper at further distances due to amplification, the decrease in visibility outweighs increases in social image returns. The second row of Table 3 Panel B shows that under this scenario, the policymaker underestimates the value of signaling at greater distances and expects to use 96 points of treatment when introducing bracelets. In reality the policymaker can reduce the number of PoTs required by a further 6% to 90.

Unaware of Social Image Returns

$$T(z, d_{ij}; \theta) = \underbrace{B(\text{control}, d_{ij})}_{\text{private benefit}}$$

Lastly, the final row of Table 3 Panel B shows the solution to the policymaker’s opti-

misation problem if they are completely unaware of social signals. For instance, if the policymaker had failed to create common knowledge of signals through a mass information campaign or had ran a pilot campaign without experimentation at scale to produce shifts in the agents equilibrium beliefs about actions. Under this scenario, the policymaker believes achieving the target deworming level is completely infeasible: even with all 144 points of treatment active they estimate deworming demand at only 17.4% of the population, despite placing each community as close as possible to the nearest point of treatment, communities only walk 0.58km on average.

Figure 3 highlights how the policymaker must be conscious of amplification and mitigation effects when determining the optimal layout of points of treatment. Under the experimental arm the density of walking distances is bi-modal – since communities are assigned to a Close or Far condition. However, once she solves Equation 9 under the Control visibility scenario she places almost everyone as close as possible to each PoT because she knows she is in an amplification situation. Since the fall in visibility in the Control scenario outweighs any increase in social image returns she faces a "double whammy" when trying to induce individuals to walk further – not only do they dislike distance, they also receive less signaling value as μ falls precipitously with distance. On the flipside, the Bracelet scenario demonstrates the large rewards a policymaker can exploit from the social multiplier. The policymaker can space out points of treatment even further, and as she does so she faces an increasingly inelastic demand curve. From the policymaker’s perspective, visibility introduces both a shift upwards of the demand curve and a flattening at higher distances.

7.2 Optimal Subsidy

Next, we follow [Bénabou and Tirole \(2011\)](#) by calculating the optimal incentive to maximize social welfare across various counterfactuals. In this context this means calculating the optimal distance to a point of treatment under different levels of visibility and the private value of the action. Given an individual’s utility function:³⁰

$$U = (w + b - \delta d)a + e\bar{a} + \mu(d)E(v|a). \quad (10)$$

The social planner maximizes social welfare, Equation 11, which is the sum of U in equilibrium, Equation 10, plus an additional shadow cost of public funds term, λ :

$$W(d) = \bar{U} + (1 - \lambda)\delta d\bar{a} \quad (11)$$

³⁰Our main specification sets the value of externalities, e , from overall deworming, \bar{a} , to 10% of the private value of deworming. In Appendix C we show how our results change as a function of the externality value.

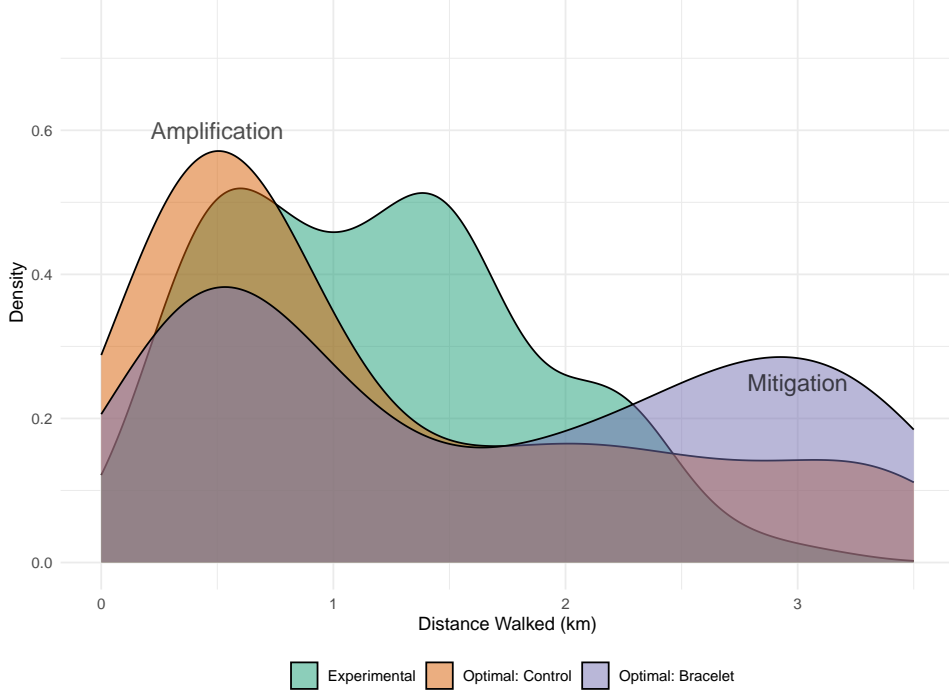


Figure 3: Density of Distance Walked by Communities

To induce a total contribution to the deworming public good \bar{a} by providing a Point of Treatment at distance d they must incur the shadow cost of funds $\lambda \geq 0$.³¹ This λ could be the deadweight loss of taxes, or enforcement costs associated with ensuring Points of Treatment are run correctly. Our main specification solves the Ramsey problem using $\lambda = 0.1$, whilst Appendix C varies λ and solves the corresponding Pigovian problem. Therefore, the planner solves

$$\begin{aligned} d^* &= \arg \max_d W(d) \\ &= \arg \max_d \int_{w^*(d)}^{\infty} (w + b + e - \lambda \delta d) f(w) dw + \mu \bar{w} \end{aligned}$$

with the solution given by the following first order condition:

$$-\frac{\delta - \mu' \Delta(w^*(d))}{1 + \mu \Delta'(w^*(d))} (w^*(d) + b + e - \lambda \delta d) - \lambda \delta \frac{[1 - F(w^*(d))]}{f(w^*(d))} = 0.$$

When choosing the optimal distance to a Point of Treatment the planner faces a key trade-off created by the interaction of visibility with the private benefit's, b , effect on social image concerns. When b is very low, most individuals do not contribute to the public good and therefore the few individuals that do contribute reap significant honor – the planner can place a PoT very far away. This dynamic appears at the far left corner of

³¹Since it is costlier to provide more Points of Treatment at closer distances we flip the sign of λ so that this can be interpreted as the additional cost a planner faces to move a PoT closer.

Figure A14, as private benefit falls, the planner can push the PoT even further away. On the other hand, when private benefits are very high, in equilibrium only a few bad apples fail to participate in deworming and incur a large amount of social stigma. Again, the planner optimally places the Point of Treatment far away, shown in the far right corner of Figure A14. When private benefit, b , is small in absolute value the planner can less rely on social image – performing or not performing the action incurs little social image return. In this case, the planner has to compensate individuals with a closer Point of Treatment, shown in the middle of Figure A14. This dynamic increases as μ increases, the red curve in Figure A14 shows the optimal PoT placement when visibility is set to the control level whilst the blue curve, which represents the effect when visibility is set to the bracelet level, is shifted higher and exhibits greater curvature at greater values of b in magnitude.

7.2.1 Private Benefit and Visibility

The importance of considering the interaction between incentives and social image concerns is shown in Figure 4, where we plot the optimal Point of Treatment distance placement while varying visibility and the private incentive. When the private benefit is small, or equivalently, when there is no shift in norms induced by the planner–deworming is a ‘modal’ act–increasing visibility has little effect on how far a planner can move a PoT, since there is little gain from revealing an individual’s type: there is not a large amount of honor or stigma at play at these equilibria. However, the returns to manipulating visibility are much higher in the tails of the private benefit support – increasing visibility when the additional private benefit is less than -2 or greater than 2 allows the planner to move a PoT up to $5km$ away because revealing an individual’s type creates large honor or stigma payoffs respectively. Figure 4 emphasises how important it is a planner is aware of the interaction of economic incentives and visibility. For instance, conditioning on Visibility = 75% (75% of individuals know someone’s deworming status) and taking a horizontal line across the contour plot shows that if the planner starts from a very negative private benefit, -2 and increases incentives, she would have to move PoTs closer to maximize social welfare, until she reaches a high private incentive of $+2$ again and can move PoTs back out to $3km$.

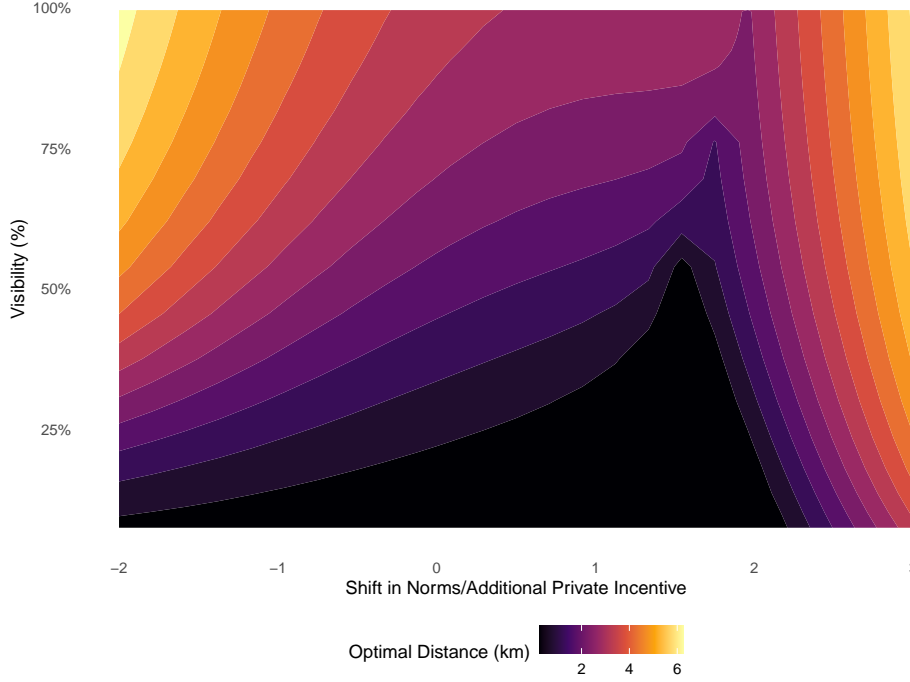


Figure 4: Optimal Point of Treatment Distance

Notes: This plot shows the optimal distance to place a Point of Treatment from a community to maximize welfare, given by Equation 11. The y-axis varies visibility as the proportion of individuals that know someone’s deworming status, where 50% corresponds to half of individuals knowing someone’s status on average. The x-axis denotes a shift in norms – shifting the distribution of w^* to the right by x – which is equivalent to an additional private incentive of x units, over the estimated bracelet private benefit. The coloured contours denote the optimal distance a planner should place a point of treatment. Equation 11 is solved using parameter values at the posterior median in the bracelet condition where $\lambda = 0.1, e = \beta_{\text{bracelet}} \times 0.1$.

8 Conclusion

Leveraging social image concerns is receiving increasing attention from policymakers to increase the provision of public goods and encourage the take-up of socially desirable behaviors. This paper demonstrates that these social image incentives do not operate in isolation, and decision-makers must consider the interactions between social image and economic incentives when designing policies. Our study yields three important insights.

First, we empirically demonstrate these interactions within a large-scale community deworming program. We reveal that the interplay between economic incentives and social image motives creates a social multiplier, affecting the marginal impact of benefits or costs on deworming take-up. By varying the visibility of deworming actions and travel distance to deworming locations, we find signals significantly impact take-up in communities with lower baseline take-up levels (far communities) more than in those with higher baseline levels (close communities). A higher cost for taking action allows individuals with stronger intrinsic motivation to credibly signal this motivation, thereby

obtaining greater social image returns. We build a structural model to directly estimate changes in the marginal type and the corresponding social multiplier effects.

Second, our findings indicate that individuals become more attentive to deworming decisions when social image incentives are introduced. By measuring adults' beliefs about others' deworming actions in communities with varying take-up rates, we observe that visibility and social image returns interact differently across control and material reward (calendar) communities, with visibility effects predominating in the latter. In contrast, in social signaling (bracelet and ink) communities, social image returns outweigh the negative impact of increased travel costs on take-up. This allows a social planner to exploit the dampening effects of social image returns and increase the spacing between deworming treatment points beyond what a static model suggests.

Third, our analysis documents the importance of these interactions for the optimal allocation of treatment points. We estimate the optimal distribution of deworming treatment locations for policymakers aiming to minimize their number while achieving a target take-up rate. Our results indicate that overlooking the interplay between social image and economic incentives can lead to misestimating the demand for deworming, either by providing more Points of Treatment than necessary or by placing them too close to households. This misestimation arises from failing to account for how equilibrium beliefs shift with changes in distance and costs, leading to a 7% over-provision of treatment points in our context and potentially placing treatment points closer than optimal for maximizing social welfare.

In summary, our paper illustrates that while signals effectively increase deworming rates, their impact must not be viewed in isolation, as interactions with other policy measures can amplify or mitigate their effects. Such interactions are not only significant but can have first-order implications for optimal policy design, especially in public health contexts within budget-constrained environments in low-income countries where leveraging social norms is often a strategy to enhance program efficacy.

References

- Roland Bénabou and Jean Tirole. Laws and Norms, November 2011. URL <https://www.nber.org/papers/w17579>.
- Leonardo Bursztyn and Robert Jensen. Social Image and Economic Behavior in the Field: Identifying, Understanding, and Shaping Social Pressure. *Annual Review of Economics*, 9(1):131–153, 2017. doi: 10.1146/annurev-economics-063016-103625. URL <https://doi.org/10.1146/annurev-economics-063016-103625>. _eprint: <https://doi.org/10.1146/annurev-economics-063016-103625>.
- Leonardo Bursztyn, Bruno Ferman, Stefano Fiorin, Martin Kanz, and Gautam Rao. Status Goods: Experimental Evidence from Platinum Credit Cards*. *The Quarterly Journal of Economics*, 133(3):1561–1595, August 2018. ISSN 0033-5533. doi: 10.1093/qje/qjx048. URL <https://doi.org/10.1093/qje/qjx048>.
- Arun G. Chandrasekhar, Cynthia Kinnan, and Horacio Larreguy. Social Networks as Contract Enforcement: Evidence from a Lab Experiment in the Field. *American Economic Journal: Applied Economics*, 10(4):43–78, October 2018. ISSN 1945-7782. doi: 10.1257/app.20150057. URL <https://www.aeaweb.org/articles?id=10.1257/app.20150057>.
- Stefano Dellavigna, John A. List, Ulrike Malmendier, and Gautam Rao. Voting to Tell Others. *The Review of Economic Studies*, 84(1):143–181, January 2017. ISSN 0034-6527. doi: 10.1093/restud/rdw056. URL <https://doi.org/10.1093/restud/rdw056>.
- Anne Karing. Social Signaling and Childhood Immunization: A Field Experiment in Sierra Leone*. *The Quarterly Journal of Economics*, page qjae025, 08 2024. ISSN 0033-5533. doi: 10.1093/qje/qjae025. URL <https://doi.org/10.1093/qje/qjae025>.
- Emily Breza and Arun G. Chandrasekhar. Social networks, reputation, and commitment: evidence from a savings monitors experiment. 87(1), 2019. ISSN 175-216.
- Roland Bénabou and Jean Tirole. Incentives and Prosocial Behavior. *American Economic Review*, 96(5):1652–1678, December 2006. ISSN 0002-8282. doi: 10.1257/aer.96.5.1652. URL <https://www.aeaweb.org/articles?id=10.1257/aer.96.5.1652>.
- Dean Karlan and Margaret A. McConnell. Hey look at me: The effect of giving circles on giving. *Journal of Economic Behavior & Organization*, 106:402–412, October 2014. ISSN 0167-2681. doi: 10.1016/j.jebo.2014.06.013. URL <https://www.sciencedirect.com/science/article/pii/S0167268114002017>.

- Judd B. Kessler. Announcements of Support and Public Good Provision. *American Economic Review*, 107(12):3760–3787, December 2017. ISSN 0002-8282. doi: 10.1257/aer.20130711. URL <https://www.aeaweb.org/articles?id=10.1257/aer.20130711>.
- Ricardo Perez-Truglia and Guillermo Cruces. Partisan Interactions: Evidence from a Field Experiment in the United States. *Journal of Political Economy*, 125(4):1208–1243, August 2017. ISSN 0022-3808. doi: 10.1086/692711. URL <https://www.journals.uchicago.edu/doi/full/10.1086/692711>. Publisher: The University of Chicago Press.
- Luigi Butera, Robert Metcalfe, William Morrison, and Dmitry Taubinsky. Measuring the welfare effects of shame and pride. *American Economic Review*, 112(1):122–68, January 2022. doi: 10.1257/aer.20190433. URL <https://www.aeaweb.org/articles?id=10.1257/aer.20190433>.
- Leonid Hurwicz. On the Structural Form of Interdependent Systems. In Ernest Nagel, Patrick Suppes, and Alfred Tarski, editors, *Studies in Logic and the Foundations of Mathematics*, volume 44 of *Logic, Methodology and Philosophy of Science*, pages 232–239. Elsevier, January 1966. doi: 10.1016/S0049-237X(09)70590-7. URL <https://www.sciencedirect.com/science/article/pii/S0049237X09705907>.
- James J. Heckman and Edward Vytlacil. Policy-Relevant Treatment Effects. *The American Economic Review*, 91(2):107–111, 2001. ISSN 0002-8282. URL <https://www.jstor.org/stable/2677742>. Publisher: American Economic Association.
- Stan Development Team. Stan Reference Manual, 2023.

A Appendix Figures

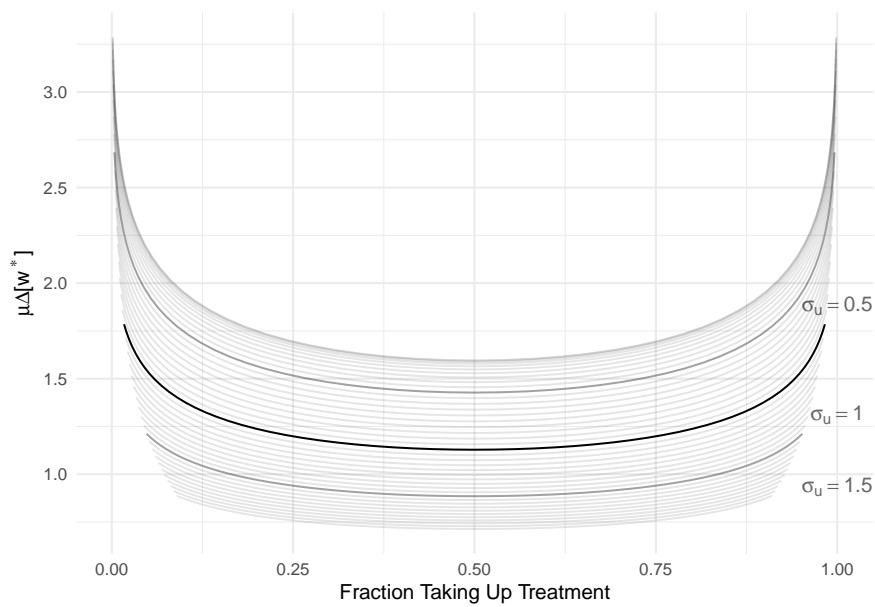


Figure A1: Equilibrium Social Image Returns Against Take-up

Notes: This figure shows how the expected social image return, $\mu(c)\Delta[w^*]$, varies as take-up, which is a function of the cutoff type, w^* , changes. As σ_u increases, the social image returns fall as it becomes harder to infer someone's type based on actions. To generate this figure we fix $\mu(c) = 1$ and calculate $\mu(c)\Delta[w^*]$ across a grid of w^* and σ_u values.

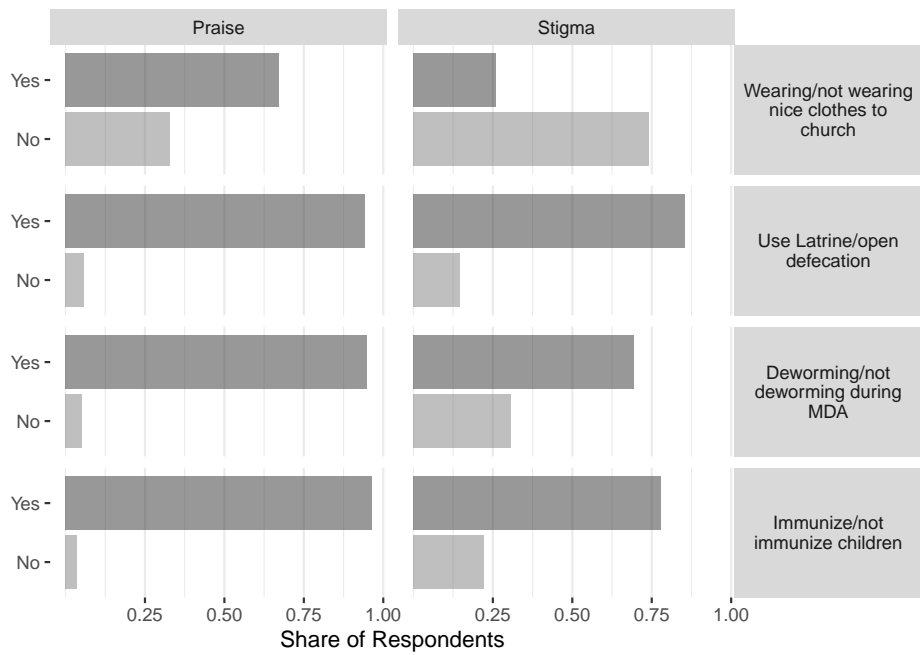


Figure A2: Social Image Concerns

Notes: This figure shows respondents' self-reported judgements of community members who engage or does not engage in a certain behavior. Respondents were asked at baseline whether they would “look down on someone” or “praise” a person if they e.g. used a latrine, or openly defecated. The sample includes all baseline respondents (N = 1,770). Each respondent was asked the immunization and deworming scenario, while people were randomly assigned to either the church or defecation scenario. There are no significant differences across experimental groups as shown in Table B19.

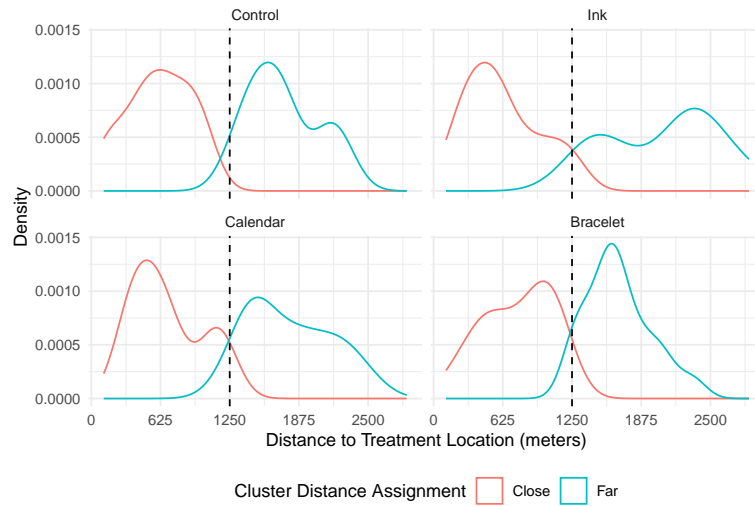


Figure A3: Random distance to treatment location

Notes: This plot shows the distribution of distance to the assigned point of treatment across conditions. communities in the Close condition walk shorter distances to the point of treatment on average compared to the Far condition. The average difference in walking distance between Close and Far treatment arms is 1.02 km.

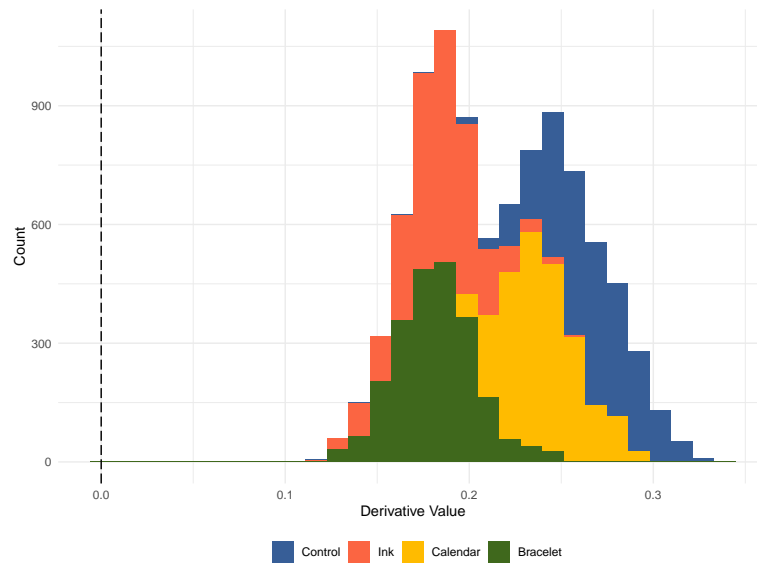


Figure A4: Posterior Draws of $\frac{\delta - \mu'(d)\Delta(w^*(d))}{1 + \mu(d)\Delta(w^*(d))}$ over Distances Used in Paper

Notes: This plot shows that $\frac{\delta - \mu'(d)\Delta(w^*(d))}{1 + \mu(d)\Delta(w^*(d))} > 0$ for the range of distances and parameter values considered in the paper and therefore rules out multiple equilibria and self-sustaining norms, analogously to [Bénabou and Tirole \(2011\)](#)'s condition: $1 + \mu'\Delta(v^*) > 0$ on page 6.



Figure A5: Bracelets

Notes: This image displays the bracelets that Community Health Volunteers give out at points of treatment. The bracelet states in Swahili, “Treat worms improve the health of your community”.



Figure A6: Calendar

Notes: This image displays the calendars that Community Health Volunteers give out at points of treatment. The calendar made no reference to deworming to minimize its social signaling value.

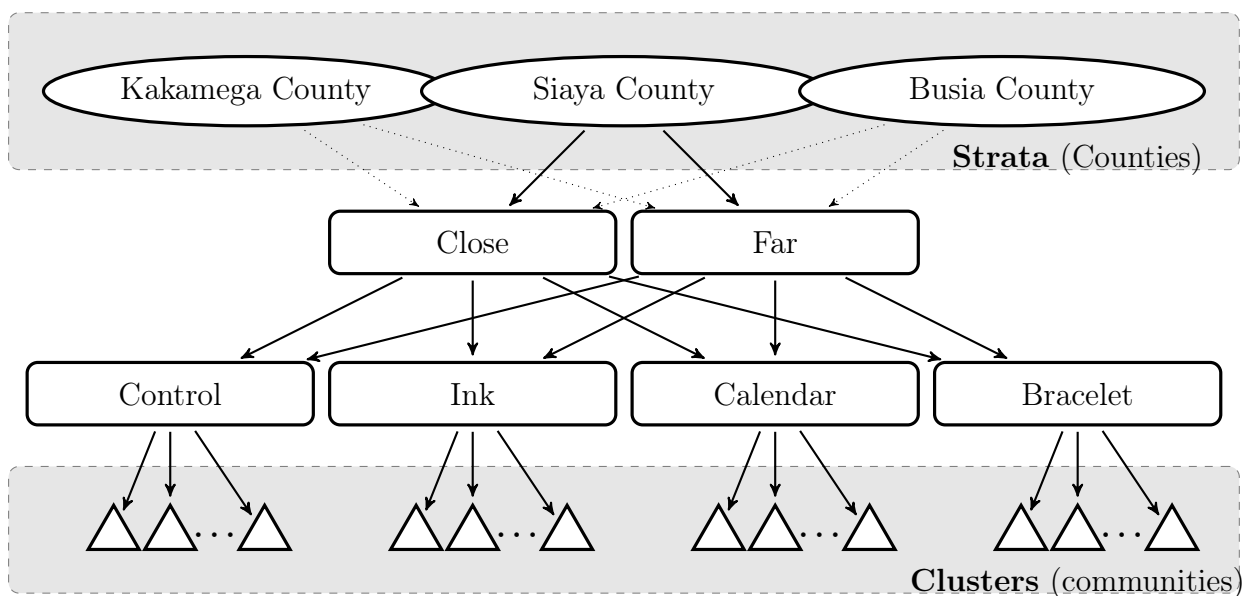


Figure A7: Experiment Design: grey boxes identify the types of population units over which treatment was assigned. The study was stratified over counties (ellipses) and clustered over communities (triangles). Boxes identify cluster (community) level treatments while circles identify individual level treatments.



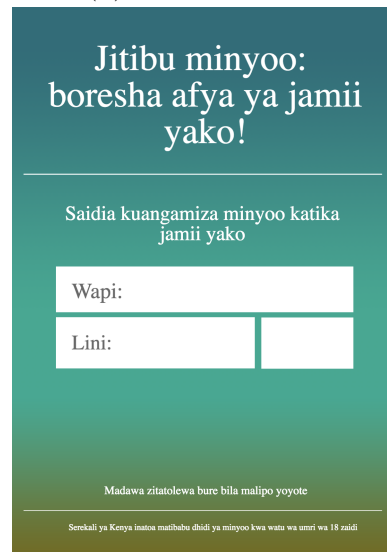
(a) Bracelet Flyer



(b) Calendar Flyer



(c) Ink Flyer



(d) Control Flyer

Figure A8: Flyers

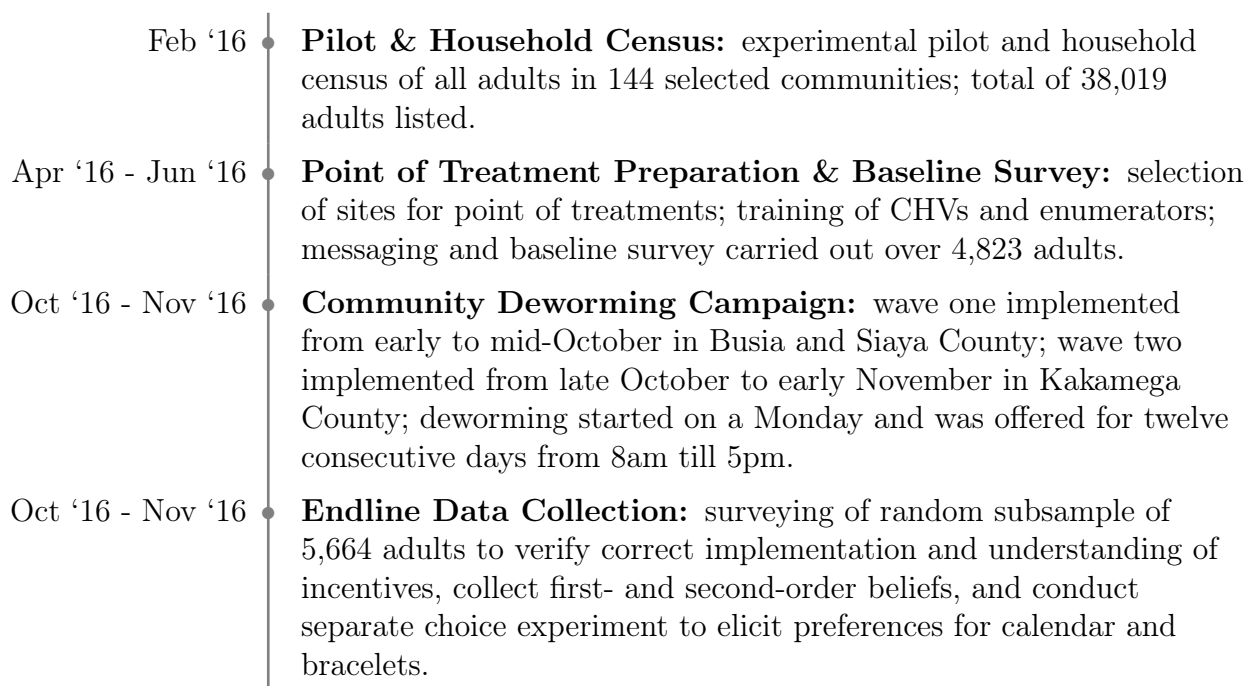


Figure A9: Timeline of the Experiment Implementation and Main Data Collection Activities

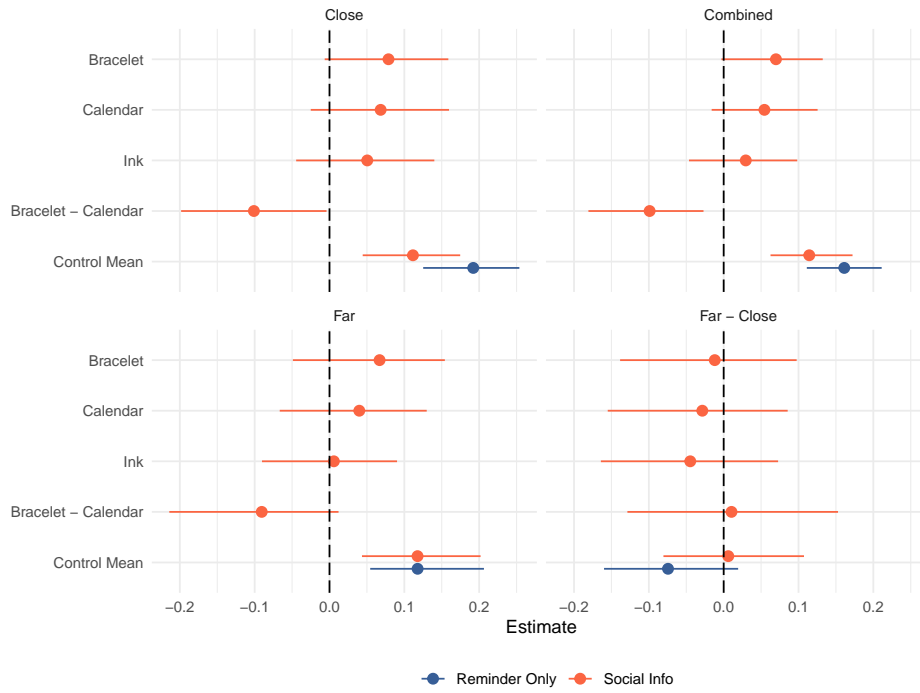


Figure A10: Treatment Effects, by SMS Condition

Notes: This figure shows the treatment effects of each incentive and distance condition cross-cut with the SMS condition.

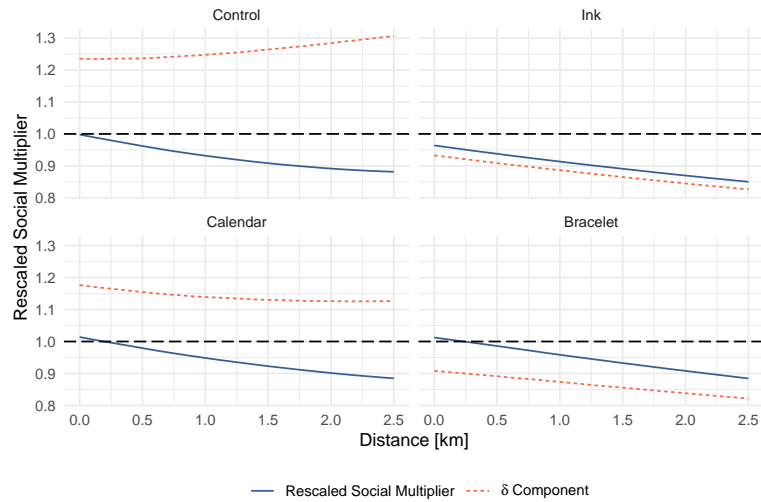


Figure A11: Estimated Social Multiplier Over Distance - Components

This plot shows the social multiplier components estimated using the structural model. The plot decomposes how much of the social multiplier is driven by the δ component versus how much is driven by changes in visibility across distance. The full line shows the entire social multiplier whilst the line shows the δ component - the difference between the two lines is driven by changes in μ visibility. Line: median.

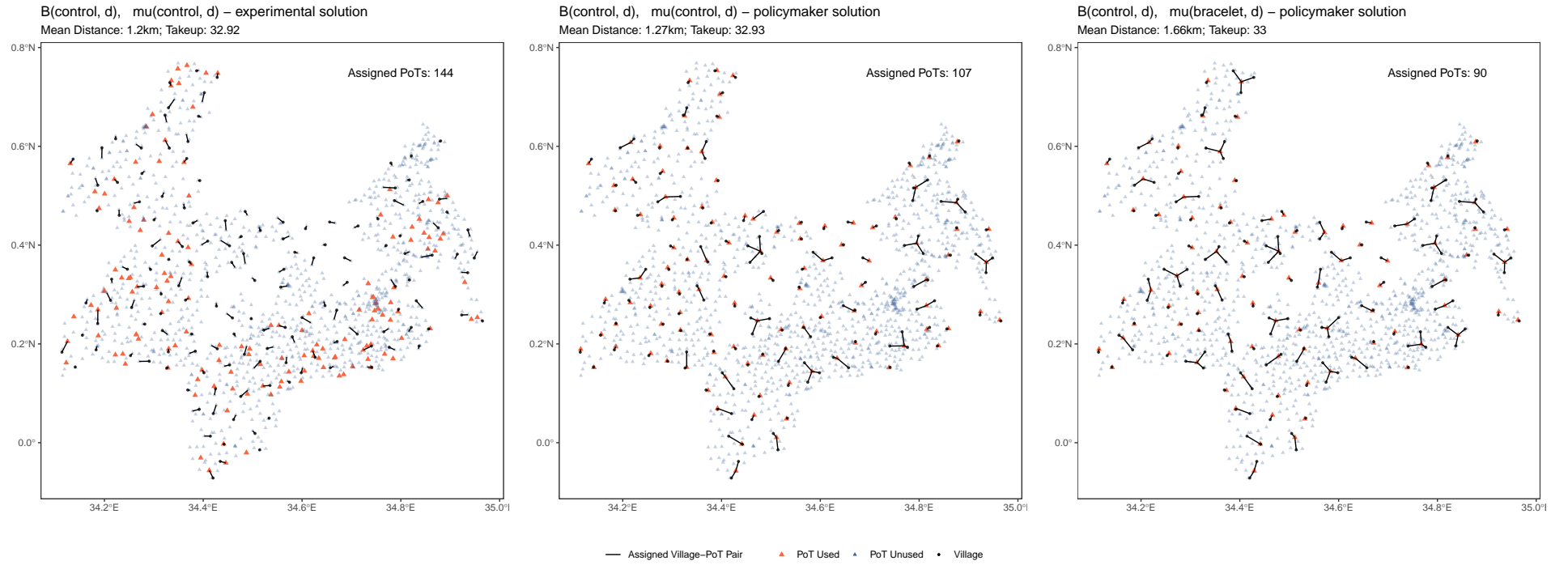


Figure A12: Policymaker's Allocation of Points of Treatment

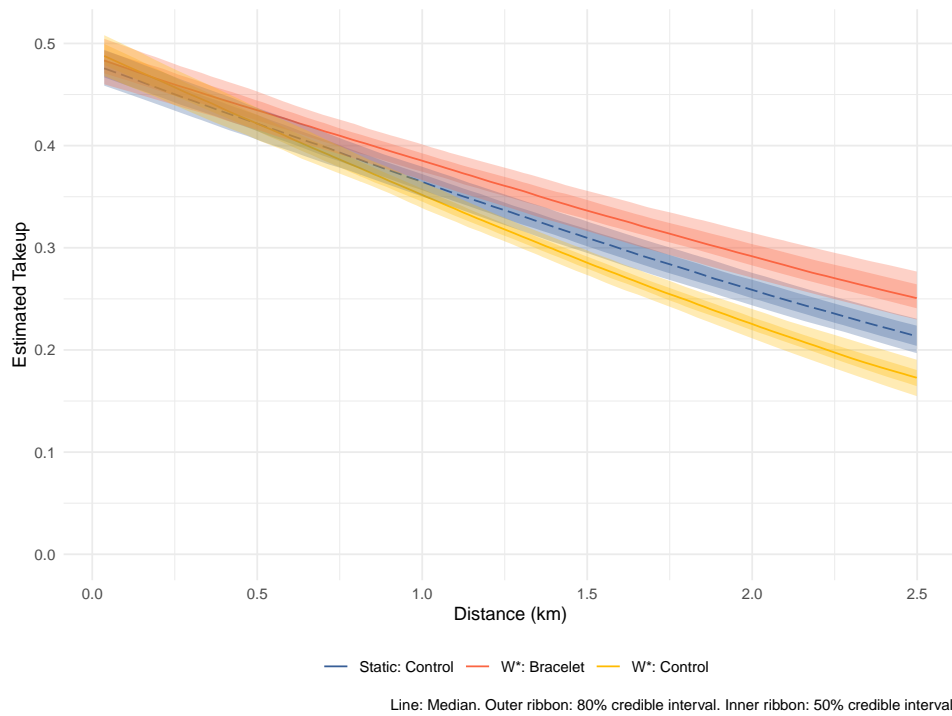


Figure A13: Demand Curve Perceived by Policymaker Across Counterfactual Scenarios

Notes: This plot shows predicted deworming takeup against distance walked under three scenarios:

- In blue: the policymaker believes social image concerns are static (fixed at 0.5km) and there's no change in $\mu\Delta[w^*]$ as a function of distance.
- In yellow: the policymaker is aware that social image concerns interact with incentives but doesn't introduce a material incentive (the control condition). There is amplification compared to the blue line.
- In red: the policymaker is aware that social image concerns interact with incentives and introduces a bracelet signal with no private incentive. There is mitigation compared to the blue line.

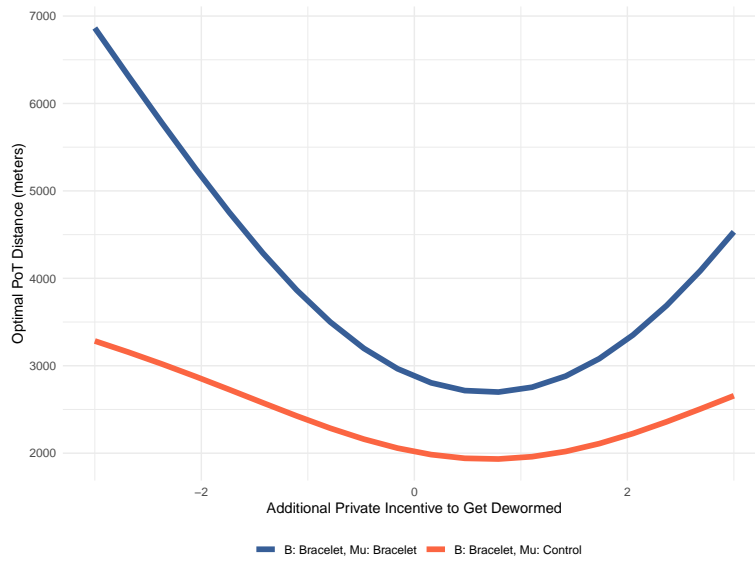


Figure A14: Optimal Point of Treatment Distance

Notes: This figure shows the expected welfare-maximizing distance to place a Point of Treatment from a community as a function of the private incentive individuals receive upon deworming, calculated by solving the optimal Pigovian subsidy under two scenarios: in blue, the optimal distance using the bracelet private incentive and visibility condition; in red, using the bracelet private incentive and control visibility.

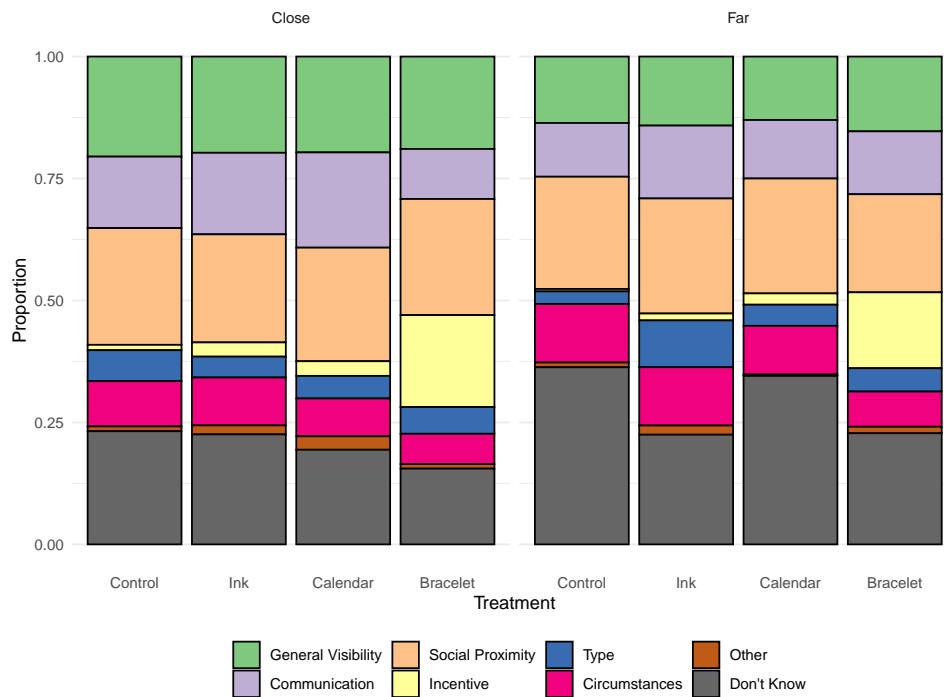


Figure A15: Second Order Beliefs - Reasons

Notes: This plot shows the reasons given by surveyed individuals for why other members of the community knew (or did not know, in grey) their deworming treatment status.

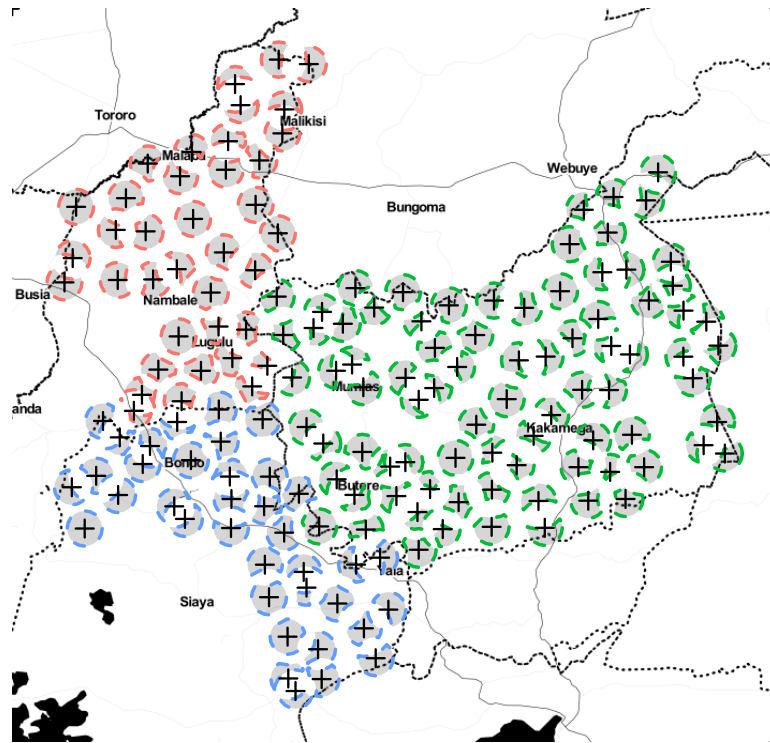


Figure A16: Site selection

Notes: This map shows the selected deworming points of treatment (black crosses), and the eligible catchment area a community could have been drawn from for a given point of treatment (the circles).

B Appendix Tables

Table B1: Balance Table

	Close						Far						
	Con	Ink - Con	Cal - Con	Bra - Con	Bra - Cal	Joint Test	Con	Ink - Con	Cal - Con	Bra - Con	Bra - Cal	Joint Test	Joint Test
Panel A: Takeup sample covariates, $N = 9,805$													
Number of individuals per community	825.127 (72.089)	-122.916 [0.119]	-124.104 [0.139]	-98.487 [0.171]	25.617 [0.708]	0.4000	741.955 (67.644)	13.533 [0.879]	-53.557 [0.428]	-85.044 [0.235]	-31.488 [0.606]	0.5469	0.5395
Female	0.543 (0.013)	-0.006 [0.673]	-0.002 [0.907]	-0.036 [0.028]	-0.034 [0.068]	0.0913	0.539 (0.014)	-0.014 [0.414]	0.002 [0.906]	-0.023 [0.182]	-0.025 [0.172]	0.4555	0.2458
Phone owner	0.816 (0.015)	0.008 [0.675]	-0.006 [0.755]	-0.005 [0.737]	0.001 [0.947]	0.9154	0.798 (0.015)	0 [0.998]	0.021 [0.307]	0.006 [0.703]	-0.015 [0.501]	0.7542	0.8231
Age	38.126 (0.758)	-0.714 [0.427]	-0.919 [0.286]	0.232 [0.813]	1.151 [0.208]	0.5221	37.995 (8.38)	-0.804 [0.403]	-0.861 [0.324]	-0.798 [0.419]	0.063 [0.945]	0.7592	0.7776
Distance to PoT	698.855 (79.393)	1.373 [0.988]	78.745 [0.411]	153.507 [0.116]	74.763 [0.452]	0.3271	1809.89 (103.125)	344.553 [0.022]	74.066 [0.544]	-60.152 [0.567]	-134.218 [0.23]	0.0366	0.0000
Panel B: Pretreat covariates, $N = 3,678$													
Completed primary schooling	0.484 (0.043)	-0.006 [0.899]	-0.043 [0.35]	-0.047 [0.277]	-0.005 [0.904]	0.4986	0.412 (0.037)	0.01 [0.818]	0.113 [0.013]	0.074 [0.114]	-0.039 [0.404]	0.0419	0.1556
Floor made of tile/cement	0.259 (0.04)	-0.054 [0.161]	-0.009 [0.844]	0.023 [0.552]	-0.014 [0.759]	0.5177	0.288 (0.061)	-0.081 [0.123]	-0.001 [0.984]	-0.051 [0.404]	-0.049 [0.333]	0.1790	0.4125
Main ethnicity/Luhya	0.5 (0.067)	0.007 [0.896]	0.02 [0.714]	-0.061 [0.354]	-0.081 [0.201]	0.6361	0.501 (0.075)	-0.097 [0.101]	-0.082 [0.463]	0.028 [0.405]	0.028 [0.635]	0.3880	0.2317
Christian	0.973 (0.012)	-0.01 [0.691]	0.004 [0.813]	0.015 [0.266]	0.012 [0.391]	0.5230	0.981 (0.008)	-0.022 [0.344]	0.004 [0.773]	-0.033 [0.165]	-0.037 [0.141]	0.3808	0.6049
Panel C: Baseline worm covariates, $N = 2,056$													
Dewormed in the past	0.75 (0.033)	-0.072 [0.072]	-0.047 [0.347]	-0.055 [0.149]	-0.008 [0.877]	0.3033	0.69 (0.036)	0.042 [0.283]	0.061 [0.138]	0.053 [0.16]	-0.007 [0.83]	0.4599	0.3361
Know how to prevent worms	0.917 (0.022)	0.045 [0.052]	0.001 [0.96]	-0.021 [0.479]	-0.023 [0.461]	0.0407	0.932 (0.021)	-0.023 [0.51]	0.017 [0.612]	-0.015 [0.961]	-0.015 [0.698]	0.8174	0.2881
Know everyone can be infected	0.68 (0.043)	-0.005 [0.912]	-0.039 [0.368]	0.05 [0.3]	0.088 [0.053]	0.2882	0.625 (0.05)	0.092 [0.094]	0.063 [0.339]	0.052 [0.407]	-0.011 [0.867]	0.4171	0.4613
Know bi-yearly treatment recommended	0.51 (0.043)	0.056 [0.309]	-0.064 [0.254]	-0.033 [0.533]	0.031 [0.568]	0.1672	0.444 (0.041)	0.009 [0.886]	0.129 [0.026]	0.034 [0.457]	-0.005 [0.073]	0.1395	0.1357
Know worms impose externality	0.27 (0.043)	0.014 [0.763]	-0.015 [0.766]	-0.042 [0.352]	-0.027 [0.561]	0.5901	0.203 (0.051)	0.029 [0.594]	0.017 [0.772]	0.099 [0.1]	0.082 [0.11]	0.2558	0.4864
Know worms spread by infected	0.27 (0.036)	0.088 [0.095]	0.063 [0.198]	0.003 [0.946]	-0.06 [0.255]	0.2539	0.289 (0.043)	0.044 [0.4]	0.006 [0.915]	0.031 [0.527]	0.026 [0.612]	0.8084	0.6261
Panel D: Implementation covariates, $N = 3,678$													
Did a CHV visit you?	0.863 (0.03)	-0.013 [0.757]	0.041 [0.159]	0.005 [0.886]	-0.036 [0.244]	0.3886	0.793 (0.043)	0.033 [0.51]	0.041 [0.415]	0.09 [0.064]	0.049 [0.212]	0.2316	0.1420
Was there an announcement about MDA in your community?	0.679 (0.118)	0.151 [0.247]	0.021 [0.904]	0.126 [0.376]	0.105 [0.468]	0.5592	0.923 (0.095)	-0.078 [0.467]	-0.078 [0.539]	-0.146 [0.259]	-0.068 [0.617]	0.7268	0.7427

Notes: The ‘‘Con’’ column denotes the baseline covariate’s control mean and corresponding standard error in parentheses. The ‘difference’ columns show the corresponding difference in means across conditions and control with p -values in parentheses below. ‘‘Joint Test’’ shows the F -stat p -value for equality of means across treatment conditions and control within the ‘Close’, ‘Far’, and across both distance conditions respectively. Standard errors are clustered at the community level with county fixed effects to reflect stratification at the county level. Only individuals eligible for deworming are surveyed.

- Number of individuals per community is calculated using the census data and aggregated to the community level so strictly speaking $N \neq 9,805$ for this covariate.
- Know everyone can be infected is equal to 1 if individuals report both adults and children can be infected when asked to list who can be infected.
- Know worms impose externality is equal to 1 if individuals respond ‘Yes’ when asked whether neighbours can infect them and respond ‘Yes’ when asked whether they can infect their neighbours.
- Distance to PoT is the distance in meters from the community center to the assigned point of treatment.

Table B2: Balance Table – Distance Condition

	Con	Con _{far - close}	Ink	Ink _{far - close}	Cal	Cal _{far - close}	Bra	Bra _{far - close}
Panel A: Takeup sample covariates, N = 9,805								
Number of individuals per community	825.127 (72.089)	-83.172 [0.311]	702.211 (61.564)	53.277 [0.539]	701.023 (70.246)	-12.625 [0.856]	726.64 (50.457)	-69.729 [0.243]
Female	0.543 (0.013)	-0.004 [0.798]	0.537 (0.011)	-0.012 [0.484]	0.541 (0.015)	0 [1]	0.507 (0.014)	0.009 [0.599]
Phone owner	0.816 (0.015)	-0.018 [0.242]	0.824 (0.017)	-0.027 [0.195]	0.81 (0.02)	0.009 [0.705]	0.811 (0.018)	-0.007 [0.693]
Age	38.126 (0.758)	-0.132 [0.889]	37.412 (0.717)	-0.222 [0.811]	37.207 (0.749)	-0.074 [0.925]	38.358 (0.949)	-1.162 [0.252]
Distance to PoT	698.855 (79.393)	1111.035 [0]	700.228 (81.478)	1454.215 [0]	777.6 (90.051)	1106.357 [0]	852.362 (83.339)	897.376 [0]
Panel B: Pretreat covariates, N = 3,678								
Completed primary schooling	0.484 (0.043)	-0.072 [0.129]	0.478 (0.031)	-0.056 [0.152]	0.441 (0.037)	0.084 [0.052]	0.437 (0.029)	0.049 [0.247]
Floor made of tile/cement	0.259 (0.04)	0.029 [0.605]	0.205 (0.032)	0.001 [0.965]	0.249 (0.049)	0.037 [0.459]	0.236 (0.033)	0.002 [0.967]
Main ethnicity/Luhya	0.5 (0.067)	0 [0.994]	0.508 (0.068)	-0.104 [0.058]	0.52 (0.067)	-0.102 [0.052]	0.439 (0.081)	0.008 [0.91]
Christian	0.973 (0.012)	0.008 [0.566]	0.963 (0.022)	-0.004 [0.905]	0.977 (0.011)	0.008 [0.603]	0.989 (0.008)	-0.04 [0.087]
Panel C: Baseline worm covariates, N = 2,056								
Dewormed in the past	0.75 (0.033)	-0.06 [0.147]	0.678 (0.034)	0.054 [0.148]	0.703 (0.043)	0.048 [0.342]	0.696 (0.031)	0.048 [0.158]
Know how to prevent worms	0.917 (0.022)	0.014 [0.572]	0.963 (0.017)	-0.054 [0.107]	0.919 (0.024)	0.03 [0.382]	0.896 (0.024)	0.037 [0.296]
Know everyone can be infected	0.68 (0.043)	-0.056 [0.305]	0.675 (0.047)	0.042 [0.394]	0.642 (0.038)	0.046 [0.421]	0.73 (0.042)	-0.054 [0.343]
Know bi-yearly treatment recommended	0.51 (0.043)	-0.067 [0.209]	0.567 (0.043)	-0.114 [0.078]	0.447 (0.046)	0.126 [0.038]	0.478 (0.039)	0 [1]
Know worms impose externality	0.27 (0.043)	-0.067 [0.261]	0.284 (0.039)	-0.052 [0.194]	0.255 (0.044)	-0.035 [0.492]	0.228 (0.034)	0.074 [0.101]
Know worms spread by infected	0.27 (0.036)	0.019 [0.685]	0.358 (0.049)	-0.024 [0.671]	0.333 (0.042)	-0.038 [0.494]	0.273 (0.039)	0.048 [0.319]
Panel D: Implementation covariates, N = 3,678								
Did a CHV visit you?	0.863 (0.03)	-0.07 [0.134]	0.849 (0.036)	-0.023 [0.629]	0.903 (0.026)	-0.069 [0.047]	0.867 (0.026)	0.016 [0.655]
Was there an announcement about MDA in your community?	0.679 (0.118)	0.244 [0.096]	0.829 (0.071)	0.016 [0.855]	0.699 (0.13)	0.145 [0.351]	0.804 (0.086)	-0.027 [0.831]

Notes: The ‘‘Con’’ column denotes the baseline covariate’s control mean and corresponding standard error in parentheses. The ‘difference’ columns show the corresponding difference in means across conditions and control with p -values in parentheses below. ‘‘Joint Test’’ shows the F -stat p -value for equality of means across treatment conditions and control within the ‘Close’, ‘Far’, and across both distance conditions respectively. Standard errors are clustered at the community level with county fixed effects to reflect stratification at the county level. Only individuals eligible for deworming are surveyed.

- Number of individuals per community is calculated using the census data and aggregated to the community level so strictly speaking $N \neq 9,805$ for this covariate.
- Know everyone can be infected is equal to 1 if individuals report both adults and children can be infected when asked to list who can be infected.
- Know worms impose externality is equal to 1 if individuals respond ‘Yes’ when asked whether neighbours can infect them and respond ‘Yes’ when asked whether they can infect their neighbours.
- Distance to PoT is the distance in meters from the community center to the assigned point of treatment.

Table B3: The Effects of Incentives on the Visibility of Deworming Decisions - Second Order Beliefs

Dependent variable: Second-order beliefs	Reduced Form			
	Combined (1)	Close (2)	Far (3)	Far - Close (4)
Control	0.641 [0.042]	0.681 [0.049]	0.592 [0.058]	-0.089 [0.067]
<i>H0</i> : Any Signal \neq No Signal, <i>p</i> -value	0.232	0.702	0.017	0.018
<i>H0</i> : Bracelet \neq Calendar, <i>p</i> -value	0.203	0.513	0.01	0.012
Ink	0.032 [0.055]	0.001 [0.069]	0.07 [0.068]	0.069 [0.081]
Bracelet	0.07 [0.054]	0.009 [0.062]	0.144 [0.078]	0.135 [0.088]
Calendar	0.015 [0.051]	0.043 [0.061]	-0.018 [0.069]	-0.061 [0.081]

Notes: Point estimates show the probability an individual responded that the community member knew about the individual’s deworming status when asked the question: “Do you think this person knows if you came for deworming?” conditional on the respondent recognizing the person within the community randomly drawn by the enumerator. Respondents were asked 10 times. ‘Control’ denotes the control mean, whilst other rows denote treatment effects relative to the control mean. “Combined”, “Close”, “Far”, and “Far - Close” average treatment effect estimates are calculated by aggregating over the predicted deworming take-up in each cell using the main specification Probit model whilst controlling for household distance to the treatment location. *H0*: Any signal $>$ No signal pools the ink and bracelet arms and the control and calendar arms and computes the *p*-value for the one sided t-test that treatment effects are greater in the signal arms than non-signal arms. *H0*: Bracelet $>$ Calendar shows the *p*-value for a one sided t-test that the Bracelet treatment effect is greater than the Calendar treatment effect. Sample consists of 999 respondents and estimates are generated using the linear probability model with strata dummies and saturated dummies for incentive treatment and incentive treatment interacted with distance to the nearest point of treatment. Results are clustered at the community level using the cluster bootstrap. Parentheses denote standard errors. Far - Close shows the difference between the close and far treatment effect.

Table B4: The Effects of Incentives on the Visibility of Deworming Decisions - Controlling for Household Distance to Treatment Location

Dependent variable: Take-up	Reduced Form			
	Combined (1)	Close (2)	Far (3)	Far - Close (4)
Control	0.69 [0.03]	0.747 [0.042]	0.622 [0.044]	-0.126 [0.06]
<i>H0</i> : Any Signal \neq No Signal, <i>p</i> -value	<0.001	0.437	<0.001	0.001
<i>H0</i> : Bracelet \neq Calendar, <i>p</i> -value	0.001	0.594	<0.001	0.002
Ink	0.084 [0.04]	0.032 [0.053]	0.147 [0.052]	0.115 [0.068]
Bracelet	0.136 [0.037]	0.051 [0.048]	0.238 [0.053]	0.187 [0.068]
Calendar	0.039 [0.039]	0.03 [0.052]	0.05 [0.055]	0.02 [0.074]

Notes: Point estimates show the probability an individual responded that they knew about a community member’s deworming status when asked the question: “Do you think this person came for deworming?” conditional on the respondent recognizing the person within the community randomly drawn by the enumerator. Respondents were asked 10 times. ‘Control’ denotes the control mean, whilst other rows denote treatment effects relative to the control mean. “Combined”, “Close”, “Far”, and “Far - Close” average treatment effect estimates are calculated by aggregating over the predicted deworming take-up in each cell using the main specification Probit model whilst controlling for household distance to the treatment location. *H0*: Any signal $>$ No signal pools the ink and bracelet arms and the control and calendar arms and computes the *p*-value for the one sided t-test that treatment effects are greater in the signal arms than non-signal arms. *H0*: Bracelet $>$ Calendar shows the *p*-value for a one sided t-test that the Bracelet treatment effect is greater than the Calendar treatment effect. Sample consists of 999 respondents and estimates are generated using the linear probability model with strata dummies and saturated dummies for incentive treatment and incentive treatment interacted with distance to the nearest point of treatment. Results are clustered at the community level using the cluster bootstrap. Parentheses denote standard errors. Far - Close shows the difference between the close and far treatment effect.

Table B5: The Effects of Incentives on Deworming Take-up - Marginal Effects at the Average

Dependent variable: Take-up	Reduced Form			
	Combined (1)	Close (2)	Far (3)	Far - Close (4)
Control	0.329 [0.028]	0.4 [0.027]	0.229 [0.036]	-0.171 [0.033]
<i>H0</i> : Any Signal \neq No Signal, <i>p</i> -value	0.51	0.654	0.073	0.049
<i>H0</i> : Bracelet \neq Calendar, <i>p</i> -value	0.02	0.267	0.021	0.34
Ink	-0.03 [0.033]	-0.053 [0.033]	0.025 [0.044]	0.078 [0.043]
Bracelet	0.079 [0.03]	0.06 [0.033]	0.117 [0.043]	0.056 [0.05]
Calendar	0.023 [0.029]	0.027 [0.031]	0.044 [0.037]	0.018 [0.039]

Notes: This table shows marginal effects at the average from a Probit model with saturated interactions between incentive treatment arms and distance to the point of treatment and strata fixed effects. “Combined”, “Close”, “Far”, and “Far - Close” average treatment effect estimates are calculated by aggregating over the predicted deworming take-up in each cell using the Probit model with continuous distance. Estimates show treatment effects compared to the control group, apart from Control which displays the level of deworming take-up in the control group. Square brackets show standard errors clustered at the community level calculated using the cluster bootstrap. Far - Close shows difference between the close and far treatment effects. *H0*: Any signal $>$ No signal pools the ink and bracelet arms and the control and calendar arms and computes the *p*-value for the one sided t-test that treatment effects are greater in the signal arms than non-signal arms. *H0*: Bracelet $>$ Calendar shows the *p*-value for a one sided t-test that the Bracelet treatment effect is greater than the Calendar treatment effect. We present a Bayesian probit model in Table B10 using a parametric form of clustering to aid comparability with the structural model. Appendix Tables B9 and B8 show results including the squared distance to a cluster’s centroid and replacing continuous distance with a binary treatment indicator for the Close and Far group respectively.

Table B6: The Effect of Incentives on Deworming Take-up - Controlling for Household Distance to Treatment Location

Dependent variable: Take-up	Reduced Form			
	Combined (1)	Close (2)	Far (3)	Far - Close (4)
Control	0.33 [0.023]	0.409 [0.024]	0.232 [0.032]	-0.176 [0.032]
<i>H0</i> : Any Signal \neq No Signal, <i>p</i> -value	0.417	0.603	0.065	0.042
<i>H0</i> : Bracelet \neq Calendar, <i>p</i> -value	0.045	0.307	0.035	0.41
Ink	-0.016 [0.031]	-0.054 [0.033]	0.031 [0.041]	0.085 [0.041]
Bracelet	0.082 [0.028]	0.057 [0.034]	0.112 [0.042]	0.054 [0.05]
Calendar	0.035 [0.027]	0.026 [0.031]	0.046 [0.035]	0.02 [0.037]

Notes: This table shows average marginal effects from the main specification Probit model with an additional control for household's distance to the treatment location. Estimates show treatment effects compared to the control group, apart from Control which displays the level of deworming take-up in the control group. Square brackets show standard errors clustered at the community level calculated using the cluster bootstrap. Far - Close shows difference between the close and far treatment effects. *H0*: Any signal $>$ No signal pools the ink and bracelet arms and the control and calendar arms and computes the *p*-value for the one sided t-test that treatment effects are greater in the signal arms than non-signal arms. *H0*: Bracelet $>$ Calendar shows the *p*-value for a one sided t-test that the Bracelet treatment effect is greater than the Calendar treatment effect.

Table B7: The Effects of Incentives on the Visibility of Deworming Decisions - Randomized Distance Group

Dependent variable: First-order beliefs	Reduced Form			
	Combined (1)	Close (2)	Far (3)	Far - Close (4)
Control	0.696 [0.031]	0.752 [0.042]	0.628 [0.044]	-0.124 [0.06]
<i>H0</i> : Any Signal \neq No Signal, <i>p</i> -value	0.001	0.625	<0.001	0.002
<i>H0</i> : Bracelet \neq Calendar, <i>p</i> -value	0.002	0.728	<0.001	0.007
Ink	0.082 [0.039]	0.021 [0.055]	0.156 [0.055]	0.135 [0.077]
Bracelet	0.127 [0.038]	0.051 [0.05]	0.22 [0.053]	0.169 [0.071]
Calendar	0.035 [0.039]	0.036 [0.054]	0.033 [0.056]	-0.002 [0.077]

Notes: Point estimates show the probability an individual responded that they knew about a community member’s deworming status when asked the question: “Do you think this person came for deworming?” conditional on the respondent recognizing the person within the community randomly drawn by the enumerator. Respondents were asked 10 times. ‘Control’ denotes the control mean, whilst other rows denote treatment effects relative to the control mean. “Combined”, “Close”, “Far”, and “Far - Close” average treatment effect estimates are calculated by aggregating over the predicted deworming take-up in each cell using the Probit model with interactions for each randomized distance group, Close and Far. *H0*: Any signal $>$ No signal pools the ink and bracelet arms and the control and calendar arms and computes the *p*-value for the one sided t-test that treatment effects are greater in the signal arms than non-signal arms. *H0*: Bracelet $>$ Calendar shows the *p*-value for a one sided t-test that the Bracelet treatment effect is greater than the Calendar treatment effect. Sample consists of 999 respondents and estimates are generated using the linear probability model with strata dummies and saturated dummies for incentive treatment and incentive treatment interacted with distance to the nearest point of treatment. Results are clustered at the community level using the cluster bootstrap. Parentheses denote standard errors. Far - Close shows the difference between the close and far treatment effect.

Table B8: The Effect of Incentives on Deworming Take-up - Randomized Distance Group

Dependent variable: Take-up	Reduced Form			
	Combined (1)	Close (2)	Far (3)	Far - Close (4)
Control	0.332 [0.022]	0.406 [0.027]	0.24 [0.035]	-0.166 [0.043]
<i>H0</i> : Any Signal \neq No Signal, <i>p</i> -value	0.37	0.528	0.058	0.06
<i>H0</i> : Bracelet \neq Calendar, <i>p</i> -value	0.03	0.323	0.026	0.347
Ink	-0.017 [0.03]	-0.06 [0.037]	0.036 [0.047]	0.096 [0.06]
Bracelet	0.083 [0.027]	0.062 [0.035]	0.108 [0.045]	0.046 [0.058]
Calendar	0.033 [0.027]	0.031 [0.036]	0.035 [0.039]	0.003 [0.052]

Notes: This table shows average marginal effects from a Probit model with saturated interactions between incentive treatment arms and the assigned distance group for a community, either close or far, and strata fixed effects. Estimates show treatment effects compared to the control group, apart from Control which displays the level of deworming take-up in the control group. Square brackets show standard errors clustered at the community level calculated using the cluster bootstrap. Far - Close shows difference between the close and far treatment effects. *H0*: Any signal $>$ No signal pools the ink and bracelet arms and the control and calendar arms and computes the *p*-value for the one sided t-test that treatment effects are greater in the signal arms than non-signal arms. *H0*: Bracelet $>$ Calendar shows the *p*-value for a one sided t-test that the Bracelet treatment effect is greater than the Calendar treatment effect.

Table B9: Reduced Form Distance Squared

Dependent variable: Take-up	Reduced Form			
	Combined (1)	Close (2)	Far (3)	Far - Close (4)
Control	0.329 [0.022]	0.411 [0.025]	0.228 [0.03]	-0.183 [0.032]
<i>H0</i> : Any Signal \neq No Signal, <i>p</i> -value	0.193	0.664	0.015	0.01
<i>H0</i> : Bracelet \neq Calendar, <i>p</i> -value	0.002	0.156	0.002	0.133
Ink	-0.017 [0.032]	-0.057 [0.034]	0.032 [0.044]	0.089 [0.042]
Bracelet	0.102 [0.027]	0.064 [0.032]	0.148 [0.04]	0.084 [0.047]
Calendar	0.036 [0.026]	0.025 [0.031]	0.05 [0.034]	0.024 [0.037]

Notes: This table shows average marginal effects from a Probit model with saturated interactions between incentive treatment arms and distance to the point of treatment and strata fixed effects – it also includes distance squared as both a main effect and interaction with treatment to control for the possibly non-linear effect of distance. “Combined”, “Close”, “Far”, and “Far - Close” average treatment effect estimates are calculated by aggregating over the predicted deworming take-up in each cell using the Probit model with continuous distance. Estimates show treatment effects compared to the control group, apart from Control which displays the level of deworming take-up in the control group. Square brackets show standard errors clustered at the community level calculated using the cluster bootstrap. Far - Close shows difference between the close and far treatment effects. *H0*: Any signal $>$ No signal pools the ink and bracelet arms and the control and calendar arms and computes the *p*-value for the one sided t-test that treatment effects are greater in the signal arms than non-signal arms. *H0*: Bracelet $>$ Calendar shows the *p*-value for a one sided t-test that the Bracelet treatment effect is greater than the Calendar treatment effect.

Table B10: The Effects of Incentives on Deworming Take-up - Bayesian Model, Average Marginal Effects

Dependent variable: Take-up	Reduced Form			
	Combined (1)	Close (2)	Far (3)	Far - Close (4)
Bracelet	0.083 (0.024, 0.143)	0.054 (-0.029, 0.14)	0.12 (0.041, 0.198)	0.066 (-0.047, 0.18)
Calendar	0.041 (-0.02, 0.102)	0.029 (-0.058, 0.114)	0.057 (-0.021, 0.133)	0.027 (-0.09, 0.152)
Ink	-0.012 (-0.07, 0.046)	-0.062 (-0.144, 0.022)	0.049 (-0.029, 0.125)	0.112 (-0.005, 0.223)
Bracelet - Calendar	0.042 (-0.014, 0.099)	0.026 (-0.058, 0.109)	0.063 (-0.019, 0.144)	0.037 (-0.079, 0.155)
Control	0.328 (0.291, 0.367)	0.408 (0.354, 0.464)	0.227 (0.184, 0.279)	-0.179 (-0.254, -0.108)

Notes: This table shows results from a probit model with saturated interactions between incentive treatment arms and community centroid’s distance to the treatment location, strata fixed effects. Inference is ‘clustered’ using a parametric community-level random-effect. Estimates show treatment effects compared to the control group, apart from Control which displays the level of deworming take-up in the control group. Point estimates show posterior means and parentheses show 95% credibility intervals. Bracelet - Calendar shows the difference in treatment effects between the bracelet and calendar arm. Far - Close shows difference between the close and far treatment effects.

Table B11: Incentive Check: Endline

	Received incentive when treated	Have incentive currently	Seen incentive	Link incentive to deworming
Bracelet	0.022* (0.012)	0.666*** (0.023)	0.277*** (0.018)	0.246*** (0.019)
Calendar	-0.001 (0.013)	0.81*** (0.021)	0.073*** (0.018)	0.021 (0.02)
Ink (Levels)	0.95 (0.009)	0.144 (0.015)	0.674 (0.013)	0.647 (0.014)

Notes: This table shows: Received incentive when treated, the proportion of individuals that report receiving a bracelet/calendar/ink when they were treated at the point of treatment, conditional on being dewormed; Have incentive currently the proportion of surveyed individuals that report still having the incentive at endline, conditional on being dewormed; Seen incentive the fraction of individuals that report seeing the incentive, unconditional on being dewormed, the ink condition asked “Have you seen ink on people’s fingers” whereas the calendar arm asked “Have you seen this calendar before”; Link incentive to deworming, the fraction of individuals that mention "deworming/medication/treatment/tablet/drug/worms" when asked what the incentive means (in their respective treatment arm), unconditional on being dewormed. The “Bracelet” and “Calendar” rows show estimated treatment effects relative to the Ink ‘control’ mean. * p -value < 0.1, ** p -value < 0.05, *** p -value < 0.01.

Table B12: Preference for Calendar Item Across Distance

	(1)	(2)	(3)
Distance group: Far	-0.0109 (0.1143)	-0.0427 (0.1023)	-0.1828 (0.2580)
Ink Treatment			-0.0185 (0.1083)
Distance to PoT			0.0802 (0.1068)
Dewormed			0.0865 (0.0897)
Observations	408	897	897
Squared Correlation	0.01237	0.00628	0.00825
Pseudo R ²	0.01050	0.00536	0.00687
BIC	471.45	1,016.7	1,035.6
county fixed effects	✓	✓	✓

Notes: This table shows frequentist probit estimates of preferences for the calendar over the bracelet. Column 1 shows estimates using only those in the control condition. Column 2 shows estimates pooling both the ink and control condition. Column 3 uses the pooled sample and controls for a range of covariates/treatment condition. The coefficient on "Distance group: Far" shows the difference in preferences for the calendar in the Far distance condition compared to the Close distance condition. Standard errors (in parentheses) are clustered at the community level.

Table B13: Willingness To Pay Estimates

Parameter	Posterior estimates
Panel A: Model parameters	
Valuation difference (KSh), mean	0.472 (0.404, 0.54)
Panel B: Estimated preferences	
Pr(Prefer calendar), offered 50KSh	0.897 (0.876, 0.917)
Pr(Prefer calendar), offered 0KSh	0.731 (0.705, 0.755)
Pr(Prefer calendar), offered -50KSh	0.486 (0.448, 0.519)

Notes: This table shows parameter estimates and implied posterior probabilities from the willingness-to-pay exercise. Posterior medians are shown as point estimates with 95% credibility intervals below. Individuals were asked: "Which one would you like, the calendar, or the bracelet?". Next, individuals were asked: "Before you take the [bracelet/calendar], I would like to make you an offer. You can take either the [bracelet/calendar] on its own, OR take the [calendar/bracelet] and x KSh."

Table B14: The Effects of Incentives on the Visibility on Deworming Decisions (Structural Model)

	First-Order Beliefs			Second-Order Beliefs		
	Combined (1)	Close (2)	Far (3)	Combined (4)	Close (5)	Far (6)
Bracelet	0.093 (0.054, 0.132)	0.035 (-0.005, 0.075)	0.148 (0.094, 0.217)	0.046 (0.003, 0.087)	0.009 (-0.044, 0.061)	0.081 (0.03, 0.139)
Calendar	0.015 (-0.019, 0.05)	-0.003 (-0.041, 0.037)	0.031 (-0.007, 0.077)	0.017 (-0.024, 0.059)	0.034 (-0.015, 0.083)	0.001 (-0.051, 0.046)
Ink	0.06 (0.019, 0.101)	0.012 (-0.029, 0.051)	0.108 (0.054, 0.168)	0.026 (-0.017, 0.067)	-0.004 (-0.053, 0.047)	0.056 (0.006, 0.109)
Control mean	0.752 (0.72, 0.784)	0.797 (0.765, 0.828)	0.709 (0.656, 0.754)	0.688 (0.654, 0.72)	0.712 (0.672, 0.749)	0.663 (0.62, 0.703)

Notes: Point estimates shown are posterior medians. Parentheses show 95% credibility intervals. Far - Close shows the posterior of the difference between the close and far treatment effect. The model is estimated using Hamiltonian Monte-Carlo in Stan with 4 chains, 400 warm-up draws, and 400 samples. Sampler diagnostics report 0 divergent transitions and split $\hat{R} < 1.1$ for all samples. Model estimated using 9,805 observations.

Table B15: The Effects of Incentives on Deworming Take-up (Structural Model)

Dependent variable: Take-up	Structural			
	Combined (1)	Close (2)	Far (3)	Far - Close (4)
Panel A: Overall				
Bracelet	0.073 (0.049, 0.098)	0.056 (0.029, 0.083)	0.095 (0.065, 0.124)	0.039 (0.013, 0.067)
Calendar	0.04 (0.017, 0.064)	0.037 (0.01, 0.065)	0.044 (0.021, 0.067)	0.008 (-0.01, 0.03)
Ink	-0.019 (-0.045, 0.005)	-0.04 (-0.071, -0.011)	0.008 (-0.019, 0.033)	0.047 (0.024, 0.075)
Bracelet - Calendar	0.033 (0.017, 0.051)	0.019 (0.006, 0.036)	0.05 (0.027, 0.075)	0.031 (0.014, 0.054)
Control mean	0.332 (0.315, 0.35)	0.399 (0.377, 0.42)	0.249 (0.228, 0.27)	-0.15 (-0.173, -0.129)

Notes: Point estimates shown are posterior medians. Parentheses show 95% credibility intervals. Bracelet - Calendar shows the posterior of the difference between the bracelet and calendar treatment effect. Far - Close shows the posterior of the difference between the close and far treatment effect. The model is estimated using Hamiltonian Monte-Carlo in Stan with 4 chains, 400 warm-up draws, and 400 samples. Sampler diagnostics report 0 divergent transitions and split $\hat{R} < 1.1$ for all samples. Model estimated using 9,805 observations. In the Table B24 we show results robust across a variety of prior specifications, and eliminating various sub-models. Table B25 shows similar results robust to adding a cluster-level shock, $\gamma_j \sim N(0, \sigma_j)$, where the shock variance, σ_j , varies at the cluster level, a parametric form of clustered standard-errors.

Table B16: The Effects of Increasing the Visibility of Deworming Decisions

Dependent variable: Take-up	Structural			
	Combined (1)	Close (2)	Far (3)	Far - Close (4)
<i>Panel A: Signal</i>				
Bracelet	0.029 (0.012, 0.049)	0.012 (-0.002, 0.029)	0.045 (0.021, 0.076)	0.033 (0.012, 0.062)
Calendar	0.004 (-0.008, 0.017)	-0.001 (-0.017, 0.013)	0.009 (-0.003, 0.025)	0.011 (-0.001, 0.027)
Ink	0.018 (0.004, 0.036)	0.004 (-0.011, 0.018)	0.033 (0.012, 0.058)	0.029 (0.011, 0.054)
Bracelet - Calendar	0.025 (0.011, 0.042)	0.013 (-0.001, 0.03)	0.036 (0.017, 0.059)	0.023 (0.008, 0.045)
Control mean	0.368 (0.335, 0.404)	0.424 (0.397, 0.452)	0.311 (0.255, 0.371)	-0.113 (-0.17, -0.056)
<i>Panel B: Private</i>				
Bracelet	0.032 (0.007, 0.058)			
Calendar	0.032 (0.007, 0.058)			
Ink	-0.044 (-0.073, -0.015)			
Bracelet - Calendar	0 (0, 0)			
Control mean	0.332 (0.315, 0.35)			

Notes: Point estimates shown are posterior medians. Parentheses show 95% credibility intervals. Bracelet - Calendar shows the posterior of the difference of the bracelet and calendar treatment effect. Model estimated using Hamiltonian Monte-Carlo in Stan with 4 chains, 400 warm-up draws, and 400 samples. Sampler diagnostics report 0 divergent transitions and split $\hat{R} < 1.1$ for all samples. Deworming sub-model estimated using 9,805 observations, WTP submodel estimated using 998 observations, belief submodel estimated using 999 observations.

Table B17: Structural ATEs – Private Distance Cost, Cluster Social Image Returns

Dependent variable: Take-up	Structural			
	Combined (1)	Close (2)	Far (3)	Far - Close (4)
Panel A: Overall				
Bracelet	0.065 (0.039, 0.087)	0.045 (0.02, 0.068)	0.092 (0.064, 0.119)	0.047 (0.032, 0.066)
Calendar	0.028 (0.005, 0.051)	0.026 (-0.003, 0.052)	0.035 (0.013, 0.057)	0.009 (-0.007, 0.028)
Ink	-0.031 (-0.056, -0.005)	-0.036 (-0.064, -0.006)	-0.031 (-0.059, -0.006)	0.005 (-0.014, 0.03)
Bracelet - Calendar	0.037 (0.021, 0.056)	0.019 (0.005, 0.038)	0.057 (0.039, 0.077)	0.038 (0.026, 0.053)
Control mean	0.34 (0.323, 0.358)	0.402 (0.38, 0.421)	0.264 (0.245, 0.285)	-0.138 (-0.156, -0.122)

Notes: This model is similar to the main specification structural model but uses the household's own distance to the treatment location in their decision to deworm and the community's social image return. That is, the household incurs a private distance cost δd_i , but only reaps social image returns associated with the cluster centroid's distance cost: $\Delta(w^*(\bar{d}_c))$. Point estimates shown are posterior means. Parentheses show 95% credibility intervals. Bracelet - Calendar shows the posterior of the difference of the bracelet and calendar treatment effect. Model estimated using Hamiltonian Monte-Carlo in Stan with 2 chains, 200 warm-up draws, and 200 samples. Sampler diagnostics report 0 divergent transitions and split $\hat{R} < 1.1$ for all samples. Deworming sub-model estimated using 9,805 observations, WTP submodel estimated using 998 observations, belief submodel estimated using 999 observations.

Table B18: Structural ATEs – Private Distance Cost, Household Social Image Returns

Dependent variable: Take-up	Structural			
	Combined (1)	Close (2)	Far (3)	Far - Close (4)
Panel A: Overall				
Bracelet	0.064 (0.039, 0.088)	0.045 (0.019, 0.07)	0.09 (0.063, 0.117)	0.045 (0.028, 0.064)
Calendar	0.025 (0.002, 0.05)	0.021 (-0.007, 0.05)	0.034 (0.009, 0.056)	0.013 (-0.003, 0.032)
Ink	-0.031 (-0.054, -0.007)	-0.035 (-0.061, -0.004)	-0.035 (-0.062, -0.01)	0 (-0.02, 0.023)
Bracelet - Calendar	0.039 (0.021, 0.055)	0.024 (0.006, 0.042)	0.056 (0.035, 0.077)	0.032 (0.019, 0.046)
Control mean	0.342 (0.325, 0.36)	0.405 (0.384, 0.427)	0.264 (0.245, 0.282)	-0.141 (-0.16, -0.122)

Notes: This model is similar to the main specification structural model but uses the household's own distance to the treatment location in their decision to deworm and solved the corresponding fixed point for that household's social image return. That is, the household incurs a private distance cost δd_i , and reaps social image returns associated with the household's distance cost: $\Delta(w^*(d_i))$. Point estimates shown are posterior means. Parentheses show 95% credibility intervals. Bracelet - Calendar shows the posterior of the difference of the bracelet and calendar treatment effect. Model estimated using Hamiltonian Monte-Carlo in Stan with 2 chains, 200 warm-up draws, and 200 samples. Sampler diagnostics report 0 divergent transitions and split $\hat{R} < 1.1$ for all samples. Deworming sub-model estimated using 9,805 observations, WTP submodel estimated using 998 observations, belief submodel estimated using 999 observations.

Table B19: Baseline Social Image Concerns by Condition

Topic	Close				Far				Joint Test
	Control	Ink	Calendar	Bracelet	Control	Ink	Calendar	Bracelet	
Panel A: Praise									
Wearing nice clothes to church	0.726 (0.046)	0.768 (0.054)	0.642 (0.055)	0.657 (0.061)	0.711 (0.047)	0.726 (0.066)	0.683 (0.07)	0.637 (0.054)	0.383
Use latrine	0.959 (0.024)	0.935 (0.032)	0.892 (0.03)	0.952 (0.027)	0.91 (0.033)	0.913 (0.041)	0.895 (0.057)	0.936 (0.029)	0.296
Deworming during MDA	0.935 (0.029)	0.947 (0.027)	0.92 (0.033)	0.922 (0.034)	0.927 (0.032)	0.927 (0.031)	0.848 (0.088)	0.933 (0.03)	0.851
Immunizing children	0.94 (0.025)	0.949 (0.023)	0.917 (0.027)	0.929 (0.032)	0.947 (0.027)	0.925 (0.026)	0.862 (0.077)	0.936 (0.028)	0.548
Panel A: Stigma									
Not wearing nice clothes to church	0.423 (0.064)	0.322 (0.065)	0.26 (0.05)	0.264 (0.053)	0.282 (0.049)	0.311 (0.079)	0.315 (0.062)	0.329 (0.064)	0.370
Open defecation	0.829 (0.053)	0.828 (0.046)	0.821 (0.042)	0.9 (0.033)	0.839 (0.049)	0.806 (0.059)	0.906 (0.04)	0.886 (0.038)	0.217
Not deworming during MDA	0.744 (0.041)	0.702 (0.035)	0.733 (0.042)	0.755 (0.033)	0.742 (0.061)	0.755 (0.038)	0.712 (0.051)	0.783 (0.036)	0.651
Not immunizing children	0.803 (0.033)	0.789 (0.04)	0.753 (0.046)	0.821 (0.033)	0.814 (0.053)	0.837 (0.04)	0.813 (0.046)	0.803 (0.032)	0.869

Notes: This table shows respondents' baseline opinions over praising and stigmatising common actions and preventative health behaviors using a sample of 3,678 correspondents. Point estimates show cell means and standard errors are in parentheses.

Table B20: Endline Table

	Close					Far					Joint F-test	F-test p -value
	Control	Ink	Calendar	Bracelet	F-test p -value	Control	Ink	Calendar	Bracelet	F-test p -value		
Know bi-yearly treatment recommended	0.635 (0.041)	0.641 [0.037]	0.617 [0.052]	0.63 [0.039]	-	0.602 (0.058)	0.57 [0.041]	0.633 [0.044]	0.559 [0.043]	-	-	
Δ Know bi-yearly treatment recommended, p -value	0	0	0.002	0	0	0	0.028	0.001	0	0	0	
Know everyone can be infected	0.781 (0.034)	0.671 [0.046]	0.776 [0.039]	0.745 [0.039]	-	0.734 (0.039)	0.769 [0.036]	0.719 [0.047]	0.759 [0.044]	-	-	
Δ Know everyone can be infected, p -value	0.624	0	0.342	0.003	0	0.084	0.422	0.217	0.02	0.032	0	
Know worms impose externality	0.305 (0.04)	0.372 [0.038]	0.348 [0.039]	0.29 [0.029]	-	0.329 (0.044)	0.315 [0.051]	0.303 [0.044]	0.364 [0.045]	-	-	
Δ Know worms impose externality, p -value	0.769	0.808	0.707	0.417	0.918	0.675	0.918	0.937	0.595	0.976	0.994	
Know worms spread by infected	0.387 (0.046)	0.483 [0.037]	0.423 [0.044]	0.392 [0.033]	-	0.406 (0.047)	0.467 [0.062]	0.44 [0.051]	0.447 [0.043]	-	-	
Δ Know worms spread by infected, p -value	0.642	0.777	0.601	0.703	0.95	0.617	0.608	0.642	0.962	0.947	0.994	

Notes: Each column shows the endline covariate level with clustered standard errors in parentheses. The Δp -value shows the p -value for the null hypothesis that baseline and endline covariate levels are the same. The F -test p -value tests for equality in changes from baseline to endline across treatment arms. I.e. There is evidence that there is differential learning about who can be infected across conditions $p \leq 1e^{-4}$ but there is insufficient evidence to reject the null that learning about externalities is the same across treatment arms from baseline to endline ($p = 0.978$). Standard errors are clustered at the community level and county fixed effects are included in all regressions.

Table B21: Predicted Deworming Takeup at Endline

	Combined	Close	Far	H0: Close = Far, p -value
Bracelet	0.103*** (0.023)	0.067*** (0.023)	0.148*** (0.043)	0.01975
Calendar	0.057** (0.024)	0.025 (0.026)	0.097** (0.043)	0.01588
Ink	0.031 (0.023)	0.007 (0.022)	0.061 (0.044)	0.00143
H0: Bracelet = Calendar, p -value	0.0114	0.128	0.0173	
Control mean	0.566 (0.034)	0.629 (0.032)	0.495 (0.048)	0.00206

Notes: Estimated using OLS. Participants are asked to predict how many individuals came to get dewormed out of a random sample of 10 adults in their community. We estimate deworm rate $_{ic} = \gamma dist_{ic} + \beta_{z,d} \sum_{z=1}^4 \sum_{d=1}^2 treatment_{icz} \times distance\ group_{icd} + \delta_s$ where δ_s represents strata dummies with clustered standard errors.

Table B22: Second Order Beliefs - Reason Category

	General Visibility	Communication	Social Proximity	Incentive	Type	Circumstances	Other
Panel A: Why do they know you came for deworming?							
Bracelet	-0.034 (0.027)	-0.042* (0.025)	-0.059 (0.037)	0.201*** (0.032)	-0.003 (0.021)	-0.064** (0.026)	0 (0.005)
Calendar	-0.021 (0.029)	0.034 (0.029)	-0.013 (0.045)	0.025*** (0.008)	-0.005 (0.022)	-0.027 (0.028)	0.008 (0.006)
Ink	-0.019 (0.029)	0.023 (0.03)	-0.038 (0.041)	0.018** (0.007)	0.015 (0.021)	-0.01 (0.027)	0.01 (0.007)
Control Mean	0.247 (0.022)	0.184 (0.021)	0.331 (0.031)	0.012 (0.004)	0.067 (0.017)	0.147 (0.021)	0.014 (0.004)
N	1538	1538	1538	1538	1538	1538	1538
Panel B: Why don't they know that you came for deworming?							
Bracelet	0.001 (0.037)	0.022 (0.041)	-0.031 (0.064)	-0.001 (0.006)	0.003 (0.003)	0.01 (0.026)	-0.004 (0.005)
Calendar	-0.001 (0.043)	-0.015 (0.036)	0.018 (0.063)	-0.005 (0.006)	0 (0)	0.008 (0.027)	-0.005 (0.005)
Ink	0.018 (0.04)	0 (0.037)	0.003 (0.062)	-0.01** (0.004)	0.003 (0.002)	-0.01 (0.024)	-0.005 (0.005)
Control Mean	0.075 (0.024)	0.152 (0.024)	0.696 (0.04)	0.01 (0.004)	0 (0)	0.06 (0.021)	0.007 (0.004)
N	4920	4920	4920	4920	4920	4920	4920

Notes: This table categorises why individuals believed others knew/didn't know their deworming status across treatment arms. Categories are generated from free text input by surveyed respondents. First, we generate regular expressions to match common phrases - this matches $\approx 60\%$ of free text responses. Next, we prompt openAI's ChatGPT API (turbo-3.5) with the remaining unclassified examples. The prompt includes a description of each category and several examples. If the LLM is unsure how to classify the string, the prompt instructs it to reply "unsure: [category/all]" and is passed a random sample from the corresponding categories' regexed results. After five attempts, the LLM is forced to provide a final response.

Examples of each category:

- General Visibility - "He was at the PoT with me", "We went together for the treatment", "I stay next to the PoT".
- Communication - "I told him", "Because we haven't talked with her about deworming", "We were talking about it at the shop".
- Social Proximity - "She's my daughter", "Because we are not close friends", "She is a neighbor".
- Incentive - "Showed her the bracelet", "She saw my calendar and asked", "I had ink when we met".
- Type - "They know I take health issues seriously", "Because [I] am the community elder and should be a good example", "Because she knows [I] am concerned with such things like health matters".
- Circumstances - "[I] am pregnant", "[I] am busy", "I have been sickly".

Table B23: First-order Beliefs

Knowledge	First-Order Beliefs		
	Combined (1)	Close (2)	Far (3)
Bracelet			
Doesn't Know	0.174 (0.14, 0.207)	0.192 (0.145, 0.24)	0.151 (0.103, 0.2)
No	0.209 (0.175, 0.243)	0.157 (0.12, 0.195)	0.27 (0.213, 0.327)
Yes	0.618 (0.577, 0.658)	0.65 (0.596, 0.704)	0.579 (0.519, 0.639)
Calendar			
Doesn't Know	0.28 (0.234, 0.325)	0.225 (0.167, 0.283)	0.338 (0.267, 0.408)
No	0.211 (0.175, 0.247)	0.173 (0.129, 0.218)	0.251 (0.194, 0.307)
Yes	0.51 (0.462, 0.557)	0.602 (0.539, 0.664)	0.412 (0.345, 0.478)
Ink			
Doesn't Know	0.219 (0.175, 0.264)	0.221 (0.162, 0.279)	0.218 (0.15, 0.285)
No	0.269 (0.228, 0.31)	0.253 (0.198, 0.308)	0.291 (0.23, 0.353)
Yes	0.512 (0.464, 0.559)	0.526 (0.462, 0.59)	0.491 (0.421, 0.562)
Control			
Doesn't Know	0.304 (0.242, 0.365)	0.248 (0.169, 0.326)	0.371 (0.276, 0.466)
No	0.243 (0.191, 0.295)	0.219 (0.149, 0.29)	0.271 (0.195, 0.348)
Yes	0.453 (0.392, 0.514)	0.533 (0.449, 0.617)	0.358 (0.275, 0.441)

Notes: Point estimates show frequentist means. Parentheses show 95% confidence intervals. Respondents were asked: “Do you think this person came for deworming?” conditional on the respondent recognizing the person within the community randomly drawn by the enumerator. Respondents were asked 10 times. Estimates use 999 individual respondents.

Table B24: Structural ATEs - Robustness

Model	Treatment	Structural			
		Combined (1)	Close (2)	Far (3)	Far - Close (4)
High WTP Prior Mean	Bracelet	0.064 (0.04, 0.089)	0.04 (0.013, 0.068)	0.095 (0.067, 0.123)	0.055 (0.03, 0.082)
High WTP Prior Variance	Bracelet	0.074 (0.048, 0.099)	0.057 (0.03, 0.084)	0.095 (0.065, 0.125)	0.037 (0.014, 0.064)
No WTP Submodel	Bracelet	0.074 (0.05, 0.099)	0.057 (0.03, 0.083)	0.095 (0.069, 0.123)	0.039 (0.016, 0.067)
No Beliefs Submodel	Bracelet	0.081 (0.055, 0.108)	0.072 (0.043, 0.102)	0.093 (0.059, 0.127)	0.021 (-0.013, 0.063)
No Submodels	Bracelet	0.082 (0.057, 0.108)	0.073 (0.044, 0.1)	0.093 (0.059, 0.128)	0.02 (-0.014, 0.056)
High WTP Prior Mean	Calendar	0.051 (0.029, 0.075)	0.047 (0.018, 0.077)	0.057 (0.033, 0.081)	0.01 (-0.013, 0.038)
High WTP Prior Variance	Calendar	0.041 (0.016, 0.065)	0.038 (0.01, 0.064)	0.045 (0.021, 0.068)	0.007 (-0.01, 0.027)
No WTP Submodel	Calendar	0.041 (0.016, 0.064)	0.037 (0.009, 0.064)	0.045 (0.021, 0.067)	0.008 (-0.011, 0.031)
No Beliefs Submodel	Calendar	0.03 (0.005, 0.056)	0.034 (0.004, 0.064)	0.025 (-0.004, 0.056)	-0.009 (-0.037, 0.023)
No Submodels	Calendar	0.03 (0.004, 0.057)	0.034 (0.005, 0.064)	0.024 (-0.004, 0.057)	-0.01 (-0.038, 0.022)
High WTP Prior Mean	Ink	-0.018 (-0.044, 0.009)	-0.046 (-0.074, -0.013)	0.016 (-0.01, 0.043)	0.062 (0.039, 0.089)
High WTP Prior Variance	Ink	-0.018 (-0.044, 0.006)	-0.039 (-0.07, -0.01)	0.008 (-0.019, 0.033)	0.046 (0.024, 0.073)
No WTP Submodel	Ink	-0.018 (-0.042, 0.009)	-0.039 (-0.068, -0.009)	0.008 (-0.016, 0.036)	0.047 (0.026, 0.074)
No Beliefs Submodel	Ink	-0.018 (-0.045, 0.01)	-0.037 (-0.069, -0.006)	0.007 (-0.025, 0.041)	0.044 (0.01, 0.084)
No Submodels	Ink	-0.019 (-0.045, 0.008)	-0.038 (-0.069, -0.006)	0.005 (-0.025, 0.039)	0.043 (0.007, 0.08)
High WTP Prior Mean	Bracelet - Calendar	0.013 (-0.005, 0.033)	-0.007 (-0.026, 0.013)	0.038 (0.013, 0.062)	0.044 (0.023, 0.066)
High WTP Prior Variance	Bracelet - Calendar	0.033 (0.015, 0.051)	0.019 (0.005, 0.036)	0.049 (0.026, 0.074)	0.03 (0.011, 0.05)
No WTP Submodel	Bracelet - Calendar	0.033 (0.018, 0.049)	0.019 (0.006, 0.036)	0.05 (0.029, 0.072)	0.031 (0.013, 0.053)
No Beliefs Submodel	Bracelet - Calendar	0.051 (0.023, 0.078)	0.038 (0.011, 0.067)	0.068 (0.029, 0.106)	0.03 (-0.011, 0.071)
No Submodels	Bracelet - Calendar	0.052 (0.024, 0.077)	0.039 (0.013, 0.068)	0.069 (0.029, 0.105)	0.03 (-0.009, 0.067)
High WTP Prior Mean	Control mean	0.331 (0.314, 0.35)	0.402 (0.379, 0.424)	0.243 (0.223, 0.263)	-0.159 (-0.181, -0.137)
High WTP Prior Variance	Control mean	0.331 (0.311, 0.35)	0.397 (0.374, 0.419)	0.248 (0.227, 0.271)	-0.149 (-0.171, -0.128)
No WTP Submodel	Control mean	0.331 (0.312, 0.35)	0.398 (0.377, 0.42)	0.248 (0.226, 0.268)	-0.15 (-0.173, -0.129)
No Beliefs Submodel	Control mean	0.332 (0.313, 0.352)	0.395 (0.372, 0.417)	0.254 (0.231, 0.276)	-0.141 (-0.167, -0.116)
No Submodels	Control mean	0.332 (0.314, 0.35)	0.395 (0.373, 0.417)	0.255 (0.231, 0.279)	-0.14 (-0.166, -0.117)

Notes: Point estimates shown are posterior medians. Parentheses show 95% credibility intervals. Bracelet - Calendar shows the posterior of the difference between the bracelet and calendar treatment effect. Far - Close shows the posterior of the difference between the close and far treatment effect. The model is estimated using Hamiltonian Monte-Carlo in Stan with 4 chains, 400 warm-up draws, and 400 samples. Sampler diagnostics report 0 divergent transitions and split $\hat{R} < 1.1$ for all samples. Model estimated using 9,805 observations. A short description of each model is given below:

- ‘High WTP Prior Mean’ - the prior mean on the value of money in terms of distance walked is given by: $N(0.265, 0.0001)$.
- ‘High WTP Prior Variance’ - the prior variance on the value of money in terms of distance walked is given by: $\log N(-10, 4)$.
- No WTP Submodel - the WTP data isn’t used in the joint likelihood.
- No Beliefs Submodel - the beliefs data isn’t used in the joint likelihood.
- No Submodel - Neither the WTP or beliefs data are used in the joint likelihood.

Table B25: Structural ATEs - Robustness to Clustering

Dependent variable: Take-up	Structural			
	Combined (1)	Close (2)	Far (3)	Far - Close (4)
<i>Panel A: Overall</i>				
Bracelet	0.086 (0.055, 0.117)	0.054 (0.019, 0.088)	0.126 (0.086, 0.163)	0.073 (0.034, 0.113)
Calendar	0.022 (-0.01, 0.055)	0.013 (-0.024, 0.049)	0.033 (-0.009, 0.072)	0.02 (-0.019, 0.058)
Ink	-0.015 (-0.05, 0.022)	-0.052 (-0.088, -0.014)	0.031 (-0.012, 0.073)	0.083 (0.047, 0.119)
Bracelet - Calendar	0.064 (0.04, 0.089)	0.041 (0.015, 0.069)	0.093 (0.059, 0.125)	0.053 (0.019, 0.089)
Control mean	0.329 (0.307, 0.356)	0.408 (0.382, 0.435)	0.231 (0.202, 0.266)	-0.177 (-0.207, -0.148)

Notes: Point estimates shown are posterior medians. Estimating equation is identical to main structural specification but also allows for variance of cluster level shock to vary with each cluster. Parentheses show 95% credibility intervals. Bracelet - Calendar shows the posterior of the difference between the bracelet and calendar treatment effect. Far - Close shows the posterior of the difference between the close and far treatment effect. The model is estimated using Hamiltonian Monte-Carlo in Stan with 4 chains, 400 warm-up draws, and 400 samples. Sampler diagnostics report 0 divergent transitions and split $\hat{R} < 1.1$ for all samples. Model estimated using 9,805 observations.

C Optimisation Appendix

Table C1: Social Planner’s Solution - Optimal Pigovian Subsidy

Treatment	Welfare Maximising Distance		
	Dynamic $\Delta(w^*)$	Fixed $\Delta(w^*) _{d=0.5km}$	Fixed - Dynamic
Bracelet	2948	2719	-228
	(1239, 5077)	(1331, 4332)	(-684, -14)
Calendar	2169	2057	-116
	(1116, 3344)	(1176, 2958)	(-302, -11)
Ink	2860	2522	-342
	(1235, 4939)	(1256, 3954)	(-956, -38)
Control	2019	1903	-116
	(1064, 2958)	(1121, 2588)	(-263, -20)

Notes: Point estimates show posterior means, parentheses show 95% posterior credibility intervals. Posterior means and credibility intervals are estimated by solving the social planner’s optimisation problem across 500 random posterior samples drawn from the relevant structural model. The ‘Dynamic’ estimates use $\Delta(w^*)$ as estimated from the structural model. The ‘Fixed’ estimates find the value of signals $\Delta(w^*(d))|_{d=0.5km}$ fixing distance at $0.5km$ but otherwise allowing distance to influence private benefit and μ .

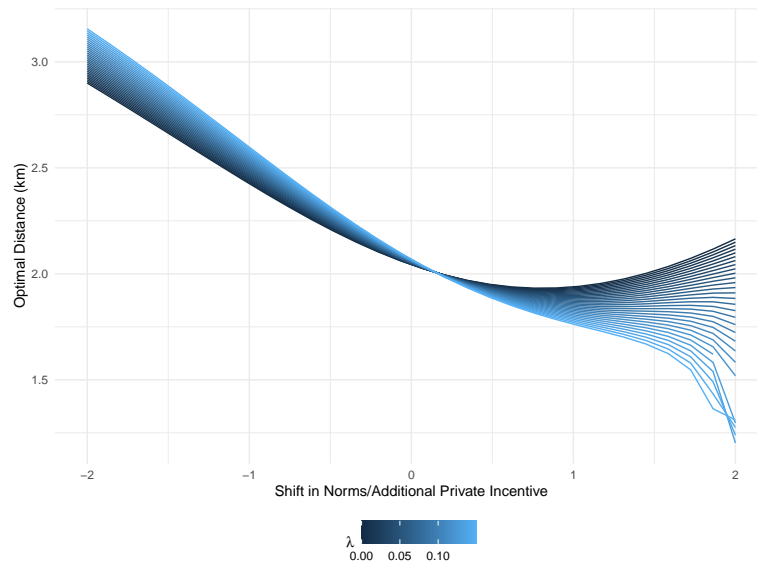


Figure C1: Optimal Point of Treatment Distance – Varying Deadweight Cost

Notes: This figure shows the expected welfare maximizing Point of Treatment distance as private incentives to deworm varies (equivalent to a shift in norms) in the control arm as the deadweight cost of public funds changes. The effect of the social multiplier, leading to amplification and mitigation and curvature in the distance-incentive trade-off, is dampened as the cost of public funds increases since the deadweight loss starts to dominate the social welfare function.

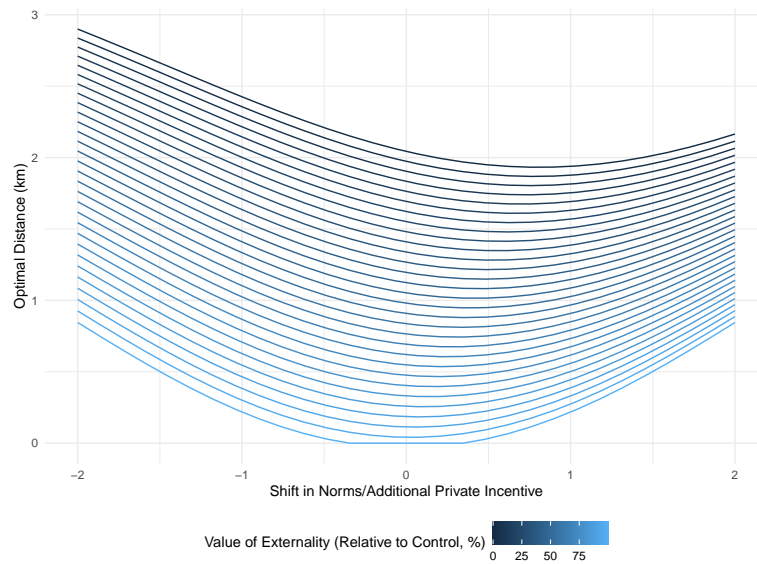


Figure C2: Optimal Point of Treatment Distance – Varying Externality

Notes: This figure shows the expected welfare maximizing Point of Treatment distance as private incentive to deworm varies in the control arm as the size of the deworming externality changes. The value of the externality is increased from 0% of the control private benefit to 100% of the control private benefit, in lighter blue. As the value of the externality increases, the curvature of the distance-incentive trade-off increases and shifts downwards.

Table C2: Posterior Estimates of Number of Points of Treatment Required

Private benefit	Visibility	Maximum distance constraint (km)	Assigned PoTs	Mean take-up	Mean distance (km)
Panel A: Random allocation					
Control	Control		144	0.33 (0.31, 0.346)	1.2
Panel B: Policymaker allocation, 2.5km					
Control	Control	2.5	116 (116, 119)	0.34 (0.329, 0.352)	1.15 (1.06, 1.167)
Control	Signal value fixed at bracelet 0.5km	2.5	116 (116, 116)	0.36 (0.339, 0.39)	1.16 (1.151, 1.167)
Control	Bracelet	2.5	116 (116, 116)	0.37 (0.344, 0.399)	1.15 (1.151, 1.167)
Control	No Visibility	2.5	144 (144, 144)	0.174 (0.101, 0.259)	0.58 (0.58, 0.58)
Panel C: Policymaker allocation, 3.5km					
Control	Control	3.5	107 (100, 114)	0.33 (0.329, 0.331)	1.26 (1.11, 1.411)
Control	Signal value fixed at bracelet 0.5km	3.5	96 (86, 105)	0.33 (0.329, 0.331)	1.52 (1.297, 1.758)
Control	Bracelet	3.5	90 (79, 102)	0.33 (0.329, 0.33)	1.68 (1.364, 1.957)
Control	No Visibility	3.5	144 (144, 144)	0.174 (0.101, 0.259)	0.58 (0.58, 0.58)
Panel D: Policymaker allocation, 4.5km					
Control	Control	4.5	107 (100, 114)	0.33 (0.329, 0.332)	1.27 (1.123, 1.416)
Control	Signal value fixed at bracelet 0.5km	4.5	96 (86, 105)	0.33 (0.329, 0.331)	1.51 (1.299, 1.758)
Control	Bracelet	4.5	90 (79, 102)	0.33 (0.329, 0.331)	1.68 (1.374, 1.957)
Control	No Visibility	4.5	144 (144, 144)	0.174 (0.101, 0.259)	0.58 (0.58, 0.58)
Panel E: Policymaker allocation, 5.5km					
Control	Control	5.5	106 (99, 113)	0.33 (0.329, 0.331)	1.33 (1.145, 1.507)
Control	Signal value fixed at bracelet 0.5km	5.5	96 (86, 105)	0.33 (0.329, 0.332)	1.52 (1.294, 1.758)
Control	Bracelet	5.5	90 (79, 102)	0.33 (0.329, 0.331)	1.67 (1.364, 1.953)
Control	No Visibility	5.5	144 (144, 144)	0.174 (0.101, 0.259)	0.58 (0.58, 0.58)
Panel F: Policymaker allocation, 10km					
Control	Control	10.0	106 (99, 113)	0.33 (0.329, 0.331)	1.51 (1.257, 1.755)
Control	Signal value fixed at bracelet 0.5km	10.0	96 (86, 105)	0.33 (0.329, 0.332)	1.57 (1.309, 1.876)
Control	Bracelet	10.0	90 (79, 102)	0.33 (0.329, 0.332)	1.69 (1.374, 2.007)
Control	No Visibility	10.0	144 (144, 144)	0.174 (0.101, 0.259)	0.58 (0.58, 0.58)

Notes: Point estimates show posterior medians, parentheses show 95% posterior credibility intervals. Credibility intervals are omitted for the random allocation panel for ‘Assigned PoTs’ and ‘Mean distance (km)’ since these are fixed across posterior draws. Posterior medians and credibility intervals are estimated by solving an integer linear program across 200 random posterior samples drawn from the relevant structural model. Maximum distance constraint denotes the furthest distance a decision maker can allocate a community to walk to reach a PoT.

Table C3: Posterior Estimates of Number of Points of Treatment Required: Fixing Model Components

Fix distance	Assigned PoTs	Mean take-up	Mean distance (km)
<i>Panel A: No Fixing</i>			
	78 (73, 83)	0.33 (0.329, 0.332)	2.02 (1.839, 2.274)
<i>Panel B: Fix μ</i>			
0	82 (77, 90)	0.33 (0.329, 0.331)	1.87 (1.654, 2.026)
1250	79 (74, 84)	0.33 (0.329, 0.332)	1.98 (1.828, 2.151)
2500	77 (73, 83)	0.33 (0.329, 0.333)	2.07 (1.856, 2.334)
<i>Panel C: Fix $\Delta(w^*)$</i>			
0	85 (79, 94)	0.33 (0.329, 0.331)	1.78 (1.567, 1.957)
1250	81 (77, 85)	0.33 (0.329, 0.331)	1.91 (1.785, 2.027)
2500	76 (73, 81)	0.33 (0.329, 0.332)	2.1 (1.895, 2.34)

Notes: This table shows the number of points of treatment required, using the bracelet private incentive and visibility condition, but fixing the μ and $\Delta(w^*)$ components respectively. Point estimates show posterior medians, parentheses show 95% posterior credibility intervals. Posterior medians and credibility intervals are estimated by solving an integer linear program across 200 random posterior samples drawn from the relevant structural model. Maximum distance constraint denotes the furthest distance a decision maker can allocate a community to walk to reach a PoT.

D Online Appendix

A Site Selection and Randomization

We randomly selected 158 clusters in the three study counties, of which 144 were used in the study.³² Each cluster was defined as a treatment location and targeted community pair. We used the location of primary schools as proxies to (i) identify acceptable locations to set up our treatment locations and (ii) to find communities to target with our informational campaign and data collection. We relied on the high geographic density of primary schools in the study counties to select both treatment locations and targeted communities.³³ To select our clusters from the pool of a total of 1,451 primary schools in our study area, we used an acceptance-rejection method whereby we randomly picked schools, checked their acceptability based on their overlap with already selected clusters, and if accepted added them to our selected sample. This process was repeated until we had selected the requisite number of clusters. If no acceptable schools remained before completion, the whole process was restarted. Each cluster, centered on its treatment location, had a 2.5 kilometer radius catchment circle and 3-4 kilometer radius buffer circle. A cluster was considered acceptable if its buffer circle did not leave any of the already selected clusters' non-overlapping catchment circles smaller than an a pre-specified size. Figure A16 shows the final cluster selection. After all clusters were selected, we randomly assigned each cluster to be either a "Close" or "Far" cluster.³⁴ We then selected for each cluster, from its non-overlapping catchment circle and according to its assigned distance treatment, a primary school as an anchor for us to locate its targeted community. Clusters were then randomly assigned, stratified over counties and distance treatment, to the different signal/incentive treatments: control, ink, calendar and bracelet. To finalize the cluster selection process, we surveyed the treatment location and target community anchor schools. For the treatment locations we confirmed that treatment would be feasible there and identified alternative treatment locations, close to the selected schools, as potential backups. For the anchor schools, we identified all the communities near them and randomly selected one community to target.³⁵

B Information Gain From Signals

Let p denote the probability an individual gets dewormed and $p_{s|d}$ the probability an individual shows a signal conditional on getting dewormed. That is, $p_{s|d}$ is the probabil-

³²We only intended to use 150 clusters, and only included eight extra clusters as fallback clusters. For various practical reasons, implementation was only possible in 144 clusters.

³³Geographic coordinates for primary schools were retrieved from the Kenya Open Data Portal (<http://www.opendata.go.ke/>).

³⁴Randomization was stratified within counties.

³⁵In some cases because the initial community was too small, we added a second community.

ity an individual keeps their bracelet/ink visible after getting dewormed. Entropy and conditional entropy are therefore defined as:

$$\begin{aligned}
H(\text{Deworm}) &= -P(d) \log(P(d)) - (1 - P(d)) \log(1 - P(d)) \\
H(\text{Deworm}|\text{Signal}) &= -P(d, s) \log\left(\frac{P(d, s)}{P(s)}\right) - P(s^c, d) \log\left(\frac{P(s^c, d)}{P(s)}\right) \\
&\quad - P(s, d^c) \log\left(\frac{P(s, d^c)}{P(s)}\right) - P(s^c, d^c) \log\left(\frac{P(s^c, d^c)}{P(s)}\right)
\end{aligned}$$

With mutual information:

$$I(\text{Deworm}; \text{Signal}) = H(\text{Deworm}) - H(\text{Deworm}|\text{Signal})$$

To calculate the probability of signaling given being dewormed, $P(S|D)$, we take the fraction of individuals that report receiving the ink incentive at the point of treatment in the ink arm (0.95), and the fraction of individuals that still have the bracelet at endline in the bracelet arm (0.81)³⁶. Given $P(S = 1|D = 0)$ is mechanically 0 and we can estimate $P(D)$ as a function of distance we have enough information to compute $I(\text{Deworm}(d); \text{Signal}(d))$. Figure B1 shows that signals become more informative about an individual's actions as distance increases, consistent with the larger treatment effects for first- and second-order beliefs observed in the Bracelet and Calendar Arm for the Far versus Close condition.

³⁶We can't use the fraction of individuals that still have ink on their thumbs since by the time of the endline survey, this has typically worn off.

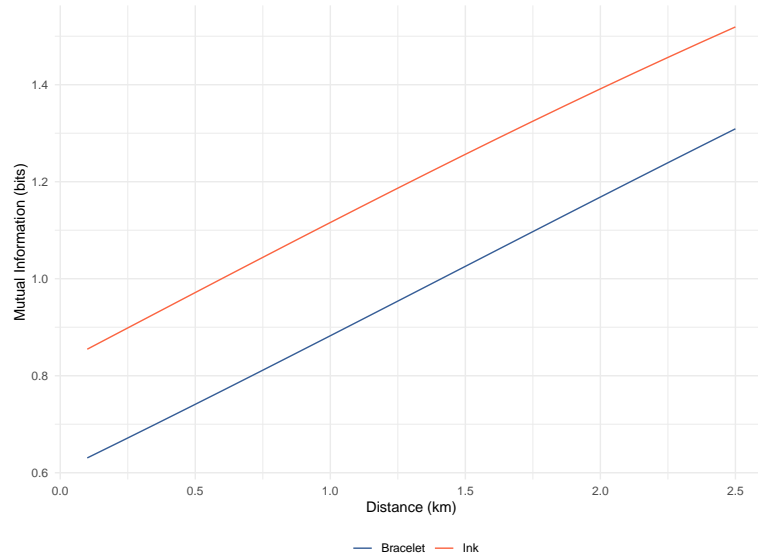


Figure B1: Reduction in Uncertainty From Conditioning On Signals (bits)

Notes: This figure shows a simulated calibration of information gain as distance increases using the deworming take-up rate in close and far and compliance with bracelet and ink wearing. As distance increases in the ink and bracelet arm, an individual's signal is more informative about their deworming status.

C Continuous Distance Randomization Inference

As an additional check to ensure distance as a continuous measure does not vary systematically with baseline covariates we regress each covariate on distance to the closest assigned point of treatment and report the t -statistic. Next, we permute through 500 random permutations of assigned distance to the point of treatment and record the distribution of t -statistics. Figure C1 shows the distribution of t -statistics under the null hypothesis with the vertical line denoting the realised t -statistic. Exact p -values are shown in the upper right-hand corner of each panel. We are unable to reject the null hypothesis for any of the 11 variables, with $p > 0.1$ throughout.

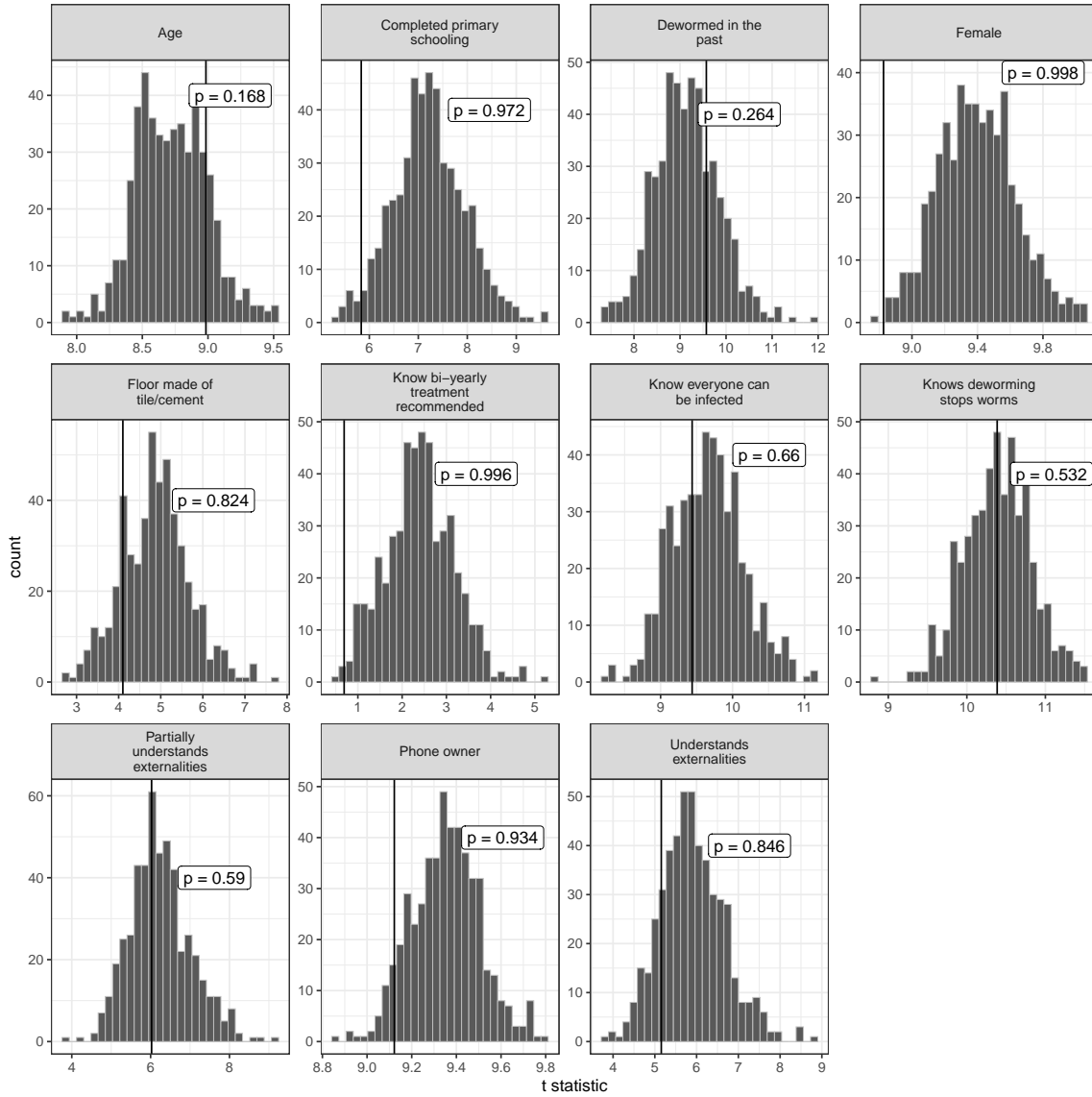


Figure C1: Randomization Distribution – Baseline Covariates and Distance to PoT

Notes: This plot shows the randomization distribution of test statistics from using OLS to regress baseline covariates on distance to the closest point of treatment, with strata fixed effects and clustered standard errors. The realised test statistic is depicted by the vertical line. The t-stat is the test statistic used in the randomization inference. Plot labels show exact p -values, that is, the probability of observing a test statistic at least as extreme as the realised test statistic. Across all baseline covariates the exact p -value is less than 10% which suggests our randomization was successful.

D Confounds

To test whether additional factors interact with social image concerns to produce heterogeneous treatment effects we construct a variety of baseline, community level covariates and regress deworming on these covariates and their interactions alongside the standard dummies for our treatment groups. Given we can only measure these factors at the community level we are not powered to detect heterogeneous treatment effects and our results should be interpreted with caution. We measure four factors: A baseline ‘Judgemental score’ which captures how likely a community is to praise or stigmatize a given health action; an ‘Externality knowledge’ covariate which measures the fraction of individuals in a given community that are aware of the externality imposed by worms; a ‘Number of people recognised in community’ average which is designed to proxy for the level of social connectedness within a community; and finally a measure of ethnic fractionalization, which we label simply ‘Fractionalization’.

Table D1 shows the results from a frequentist Probit regression of deworming on the standard saturated Close/Far and incentive dummies alongside each covariate listed above. The only precisely measured effect is in column 3 which shows that the level of deworming takeup is higher in communities with a greater social connectedness index. The binomial likelihood in our beliefs sub-model in the structural model explicitly accounts for the fact that some individuals recognize more people in their community so this cannot drive our main result alone. Unfortunately, whilst the coefficient on ‘Judgemental score’ is positive and corroborates our hypothesis that social norms are a strong incentive for individuals to get dewormed, the standard error is larger than the point estimate and it is hard to conclude much given the level of uncertainty. This shouldn’t be too surprising since we see very little variation in judgemental score across communities so precisely estimating an effect is particularly hard in our setting.

Table D1: Deworming Takeup: Additional Covariates

Model:	(1)	(2)	(3)	(4)
<i>Variables</i>				
Judgemental score	0.1017 (0.1788)			
Externality knowledge		0.2289 (0.2074)		
Number of people recognised in community, village mean			0.0725*** (0.0214)	
Fractionalisation				0.2370 (0.9701)
<i>Fixed-effects</i>				
county	Yes	Yes	Yes	Yes
<i>Fit statistics</i>				
Observations	9,626	9,746	9,805	9,805
Squared Correlation	0.03024	0.03132	0.03829	0.03113
Pseudo R ²	0.02393	0.02479	0.02990	0.02454
BIC	12,327.6	12,466.2	12,507.0	12,566.4

Clustered (cluster.id) standard-errors in parentheses
*Signif. Codes: ***: 0.01, **: 0.05, *: 0.1*

Notes: This table shows frequentist probit estimates of deworming, controlling for additional covariates. Each specification estimates $Pr(Y_{ic}) = \Phi(X_{ic}\beta + \sum_{z=1}^4 \sum_{d=1}^2 \beta_{z,d} \text{treatment}_{ic,z} \times \text{distance group}_{ic,d})$, where X_c corresponds to the cluster (community) level covariate defined below. Judgemental score is defined as the probability an individual praises deworming and stigmatises not deworming, averaged at the community level. Externality knowledge is defined as the fraction of individuals in a community aware that they can infect their neighbours with worms or vice versa. Number of people recognised in community is defined as the number of people randomly sampled from the community out of 10 that a respondent recognises, averaged at the community level. Fractionalization is defined as $1 - \sum_j s_{ij}^2$ where s_{ij} refers to the share of individuals identifying as ethnicity j in community i .

In Table D2 we interact the baseline covariate with a dummy if the community was in any treatment arm that received an incentive in a bid to pool sample and increase power. Again, the social connectedness index is the only significant predictor but we fail to reject, across all covariates, the null hypothesis of homogeneous treatment effects across the incentive and non-incentive arms. Given our limited power to detect even level shifts we have little chance of precisely capturing differential treatment effects – overall, it seems safe to conclude there aren't huge differential effects across arms but it is difficult to say much more conclusively.

Table D2: Deworming Takeup: Treatment Heterogeneity Additional Covariates

Model:	(1)	(2)	(3)	(4)
<i>Variables</i>				
Judgemental score \times (Any incentive = False)	0.2475 (0.3985)			
Judgemental score \times (Any incentive = True)	0.0385 (0.1840)			
Externality knowledge \times (Any incentive = False)		0.5839 (0.6165)		
Externality knowledge \times (Any incentive = True)		0.1096 (0.1821)		
Number of people recognised in community, village mean \times (Any incentive = False)			0.0696** (0.0345)	
Number of people recognised in community, village mean \times (Any incentive = True)			0.0738*** (0.0271)	
Fractionalisation \times (Any incentive = False)				0.9721 (2.953)
Fractionalisation \times (Any incentive = True)				0.0682 (0.8820)
Homogeneous effects across ‘Any incentive’, p -value	0.6299	0.4682	0.9237	0.7611
<i>Fixed-effects</i>				
county	Yes	Yes	Yes	Yes
<i>Fit statistics</i>				
Observations	9,626	9,746	9,805	9,805
Squared Correlation	0.03032	0.03174	0.03828	0.03116
Pseudo R ²	0.02405	0.02531	0.02991	0.02456
BIC	12,335.3	12,468.9	12,516.2	12,575.3

Clustered standard-errors in parentheses

Significance level: ***: 0.01, **: 0.05, *: 0.1

Notes: This table shows frequentist probit estimates of deworming, controlling for additional covariates. Each specification estimates $Pr(Y_{ic}) = \Phi(X_c\beta + X_c \times \text{any incentive}_c\gamma + \sum_{z=1}^4 \sum_{d=1}^2 \beta_{z,d} \text{treatment}_{cz} \times \text{distance group}_{cd})$, where ‘any incentive’ is a dummy variable taking value 1 if the community is assigned to the bracelet, calendar, or ink condition. X_c corresponds to the cluster (community) level covariate defined below. Homogeneous effects across ‘Any incentive’, p -value test the null hypothesis that $\beta = \gamma$ i.e. additional covariates have no heterogeneous effects across control and treatment arms. Judgemental score is defined as the probability an individual praises deworming and stigmatises not deworming, averaged at the community level. Externality knowledge is defined as the fraction of individuals in a community aware that they can infect their neighbours with worms or vice versa. Number of people recognised in community is defined as the number of people randomly sampled from the community out of 10 that a respondent recognises, averaged at the community level. Fractionalization is defined as $1 - \sum_j s_{ij}^2$ where s_{ij} refers to the share of individuals identifying as ethnicity j in community i .

E Priors

We use a Bayesian approach to estimate this structural model directly as it is specified above, and therefore we need to further specify the distributions from which we draw our parameters,

$$\begin{aligned}\theta^{\text{takeup}} &= (\beta^{\text{intercept}}, \beta^{\text{ink}}, \beta^{\text{calendar}}, \gamma, \mu_0, \sigma_u)' \\ \theta^{\text{wtp}} &= (\mu^{\text{wtp}}, \sigma^{\text{wtp}})' \\ \theta^{\text{bel}} &= (\beta^{\text{bel}}, \delta^{\text{bel}})'\end{aligned}$$

For treatment effect parameters such as the β parameters, we use regularizing priors that center on zero. This means that unless there is sufficient evidence from the data we will assume that the incentives do not change people's beliefs about the observability of their actions and do not give them an extra private benefit. In other words, we do not exclude the possibility of social signaling for all the incentives, rather we assume that they are not different.

We set informative priors on two other parameters that are not well identified in this model. For the γ parameter we set a strongly informative prior keeping it positive, but very close to zero. What we are modeling here is our ignorance about the utility of the difference in the monetary value of calendars and bracelets. Similarly, for the σ_u parameters we set an inverse Gamma distribution prior, keeping this parameter away from a small region close to zero. We make this assumption for algorithm tractability, but again this conservative assumption would only make it harder for us to pick up any social signaling effects; higher values of σ_u make the Δ^* function flatter as people find it harder to separate the private and prosocial motivation of those who get dewormed.

F Alternative Model Results

F.1 Private Costs and Community Social Image Returns

One alternative model incorporates household’s distance cost directly in the decision to deworm, but due to uncertainty in the community over the distance cost a household faces, they only reap the social image return associated with traveling from the community centroid. That is, the cut-off type is determined by the centroid’s distance cost, \bar{d} , but individuals choose to take the action based off their own private cost, d , aware of the fact they will earn a social image return from $w^*(\bar{d})$.³⁷ This gives rise to the following model:

$$w^*(z, \bar{d}) = -(z \cdot \beta_z - \bar{d} \cdot \delta) - \mu(z, \bar{d})\Delta(w^*(z, \bar{d}))$$

Therefore, an individual decides to deworm if:

$$z \cdot \beta_z - d \cdot \delta + \mu(z, \bar{d})\Delta(w^*(z, \bar{d})) + w > 0$$

which, after substituting $w^*(z, \bar{d})$ into the inequality, gives the probability of deworming as:

$$Pr(\text{Deworm}|d, \bar{d}, z) = F_w(-w^*(z, \bar{d}) + \delta(\bar{d} - d))$$

i.e., an individual’s decision to deworm corresponds to the cut-off type plus an additional offset depending on how much further or closer they are to the treatment location compared to the community centroid. Table F1 shows results from the adjusted model. Ink has a negative treatment effect, even in far communities, but again displays a more positive effect in far compared to close communities, although the difference is not statistically significant. The Control mean and treatment effects for Bracelet and Calendar are similar to those in our main specification.

F.2 Private Costs and Full Information

Alternatively a household’s distance cost enters in both the private decision to deworm and the social image return an individual reaps – each individual has full knowledge of everyone’s location and therefore private cost. This model is essentially identical to our main specification but instead of solving the fixed point for each community, it solves the fixed point determining social image returns at each observed household distance. Table F2 shows results from this model. Ink has a negative treatment effect, even in far communities, but effects are now flat across far and close communities. The Control mean

³⁷Here we ignore any higher order beliefs about the type of people that would deworm since those closer to the treatment location earn a higher social image return than they ‘should’ given their private distance cost, and so therefore have on average a lower type than the cut-off type.

and treatment effects for Bracelet and Calendar are similar to our main specification.

Table F1: Structural ATEs – Household Distance Cost, Community Social Image Returns

Dependent variable: Take-up	Structural			
	Combined (1)	Close (2)	Far (3)	Far - Close (4)
Panel A: Overall				
Bracelet	0.065 (0.041, 0.09)	0.041 (0.016, 0.066)	0.098 (0.072, 0.128)	0.057 (0.035, 0.084)
Calendar	0.027 (0.004, 0.051)	0.025 (-0.005, 0.052)	0.035 (0.014, 0.058)	0.01 (-0.007, 0.034)
Ink	-0.031 (-0.055, -0.006)	-0.041 (-0.072, -0.011)	-0.025 (-0.048, -0.002)	0.016 (-0.008, 0.044)
Bracelet - Calendar	0.038 (0.023, 0.053)	0.016 (0.002, 0.032)	0.063 (0.044, 0.087)	0.046 (0.031, 0.067)
Control mean	0.34 (0.322, 0.36)	0.407 (0.382, 0.43)	0.258 (0.239, 0.277)	-0.149 (-0.171, -0.127)

Notes: This model uses community centroid distance to the treatment location to solve for the fixed point, giving the cut-off type at each community, but the household distance enters the private decision to deworm. Point estimates shown are posterior medians. Parentheses show 95% credibility intervals. Far - Close shows the posterior of the difference between the close and far treatment effect. The model is estimated using Hamiltonian Monte-Carlo in Stan with 2 chains, 400 warm-up draws, and 400 samples. Sampler diagnostics report 0 divergent transitions and split $\hat{R} < 1.1$ for all samples. The model is estimated using 9,805 observations.

Table F2: Structural ATEs – Household Distance Cost, Household Social Image Returns

Dependent variable: Take-up	Structural			
	Combined (1)	Close (2)	Far (3)	Far - Close (4)
Panel A: Overall				
Bracelet	0.064 (0.039, 0.088)	0.045 (0.019, 0.07)	0.09 (0.063, 0.117)	0.045 (0.028, 0.064)
Calendar	0.025 (0.002, 0.05)	0.021 (-0.007, 0.05)	0.034 (0.009, 0.056)	0.013 (-0.003, 0.032)
Ink	-0.031 (-0.054, -0.007)	-0.035 (-0.061, -0.004)	-0.035 (-0.062, -0.01)	0 (-0.02, 0.023)
Bracelet - Calendar	0.039 (0.021, 0.055)	0.024 (0.006, 0.042)	0.056 (0.035, 0.077)	0.032 (0.019, 0.046)
Control mean	0.342 (0.325, 0.36)	0.405 (0.384, 0.427)	0.264 (0.245, 0.282)	-0.141 (-0.16, -0.122)

Notes: Model uses household distance to the treatment location to solve for both the fixed point, giving the cut-off type at each household, and private decision to deworm. Point estimates shown are posterior medians. Parentheses show 95% credibility intervals. Far - Close shows the posterior of the difference between the close and far treatment effect. The model is estimated using Hamiltonian Monte-Carlo in Stan with 2 chains, 400 warm-up draws, and 400 samples. Sampler diagnostics report 0 divergent transitions and split $\hat{R} < 1.1$ for all samples. Model estimated using 9,805 observations.

Table F3: Structural ATEs – Overdispersed Clusters Removed

Dependent variable: Take-up	Structural			
	Combined (1)	Close (2)	Far (3)	Far - Close (4)
<i>Panel A: Overall</i>				
Bracelet	0.07 (0.046, 0.094)	0.056 (0.029, 0.081)	0.089 (0.061, 0.118)	0.033 (0.012, 0.058)
Calendar	0.041 (0.018, 0.067)	0.041 (0.013, 0.07)	0.042 (0.02, 0.066)	0.001 (-0.016, 0.022)
Ink	-0.025 (-0.052, 0)	-0.042 (-0.071, -0.012)	-0.004 (-0.028, 0.02)	0.038 (0.018, 0.063)
Bracelet - Calendar	0.029 (0.013, 0.048)	0.015 (0.001, 0.031)	0.047 (0.022, 0.071)	0.032 (0.013, 0.053)
Control mean	0.334 (0.315, 0.354)	0.398 (0.374, 0.422)	0.252 (0.23, 0.276)	-0.147 (-0.172, -0.12)

Notes: Model uses main specification but clusters with a mean squared distance to the cluster centroid of each household greater than 0.5km are removed. Point estimates shown are posterior medians. Parentheses show 95% credibility intervals. Far - Close shows the posterior of the difference between the close and far treatment effect. The model is estimated using Hamiltonian Monte-Carlo in Stan with 2 chains, 400 warm-up draws, and 400 samples. Sampler diagnostics report 0 divergent transitions and split $\hat{R} < 1.1$ for all samples.

G Sensitivity to w Distributional Assumptions

This section discusses the implications of alternative distributional assumptions over w and provides simulations when w follows a bimodal distribution.

The social multiplier will exist provided A) $\mu \neq 0$ i.e there must be visibility, and B) $\Delta' \neq 0$ – as the cut-off type changes, there must be a change in social image returns. One case where the latter doesn't hold is for the uniform distribution over types, if this is the case there's no change in honor or stigma from a change in cut-off type as the gain in honor is exactly offset by the decrease in stigma and vice-versa. One concern may be that there exists a bi-modal distribution of types, those that care about deworming and those who vehemently oppose deworming, and that this distribution of types is somehow correlated with the distance individuals have to travel to get treated. Below we show, using simulations, that if this is the case, we'd expect a distance region to exist where treatment effects are flat – i.e. we are moving between the two modes where there's no density and therefore in this region the density is approximately flat and no social multiplier exists. Whilst we observe a "flattening" of the demand curve for deworming takeup as a function of distance, we never observe regions which are invariant to the effect of distance. Therefore, whilst the Gaussianity assumption we make is a strong one, to generate a social multiplier we only require the density of types to be locally non-flat in the region of the experiment considered. Finally, our model essentially nests the case where $\Delta' = 0$ by allowing for the idiosyncratic shock u_i – if σ_u is large enough the Gaussian density will essentially be flat over the small region of w we consider and therefore the social multiplier will equal approximately one. In reality, we estimate that σ_u is relatively small and the net social image return displays significant curvature, generating the amplification and mitigation effects we observe in our study.

Figure F1 shows two simulated densities for v^* , in red is a unimodal, Gaussian density and in blue a Gaussian mixture model with two, distinct modes designed to represent pro-deworming and anti-deworming groups. Figure F2 shows the effect of changing the private incentives, i.e. reducing distance as b increases, on deworming take-up. The bi-modality, where both groups are distinct, leads to flat regions where distance has no effect on takeup. In turn, this leads to the net social image return shown in Figure F3 – there are regions where the social image return is constant since changing distance leads to no change in the cut-off type over this region. Finally, we show the implications for the social multiplier in Figure F4, whilst the Gaussian density always admits a multiplier not equal to one, there are regions of the private incentive where the multiplier is flat under a bimodal type density.

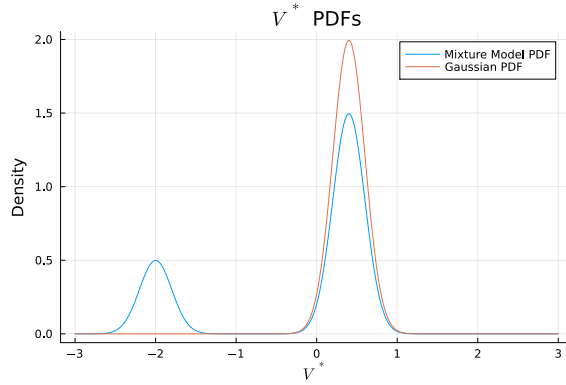


Figure F1: Bimodal Density for V Versus Unimodal (Gaussian)

Notes: This plot shows the simulated density for a bimodal type distribution vs unimodal type distribution

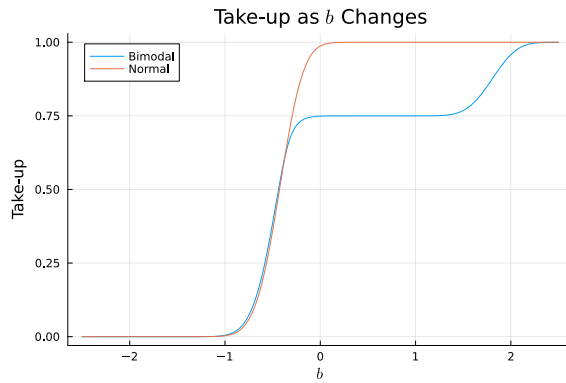


Figure F2: Take-up as Private Incentive Changes, Unimodal vs Bimodal

Notes: This plot shows the simulated take-up of deworming pills for a bimodal type distribution vs unimodal type distribution.

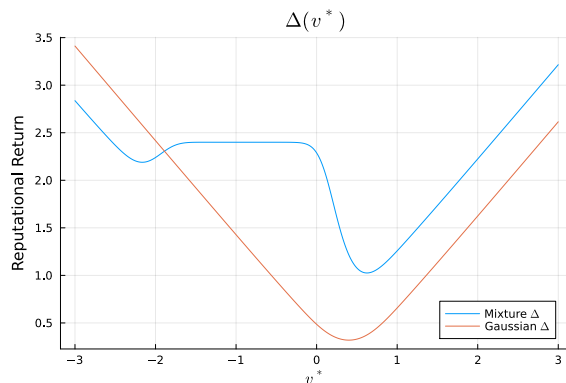


Figure F3: $\Delta(v^*)$ as Private Incentive Changes, Unimodal vs Bimodal

Notes: This plot shows the simulated social image return for a bimodal type distribution vs unimodal type distribution

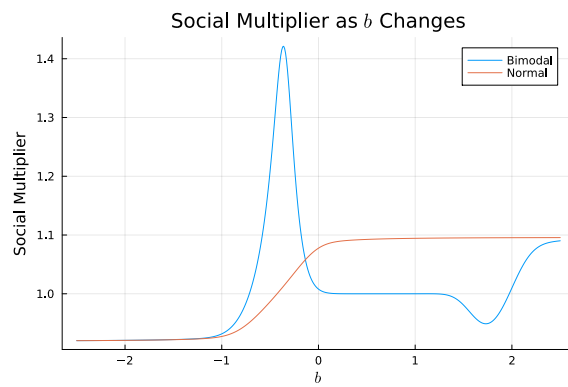


Figure F4: Social Multiplier as Private Incentive Changes, Unimodal vs Bimodal

Notes: This plot shows the simulated social multiplier for a bimodal type distribution vs unimodal type distribution

H Rate of Change Results

Since the social multiplier estimates confound both the direct visibility effect, a change in μ , with the indirect effect of visibility, w^* changing as equilibrium beliefs change. We also report results that fix the cutoff type w^* at the control level:

$$\Gamma(\tilde{z}, \tilde{d}) = \left. \frac{\partial E[Y(z, d, w)]}{\partial d} \right|_{\substack{z=\tilde{z} \\ d=\tilde{d} \\ w=w^*(\text{control}, \tilde{d})}} - \left. \frac{\partial E[Y(z, d, w)]}{\partial d} \right|_{\substack{z=\text{control} \\ d=\tilde{d} \\ w=w^*(\text{control}, \tilde{d})}}$$

where $\frac{\partial E[Y(z, d, w)]}{\partial d} = -f_w(w) \cdot \frac{\delta - \frac{\partial \mu(z, d)}{\partial d} \Delta(w)}{1 + \mu(z, d) \Delta'(w)}$ which gives the direct effect of visibility, with no endogenous adjustment of the cutoff type. Fixing w^* let's us decompose the direct effect of a change in visibility, $\mu_{\text{control}} \Rightarrow \mu_{\text{bracelet}}$, from the indirect effect on social image returns due to a change in agents' inference about the marginal type, $\Delta[w^*(\text{control}, d)] \Rightarrow \Delta[w^*(\text{bracelet}, d)]$.

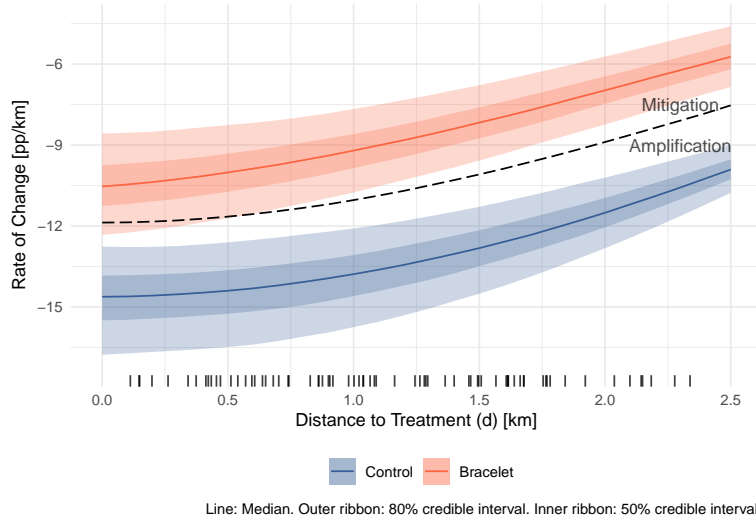


Figure F5: Rate of Change

Notes: This plot shows the rate of change (the derivative of takeup with respect to distance) fixing w^* at the control level. This isolates the effect of changing social image returns on deworming takeup's sensitivity to distance by fixing w^* - there is no change in the marginal type. The dashed line corresponds to a social multiplier of 0 ($\mu = 0$, no visibility), it is curved because of the probit density - a marginal change in cost doesn't lead to a constant, linear change in the probability of taking up treatment. Estimates above the dashed line correspond to mitigation of a cost increase. For a given increase in cost, takeup decreases less than the no visibility case. Estimates below the dashed line show amplification. For a given increase in costs, there is a larger decrease in deworming takeup compared to the no visibility case.

In Figure F5, the dashed black line denotes the rate of change if there was no visibility of actions. At 0km, with no visibility of actions, a marginal increase in distance costs leads to fall in deworming takeup of 12 percentage points per kilometer. At 2.5km this rises

to a fall of only 7.5 percentage points per kilometer³⁸. However, introducing bracelets would lead to a fall in deworming demand of only 10.5 percentage points per kilometer for communities situated 0km from a PoT, holding fixed the cutoff type.

This mitigating effect increases to a fall of only 6 percentage points per kilometer at 2.5km. Alternatively, the control again leads to an increase in deworming takeup's response to distance. Figure F6 reproduces the same result but highlights the prior-predictive distribution in grey. This shows the rate-of-change estimates implied by the model priors before conditioning on the data.

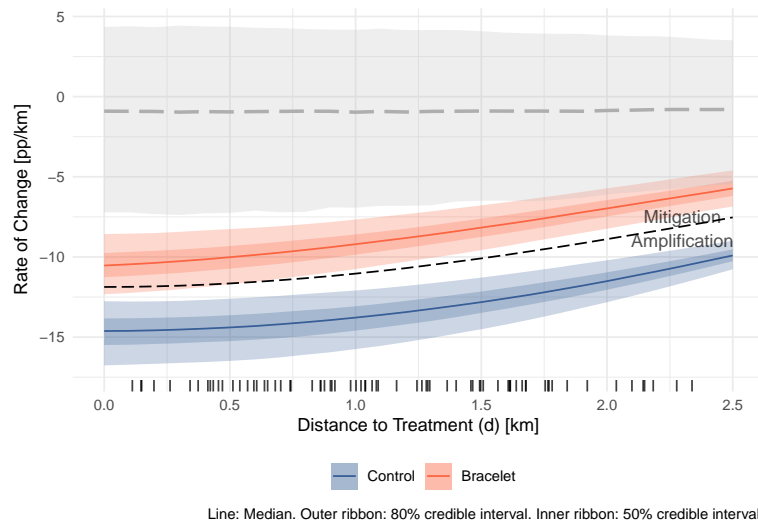


Figure F6: Rate of Change With Prior Predictive Distribution

Notes: This plot shows the rate of change (the derivative of takeup with respect to distance) fixing w^* at the control level. This isolates the effect of changing social image returns on deworming takeup's sensitivity to distance by fixing w^* - there is no change in the marginal type. The dashed line corresponds to a social multiplier of 0 ($\mu = 0$, no visibility), it is curved because of the probit density - a marginal change in cost doesn't lead to a constant, linear change in the probability of taking up treatment. Estimates above the dashed line correspond to mitigation of a cost increase. For a given increase in cost, takeup decreases less than the no visibility case. Estimates below the dashed line show amplification. For a given increase in costs, there is a larger decrease in deworming takeup compared to the no visibility case. The prior predictive distribution - i.e. the effect implied by the model priors before conditioning on the data is shown in light-grey.

³⁸This curvature with no visibility is entirely induced by the Probit density not having a constant marginal effect.

I Equilibrium Inference Derivation

J Unbounded Type

J.1 $\Delta^*(b, c)$ Derivation

We want to find:

$$\Delta^*(b, c) = \frac{-1}{F_w(w^*(b, c))[1 - F_w(w^*(b, c))]} \int_{-\infty}^{\infty} v F_u(w^*(b, c) - v) f_v(v) dv$$

We suppress $w^*(b, c)$ notation and just write w . $V \sim N(0, 1)$, $U \sim N(0, \sigma)$ and the two are independent.

Ignoring the first fraction:

$$\begin{aligned} & \int v F_u(w^*(b, c) - v) f_v(v) dv \\ &= \int \underbrace{v \phi(v)}_{d(-\phi(v))} \Phi\left(\frac{w-v}{\sigma}\right) dv \\ &= \int -\Phi\left(\frac{w-v}{\sigma}\right) d\phi(v) \\ &= \left[-\phi(v) \Phi\left(\frac{w-v}{\sigma}\right)\right]_{-\infty}^{\infty} - \int \frac{-1}{\sigma} \phi\left(\frac{w-v}{\sigma}\right) (-)\phi(v) dv \quad (\text{Integration by parts}) \\ &= \left[-\phi(v) \Phi\left(\frac{w-v}{\sigma}\right)\right]_{-\infty}^{\infty} - \frac{1}{\sigma} \int \phi\left(\frac{w-v}{\sigma}\right) \phi(v) dv \end{aligned}$$

Now focus solely on the remaining integral:

$$\begin{aligned} \int \phi\left(\frac{w-v}{\sigma}\right) \phi(v) dv &= \frac{1}{\sqrt{2\pi}} \frac{1}{\sqrt{2\pi}} \int \exp\left[-\frac{1}{2}\left(\left(\frac{w-v}{\sigma}\right)^2 + v^2\right)\right] dv \\ &= \frac{1}{\sqrt{2\pi}} \frac{1}{\sqrt{2\pi}} \int \exp\left[-\frac{1}{2}\left(\left(\frac{w}{\sigma}\right)^2 + \left(\frac{v}{\sigma}\right)^2 - \left(\frac{2wv}{\sigma}\right)^2 + v^2\right)\right] dv \\ &= \frac{1}{\sqrt{2\pi}} \frac{1}{\sqrt{2\pi}} \int \exp\left[-\frac{1}{2}\left(\left(\frac{w}{\sigma}\right)^2 + v^2 \frac{\sigma^2 + 1}{\sigma^2} - \left(\frac{2wv}{\sigma}\right)^2\right)\right] dv \\ &= \frac{1}{\sqrt{2\pi}} \frac{1}{\sqrt{2\pi}} \int \exp\left[-\frac{1}{2}\left(\left(\frac{w}{\sigma}\right)^2 + \frac{\sigma^2 + 1}{\sigma^2} \left[\left(v - \frac{w}{\sigma^2 + 1}\right)^2 - \frac{w^2}{(\sigma^2 + 1)^2}\right]\right)\right] dv \\ & \quad (\text{Completing The Square}) \\ &= \frac{1}{\sqrt{2\pi}} \frac{1}{\sqrt{2\pi}} \int \exp\left[-\frac{1}{2}\left(\frac{w^2}{\sigma^2 + 1} + \frac{\sigma^2 + 1}{\sigma^2} \left(v - \frac{w}{\sigma^2 + 1}\right)^2\right)\right] dv \\ &= \frac{1}{\sqrt{2\pi}} \frac{1}{\sqrt{2\pi}} \exp\left(-\frac{1}{2} \frac{w^2}{\sigma^2 + 1}\right) \int \exp\left[-\frac{1}{2} \frac{\sigma^2 + 1}{\sigma^2} \left(v - \frac{w}{\sigma^2 + 1}\right)^2\right] dv \end{aligned}$$

The first exponential term is just a function of w and σ whilst the the second term is very nearly a normal pdf:

$$\begin{aligned} \frac{1}{\sqrt{2\pi}} \int \exp \left[-\frac{1}{2} \frac{\sigma^2 + 1}{\sigma^2} \left(v - \frac{w}{\sigma^2 + 1} \right)^2 \right] dv &= \sqrt{\frac{\sigma^2}{\sigma^2 + 1}} \times \frac{1}{\sqrt{2\pi}} \frac{1}{\sqrt{\frac{\sigma^2}{\sigma^2 + 1}}} \int \exp \left[-\frac{1}{2} \left(\frac{v - \frac{w}{\sigma^2 + 1}}{\sqrt{\frac{\sigma^2}{\sigma^2 + 1}}} \right)^2 \right] dv \\ &= \sqrt{\frac{\sigma^2}{\sigma^2 + 1}} \end{aligned}$$

Putting this back together:

$$\begin{aligned} \left[-\phi(v) \Phi \left(\frac{w-v}{\sigma} \right) \right]_{-\infty}^{\infty} - \frac{1}{\sigma} \int \phi \left(\frac{w-v}{\sigma} \right) \phi(v) dv \\ = \left[-\phi(v) \Phi \left(\frac{w-v}{\sigma} \right) \right]_{-\infty}^{\infty} - \frac{1}{\sigma} \frac{\exp \left[-\frac{1}{2} \frac{w^2}{\sigma^2 + 1} \right]}{\sqrt{2\pi}} \times \sqrt{\frac{\sigma^2}{\sigma^2 + 1}} \\ = \frac{-1}{\sigma} \frac{\exp \left[-\frac{1}{2} \frac{w^2}{\sigma^2 + 1} \right]}{\sqrt{2\pi}} \times \sqrt{\frac{\sigma^2}{\sigma^2 + 1}} \end{aligned}$$

Plus the original fraction we ignored:

$$\begin{aligned} \Delta^*(b, c) &= \frac{-1}{F_w(w^*(b, c)) [1 - F_w(w^*(b, c))]} \int_{-\infty}^{\infty} v F_u(w^*(b, c) - v) f_v(v) dv \\ &= \frac{1}{\Phi \left(\frac{w}{\sqrt{\sigma^2 + 1}} \right) \left[1 - \Phi \left(\frac{w}{\sqrt{\sigma^2 + 1}} \right) \right]} \times \frac{1}{\sigma} \frac{\exp \left[-\frac{1}{2} \frac{w^2}{\sigma^2 + 1} \right]}{\sqrt{2\pi}} \times \sqrt{\frac{\sigma^2}{\sigma^2 + 1}} \end{aligned}$$

J.2 $\Delta^*(b, c)$ Derivation

$$\begin{aligned} \Delta'[w] &= \frac{\int_{-\infty}^{\infty} v f_u(w-v) f_v(v) dv + f_w(w) [1 - 2F_w(w)] \Delta[w]}{F_w(w) (1 - F_w(w))} \\ &= \frac{\int_{-\infty}^{\infty} v \frac{1}{\sigma} \phi \left(\frac{w-v}{\sigma} \right) \phi(v) dv + \frac{1}{\sqrt{1+\sigma^2}} \phi \left(\frac{w}{\sqrt{1+\sigma^2}} \right) \left[1 - 2\Phi \left(\frac{w}{\sqrt{1+\sigma^2}} \right) \right] \Delta[w]}{\Phi \left(\frac{w}{\sqrt{1+\sigma^2}} \right) \left(1 - \Phi \left(\frac{1}{\sqrt{1+\sigma^2}} \right) \right)} \end{aligned}$$

Focusing on the integral and recognising we've derived this above:

$$\begin{aligned} \int_{-\infty}^{\infty} v \frac{1}{\sigma} \phi\left(\frac{w-v}{\sigma}\right) \phi(v) dv \\ = \frac{1}{\sigma} \frac{\exp\left(-\frac{1}{2} \frac{w^2}{\sigma^2+1}\right)}{\sqrt{2\pi}} \Sigma \times \frac{1}{\sqrt{2\pi}} \frac{1}{\Sigma} \int_{-\infty}^{\infty} v \exp\left(-\frac{1}{2} \left(\frac{v-\mu}{\Sigma}\right)^2\right) dv \end{aligned}$$

Where $\mu = \frac{w}{\sigma^2+1}$, $\Sigma = \sqrt{\frac{\sigma^2}{\sigma^2+1}}$. Define:

$$H = \frac{1}{\sigma} \frac{\exp\left(-\frac{1}{2} \frac{w^2}{\sigma^2+1}\right) \Sigma}{\sqrt{2\pi}}$$

Now perform change of variables:

$$\begin{aligned} \frac{v-\mu}{\Sigma} &= y \\ dy &= dv \frac{1}{\Sigma} \end{aligned}$$

Giving:

$$\begin{aligned} H \frac{1}{\sqrt{2\pi}} \frac{\Sigma}{\Sigma} \int_{-\infty}^{\infty} (\Sigma y + \mu) \exp\left(-\frac{1}{2} y^2\right) dy &= H \Sigma [-\phi(y)]_{-\infty}^{\infty} + H \mu \\ &= H \mu \end{aligned}$$

Plugging this back into the formula:

$$\Delta'[w] = \frac{H \mu + \frac{1}{\sqrt{1+\sigma^2}} \phi\left(\frac{w}{\sqrt{1+\sigma^2}}\right) \left[1 - 2\Phi\left(\frac{w}{\sqrt{1+\sigma^2}}\right)\right] \Delta[w]}{\Phi\left(\frac{w}{\sqrt{1+\sigma^2}}\right) \left(1 - \Phi\left(\frac{1}{\sqrt{1+\sigma^2}}\right)\right)}$$

K Bounded Type

Now we go back and bound types between \underline{v}, \bar{v} . There are three things we need to do here: keep any terms that dropped out due to integration limits being infinite before, replace the normal pdf with the truncated normal pdf for V , and calculate the convolution of $W \sim V + U$ when V is truncated normal.

K.1 $\Delta^*(w)$ Derivation

$$\Delta^*(w) = \frac{-1}{F_w(w)(1 - F_w(w))} \frac{1}{\Phi(\bar{v}) - \Phi(\underline{v})} \times \left(\left[-\phi(v)\Phi\left(\frac{w-v}{\sigma}\right) \right]_{\underline{v}}^{\bar{v}} - \Gamma \left[\Phi\left(\frac{v - \frac{w}{\sigma^2+1}}{\frac{\sigma}{\sqrt{\sigma^2+1}}}\right) \right]_{\underline{v}}^{\bar{v}} \right)$$

Where:

$$\Gamma = \frac{1}{\sigma} \exp\left(-\frac{1}{2} \frac{w^2}{1+\sigma^2}\right) \times \sqrt{\frac{\sigma^2}{\sigma^2+1}}$$

and:

$$F_w(w) = \int_{\underline{v}}^{\bar{v}} \Phi\left(\frac{w-t}{\sigma}\right) \frac{\phi(t)}{\Phi(\bar{v}) - \Phi(\underline{v})} dt$$

$$(\Phi(\bar{v}) - \Phi(\underline{v}))F_w(w) = \int_{\underline{v}}^{\bar{v}} \Phi\left(\frac{w-t}{\sigma}\right) \phi(t) dt$$

That is, the convolution of two independent r.v.s. It can be shown that the RHS:

$$\begin{aligned} RHS &= \frac{1}{2} (\Phi(z_h) - \Phi(z_l)) \\ &\quad - \frac{1}{2} \left[\frac{\mu}{z_h} < 0 \right] \\ &\quad + \frac{1}{2} \left[\frac{\mu}{z_l} < 0 \right] \\ &\quad - T\left(z_h, \frac{h}{z_h}\right) \\ &\quad + T\left(z_l, \frac{l}{z_l}\right) \\ &\quad - T\left(\frac{\mu}{\rho}, \frac{\mu\sigma + z_h\rho^2}{\mu}\right) \\ &\quad + T\left(\frac{\mu}{\rho}, \frac{\mu\sigma + z_l\rho^2}{\mu}\right) \end{aligned}$$

where: $U \sim N(0, \gamma)$, $\mu = \gamma^{-1}z$, $\sigma = -\gamma^{-1}$, $\rho = \sqrt{1 + \sigma^2}$, $z_l = \frac{l-\mu}{\sigma}$, $z_h = \frac{h-\mu}{\sigma}$, $h = \frac{z-\bar{v}}{\gamma}$, $l = \frac{z-\underline{v}}{\gamma}$

We do the above because we need to perform change of variables so that we have:

$$\int_l^h \Phi(x) \frac{1}{\sigma} \phi\left(\frac{x-\mu}{\sigma}\right) dx$$

So everything looks weird to transform the $\Phi(\dots)$ term into $\Phi(x)$ and we can use the known result above. T stands for Owen's T.